Ecole Doctorale BioSE (Biologie-Santé-Environnement)

Thèse

Présentée et soutenue publiquement pour l'obtention du titre de

DOCTEUR DE l'UNIVERSITE DE LORRAINE

Mention : « Sciences de la Vie et de la Santé » par

Xing LIU

A contribution to the selection of suitable cells, scaffold and biomechanical

environment for ligament tissue engineering

Thèse dirigée par : Natalia DE ISLA, Cédric LAURENT et Xiong WANG

Le 1 Juillet 2019

Composition du Jury

Rapporteurs :	Véronique MIGONNEY	Professeur, Université Paris 13
	Florence FIORETTI	MCU-PH, Université de Strasbourg
Ex-examinateur :	Yun CHEN	Professeur, Université de Wuhan
Examinateurs :	Natalia DE ISLA	MCF-HDR, Université de Lorraine (Directeur de thèse)
	Cédric LAURENT	MCF, Université de Lorraine (Co-directeur de thèse)
	Xiong WANG	Professeur, Université de Lorraine (Co-directeur de thèse)
Membre invité :	Gilles ARNOLD	MCF, Université de Haute Alsace

UMR 7365 CNRS-Université de Lorraine, Ingénierie Moléculaire et Physiopathologie Articulaire (IMoPA)

Acknowledgements

First at all, I would like to express my sincere gratitude to my supervisors, **Dr. Natalia De Isla**, **Dr. Cédric Laurent** and **Pr. Xiong Wang**. Firstly, I would like to thank **Dr. Natalia De Isla** for having accepted me to be her PhD student. Her patience to teach me the experiments and kindness to help me whenever I had some issues were particularly crucial to me. It was also my great pleasure to work with **Dr. Cédric Laurent,** and benefit from his concentration, efficiency, intelligence. His way to work influenced me a lot, and I would like to thank him a lot for all he did for my thesis. I also would like to thank **Pr. Xiong Wang**, for guiding me for my thesis, his encouragement and help. I am grateful for all they have done for me.

I also would like to show my best appreciation to **Pr. Yun Chen**, with whom it was my great pleasure to work. He always put himself in our place, and I feel very lucky to be his student. He taught me not only how to do research, but also to be a person. His wisdom and humor influence me a lot.

I want to thank **Ghislaine Cauchois,** for helping me and other chinese students a lot in our team. She helped me to solve the problems encountered during my experiments, to communicate with my supervisors and others in the laboratory, and also to improve my French. We had a good time together.

Then, I would like to thank the director of IMoPA, **Pr. Jean-Yves Jouzeau**, for allowing me to work this laboratory, and **Pr. Patrick Menu** for his encouragement and his help concerning the doctoral school BioSE.

I would like to thank **Pr. Jean-Francois Stoltz** and **Dr. Jacques Magdalou** who contributed a lot to the collaboration between Nancy and Wuhan and gave me the opportunity to study in France.

I want to show my appreciation to **Pr. Véronique Migonney**, **Dr. Florence Fioretti**, and **Dr. Gilles Arnold** for having accepted to be present in my defense and to evaluate my work.

I would also like to thank **Dominique Dumas** for helping me to work in the platform of confocal microscopy, **Christel Henrionnet**, for helping me with histological experiments, **Frédéric Velard**, for taking charge of scanning electronic microscopy, **Adrien Baldit** and **Emilie de Brosses**, for working on micro-CT and mechanical tests, **Naceur Charif,** for preparing the experiments in the team.

Table of contents

Summary in French

Les lésions ligamentaires constituent l'un des troubles musculosquelettiques les plus fréquents, surtout chez les personnes pratiquant des activités physiques rigoureuses, souffrant de traumatismes aigus, chez les personnes âgées, ou lors d'accidents. L'endommagement du ligament ou de son rôle physiologique peut devenir une source de douleurs, d'inflammations et d'instabilités, ce qui peut entraîner une limitation des mouvements et une réduction de la qualité de vie des patients. Après une blessure du ligament, le processus de guérison comprend trois phrases : i) la phase inflammatoire aiguë, ii) la phase réparatrice / proliférative, iii) la phase de remodelage des tissus. Physiologiquement, ce tissu est principalement constitué de fibroblastes et de matrice extracellulaire, celle-ci étant constituée de collagène, de protéoglycanes, de tenascine-C, d'élastine et d'eau. Cependant, en raison d'un apport sanguin relativement faible et de la faible quantité de cellules, le ligament a une faible capacité d'autoréparation ou d'autorégénération.

La cicatrisation ligamentaire doit permettre l'obtention d'un tissu aux propriétés mécaniques et biochimiques comparables au tissu natif. De nombreux efforts ont été faits pour proposer une solution efficace afin de rétablir la fonction des ligaments lésés. Les traitements conservateurs tels que les orthèses et les programmes d'entraînement neuromusculaires ne sont pas suffisants pour les athlètes ou dans le cas d'une rupture grave. De nos jours, le traitement par intervention chirurgicale constitue l'approche principale pour réparer les lésions ligamentaires. Les greffons utilisés dans ce type de

traitement chirurgical comprennent les autogreffes, les allogreffes et les substituts artificiels. Par exemple, la ligamentoplastie appliquée au traitement de ruptures du ligament du genou est une intervention chirurgicale qui permet des résultats satisfaisants pour les patients. Le principe de cette intervention consiste à remplacer le ligament altéré par des greffons prélevés en général sur le tendon ischio-jambier, le tendon rotulien, le fascia lata ou les quadriceps provenant de patients ou de donneurs. Cependant, une telle chirurgie possède nécessairement une série d'inconvénients, incluant notamment la morbidité du site du donneur, le rejet immunitaire ou la disponibilité limitée des sources de greffe. Aujourd'hui l'ingénierie tissulaire ligamentaire apparaît comme une approche nouvelle et une alternative prometteuse pour réparer la fonction du ligament endommagé. Les trois piliers essentiels de l'ingénierie tissulaire ligamentaire sont la matrice de support (aussi appelée *scaffold*), la source cellulaire, ainsi que l'apport de stimulations biomécaniques/biochimiques. Dans l'étude qui constitue le présent travail de thèse, l'optimisation d'une matrice de support appropriée, le choix d'une source des cellules adaptée, ainsi que l'apport d'une stimulation mécanique sont étudiés.

La première partie de cette étude concerne le choix de la source cellulaire. Les cellules souches mésenchymateuses en gelée de Wharton (WJ-MSCs) et les cellules souches mésenchymateuses de la moelle osseuse (BM-MSCs) ont toutes les deux été évaluées et comparées en tant que sources cellulaires potentielles, principalement en raison de leur capacité d'auto-renouvellement et de leur potentiel de différenciation. Avant

d'étudier l'interaction de ces cellules avec la matrice de support, une série de caractérisations biologiques ont été effectuées pour confirmer la « propriété de souche » de ces cellules mais également pour évaluer leur qualité. Les propriétés classiques permettant d'évaluer ces cellules incluent les unités de formation de colonies-fibroblastes (CFU-F), les potentiels de différenciation multilignes, l'expression phénotypique, et aussi la sénescence cellulaire. Les résultats ont montré que les WJ-MSC et les BM-MSC présentaient une clonogénicité, et que davantage de colonies étaient formées par les BM-MSC que par les WJ-MSC. Nous avons également constaté que les deux types de cellules étaient capables de se différencier en tissus adipeux, osseux et cartilagineux, d'exprimer positivement les enzymes CD73, CD90, CD166, et d'exprimer négativement les enzymes CD34, CD45, HLA-DR, qui permettent d'identifier les MSC. Les résultats de la sénescence ont montré que les BM-MSC présentaient une meilleure capacité de prolifération et moins de cellules sénescentes en comparaison aux WJ-MSC. En guise de première conclusion, les deux types de cellules ont été identifiées comme étant des cellules souches mésenchymateuses et ont été utilisées dans les études suivantes.

La deuxième partie de cette étude porte sur le choix de la matrice de support. Le polymère synthétique poly (L-lactide-co-ε-caprolactone) (PLCL) ainsi que la soie naturelle ont été utilisés et comparés. Le PLCL est un copolymère synthétique biodégradable à haute élasticité. Il a été démontré qu'il possédait une bonne cytobiocompatibilité et ainsi qu'une biodégradabilité ne générant pas de produits

toxiques dans un laps de temps déterminé. Lors d'une étude précédente réalisée par notre équipe, le PLCL a été sélectionné pour le développement d'une matrice tressée multicouches, et il a été montré qu'une telle matrice pouvaient offrir les propriétés mécaniques et de dégradation nécessaires à la régénération ligamentaire. Cependant, une étude concernant la stimulation mécanique de cette matrice (associée à des cellules souches humaines) par le biais d'un bioréacteur de traction-torsion a montré que, bien que les cellules présentaient de bonnes adhésion et prolifération initiales, elles ne se répartissaient pas de façon homogène sur la matrice. Cette observation est à l'origine de la première question qui a été abordée dans la présente étude.

La modification couche par couche (en anglais *Layer-By-Layer,* LBL) est l'une des méthodes permettant de modifier la surface d'une matrice de support, et ainsi d'améliorer l'interaction entre les cellules et la matrice. Il s'agit d'un procédé de fabrication de films multicouches de polyélectrolyte (PEM) par dépôt de couches alternées de matériaux avec des charges opposées. Ce procédé a été utilisé pour développer des solutions de distribution de facteurs de croissance en les incorporant au sein de ces couches alternées. En effet, les facteurs de croissance jouent un rôle essentiel dans la différenciation cellulaire. Par conséquent, la deuxième partie de la présente étude s'intéresse au développement et à la caractérisation des comportements cellulaires sur ces multicouches de polyélectrolytes. Tout d'abord, le développement de couches de polyélectrolytes constitués d'alternances poly(l-lysine) /acide hyaluronique (PLL/HA) a été réalisé afin de modifier les propriétés des matrices de support. Dans la

littérature, il a été démontré que ces modifications étaient affectées par la concentration de la solution, par le pH de l'environnement, et par les charges des électrolytes. Ces différents facteurs ont été étudiés dans notre cas, en particulier l'influence de deux valeurs de pH différentes (pH 6.0-6.5 et pH 7.4), la nature de la couche finale (PLL ou HA) et le nombre de bicouches qui constituent cette modification de surface. A partir des résultats de l'analyse de l'activité métabolique cellulaire, la couche de PLL a été sélectionnée pour constituer la couche finale, le nombre de couches de polyélectrolytes a été fixé à une seule pour les deux types de cellules, et le pH 6.0-6.5 a été utilisé. A l'issue de cette partie, un protocole a donc été développé pour la modification de surface des matrices de support de PLCL.

Les propriétés physico-chimiques des matrices tressées de PLCL avec ou sans modifications de surface ont également été étudiées. Les images issues de microscopie électronique à balayage (MEB) ont montré que les matrices présentaient une structure poreuse stable avant et après modification, tandis que des images issues de microscopie par force atomique ont mis en exergue l'apparition d'une topologie rugueuse due à la modification de surface. Les propriétés mécaniques n'ont quant à elles pas montré d'évolutions significatives lors de ces modifications. Les caractéristiques biologiques liées à l'adhésion cellulaire, la prolifération, la migration et la synthèse de matrice extra-cellulaire sur les matrices, ont été étudiées. Les résultats ont révélé que les deux types de cellules présentaient une activité métabolique satisfaisante sur les matrices, qu'elles présentaient une forme allongée dans la direction longitudinale des fibres, et qu'elles

établissaient des ponts cellulaires entre les fibres. Le collagène de type I, le collagène de type III et la ténascine-C secrétés par les CSM ont été détectés au jour 14. De plus, nous avons montré que les matrices modifiées par le procédé LBL présentait des propriétés supérieures concernant la chimiotaxie. En deuxième conclusion de la présente étude, les résultats indiquent donc que la matrice de PLCL tressée associée à une modification de surface par une couche de polyélectrolytes offre un fort potentiel d'utilisation en ingénierie tissulaire du ligament, tant aux niveaux biologique que mécanique.

Néanmoins, aucune amélioration de l'homogénéité de la distribution cellulaire n'a été observée à la suite de ces modifications, puisque des amas de cellules ont été observés sur la matrice au niveau des croisements entre les fibres. Toutefois, dans le futur, cette modification peut permettre la mise au point d'un système de distribution de facteurs de croissance, en les incorporant au sein des couches de polyélectrolytes. Cette étude valide par conséquent la biocompatibilité de la matrice de support avec la modification PLL/HA, ce qui ouvre de nouvelles perspectives concernant son application à l'ingénierie tissulaire ligamentaire, et notamment concernant le recrutement des cellules endogènes après implantation.

En parallèle, notre groupe a étudié la dégradation du PLCL et a montré que les fibres de PLCL présentaient un comportement fragile après une période de dégradation de deux mois. Ce résultat laisse penser que la matrice de support pourrait être associée à

un risque prématuré d'endommagement postopératoire. Par conséquent, la proposition de biomatériaux alternatifs au PLCL pour la régénération ligamentaire constitue un défi crucial, défi qui fait l'objet de la partie suivante de ce travail de thèse.

La soie est un polymère naturel largement utilisé pour la recherche biomédicale, principalement en raison de sa biocompatibilité et de ses excellentes propriétés mécaniques. La soie est également le polymère naturel le plus communément utilisé pour une application en ingénierie tissulaire du ligament. La troisième partie de cette étude concerne donc l'étude de l'utilisation de la soie dans une matrice de support pour l'ingénierie tissulaire du ligament. Concernant l'architecture de cette matrice, la structure tressée multicouche utilisée précédemment a été conservée et utilisée pour le développement d'une matrice de support en soie. Cette structure semblable au tissu natif montre en effet une structure poreuse facilitant l'échange de nutriments ou de gaz nécessaires à la croissance des cellules ou des tissus. Le nombre de couches constituant cette matrice de soie a été déterminé à la suite d'essais mécaniques, lors desquels il a été observé que les propriétés mécaniques n'augmentaient pas lorsque le nombre de couches était supérieur à 3. De plus, le temps de dégradation de la soie est connu pour être supérieur à 18 mois après l'implantation, et la soie est classée comme un biomatériau "non dégradable" par la FDA. Sur cette base, il a été considéré que l'ajout de PLCL à une matrice de soie pourrait permettre d'ajuster sa vitesse de dégradation tout en maintenant des propriétés mécaniques suffisantes à son utilisation en ingénierie du ligament.

Des matrices de supports tressées multicouches en soie (n=1,2,3), ainsi que des matrices composites soie/PLCL/soie (SP) ont été développées, et leur les propriétés physico-chimiques (morphologie, porosité, propriétés mécaniques) et biologiques (morphologie cellulaire, fixation, prolifération, distribution ces cellules vivantes et mortes) ont été évaluées. Les images de MEB ont montré que les matrices de soie et la matrice composite soie/PLCL présentaient une structure poreuse, et que leur compacité augmentait en même temps que le nombre de couches, ce qui a été corroboré par des mesures de porosité par μ-CT. Pour un même nombre de couches, il a été observé que la porosité de la matrice composée de soie uniquement était bien inférieure à celle de la matrice composite soie/PLCL. Du point de vue mécanique, les propriétés en traction des quatre matrices différentes étaient comparables à celles d'un ligament natif. Il a été néanmoins considérée que le choix de la matrice composite soie/PLCL pouvait diminuer le risque de rupture du biosubstitut lorsqu'il était soumis à de très fortes contraintes, en raison de la grande déformabilité du PLCL.

Dans cette partie, les deux types de cellules souches (WJ-MSCs et BM-MSCs) ont été sélectionnées comme étant des sources cellulaires potentiellement adaptées à l'ingénierie tissulaire du ligament. Nous avons observé que l'activité métabolique cellulaire augmentait de J1 à J7 pour les deux types de cellules, avec une activité métabolique moindre pour la matrice de soie S3 (3 couches en soie). Les images MEB ont montré que les cellules adhéraient et proliféraient de façon satisfaisante sur les différentes matrices, et que des films de cellules recouvraient la surface des matrices.

Les colorations de cellules vivantes/mortes ont indiqué que les cellules présentaient une forme allongée, et proliféraient dans la direction des fibres de soie, tandis que davantage de cellules mortes ont été observées pour les cellules de la gelée de Wharton, en particulier sur la matrice S3. L'essai de migration a montré que la matrice composite soie/PLCL favorisait la migration cellulaire en comparaison aux matrices composées uniquement de soie, tandis que cette migration était en particulier accentuée pour les cellules de la moelle osseuse. Les résultats histologiques de la coloration HES ont révélé que l'augmentation du nombre de couches dans la matrice tressée était associée à une diminution de la colonisation de la matrice, en particulier pour la matrice S3. En effet, davantage de matrice extracellulaire a été observée à la surface et au cœur des matrices S1, S2 et SP, tandis qu'une matrice moins importante a été observée la matrice S3. Aucune différence significative n'a été observée entre les deux types de cellules. Les résultats du test Red sirious ont mis en exergue l'expression du collagène dans la matrice extracellulaire sécrétée, et souligné la prédominance du collagène I sur le collagène III. En conclusion de cette troisième partie, sur la base de la combinaison de ces propriétés physico-chimiques et biologiques, la matrice composite soie/PLCL semble être le candidat le plus approprié pour une application en ingénierie tissulaire du ligament. Toutefois, des études sur la dégradation de cette matrice devront être effectuées dans le futur, afin de confirmer ou infirmer les hypothèses formulées concernant sa capacité de biodégradation.

Sur la base de l'ensemble des résultats obtenus, la matrice de support composite

soie/PLCL développée dans le présent travail semble constituer un support de culture adapté à l'ingénierie du ligament, tandis que les deux types de cellules BM-MSC et WJ-MSC ont montré une bonne biocompatibilité sur cette matrice. Par conséquent, l'étape suivante de la démarche d'ingénierie tissulaire considérée ici consiste à tenter d'améliorer le microenvironnement cellulaire afin de promouvoir la régénération tissulaire. L'effet d'un chargement mécanique dynamique sur la différentiation cellulaire vers un phénotype ligamentaire a été donc évalué dans le cadre d'une étude préliminaire en utilisant un bioréacteur de traction-torsion développé précédemment dans notre équipe, étude qui constitue le dernier volet du présent manuscrit. Les paramètres concernant le chargement cyclique ont été fixés à 2.5% de déformation, à 1 Hz pendant 2 min toutes les 30 min et pendant 8 h par jour. Les résultats ont montré que la stimulation mécanique favorisait d'abord la prolifération cellulaire durant les 4 premiers jours, puis la viabilité cellulaire diminuait les jours suivants. Bien que les cellules aient présenté une forme allongée et une prolifération le long de la direction des fibres, nous n'avons pas observé un nombre important de cellules effectivement fixées sur la matrice de support. Par conséquent, d'autres études concernant l'effet d'un chargement mécanique devront être effectuées dans le futur afin d'une part d'améliorer la fixation, la prolifération et la synthèse de matrice extracellulaire ligamentaire, et d'autre part de comprendre les mécanismes sous-jacents du comportement cellulaire en réponse à une stimulation mécanique.

En conclusion, le PLCL et la soie constituent deux biomatériaux particulièrement

intéressants tant au niveau de leur propriétés biologiques et mécaniques pour l'ingénerie du ligament. Les cellules souches de la moelle osseuse et de la gelée de Wharton (WJ-MSCs et BM-MSCs) ont montré un comportement similaire et satisfaisant, en particulier en combinaison avec la matrice de support composite soie/PLCL développée dans ce travail. L'une des perspectives principales concerne désormais l'administration de facteurs de croissance au sein de cette matrice en utilisation la modification de surface LBL étudiée dans une première partie de ce travail. Une seconde perspective concerne l'utilisation du bioréacteur pour définir l'environnement mécanique optimisant la promotion de la différenciation ligamenteuse au sein de cette matrice.

Scientific work

Publications

1. **Liu X**, Velard F, Baldit A, Chen Y, Wang X, De Isla, N, Laurent C

   Characterization of WJ-MSC and BM-MSC response on multilayer braided silk

   and silk/ PLCL scaffold for ligament tissue engineering. (In preparation)

2. **Liu X**, Laurent C, Du Q, Targa L, Cauchois G, Chen Y, Wang X, de Isla N.

   Mesenchymal stem cell interacted with PLCL braided scaffold coated with poly-

   L-lysine/hyaluronic acid for ligament tissue engineering. *J Biomed Mater Res*

   Part A 2018:106A:3042–3052

3. Laurent C P, **Liu X**, De Isla, N, Wang, X, Rahouadj, R. Defining a scaffold for

   ligament tissue engineering: what has been done, and what still needs to be done.

   Journal of Cellular Immunotherapy 2018:4(1) 4-9

4. Laurent C P, Vaquette C, **Liu X**, Schmitt J, Rahouadj R. Suitability of a PLCL

   fibrous scaffold for soft tissue engineering applications: A combined biological and

   mechanical characterization. *Journal of biomaterials applications, 2018, 32(9):*

   1276-1288

5. Yu H, Li W, **Liu X**, Li C, Ni H, Wang X, Huselstein C, Chen Y. Improvement of

   functionality after chitosan-modified zein biocomposites. *J Biomater Sci Polym Ed.*

Communications

1. **Liu X,** Laurent C.P, Wang X, Chen Y, De Isla N. Comparison of different cell types and surface modification for ligament tissue engineering. ***16ème édition du congrès de la Société Française de Génie des Procédés.*** *July 11 -13, 2017, Nancy, France.* (Oral presentation)

2. **Liu X**, Laurent C, Chen Y, Wang X, De Isla N. Optimization of mesenchymal stem cell cultured in PLCL-braided scaffold for ligament tissue engineering. ***European Chapter Meeting of the Tissue Engineering and Regenerative Medicine, International Society****. June 26-30, 2017 Davos, Switzerland* (Oral presentation)

3. **Liu X,** Laurent C, Chen Y, Li Y, Wang X, De Isla N. Optimization of mesenchymal stem cell cultured in PLCL-braided scaffold for ligament tissue engineering. ***6th International Symposium Europe China, Molecular, cellular and tissue engineering, and clinical applications. 1st meeting of the CNRS GDRI France-China « Mesenchymal Stem Cells and Regenerative Medecine »*** *July 11-13th, 2016, Faculty of Medecine, Vandoeuvre-les-Nancy, FRANCE* (Poster)

List of tables, figures and abbreviations

Tables

Figures

Abbreviations

AB	Alamar Blue
ACL	Anterior Cruciate Ligament
AFM	Atomic Force Microscopy
ALP	Alkaline Phosphatase
AT	Achilles Tendon-derived cells
BM	Bone Marrow
BMP-12	Bone Morphogenic Protein-12
CFU-F	Colony Forming Unit-fibroblast
CLSM	Confocal Laser Scanning Microscopy
Col I	Collagen type I
Col II	Collagen type II
Col III	Collagen type III
DAPI	4′,6-diamidino-2-phenylindole
DHLNL	Dihydroxulysinonorleucine
ECM	Extracellular Matrix
EGF	Epidermal Growth Factor
EM	Elastic Modulus
FBS	Fetal Bovine Serum
FTIR	Fourier Transform Infrared Spectroscopy
Fn	Fibronectin
GAGs	Glycosaminoglycane

GMSC	Gingival Mesenchymal Stem Cell
GDF-5	Growth Differentiation Factor-5
HA	Hyaluronic Acid
HES	Hematoxylin/Eosin/Safran
HHMD	Histidinohydroxymerodesmosine
HP	Hydroxyproline
HLNL	Hydroxulysinonorleucine
IHC	Immunohistochemistry
IGF-1	Insulin-like Growth Factor-1
IL-1	Interleukin-1
KDR	Key receptors Kinase Domain Receptor
LBL	Layer-by-layer
LCL	Lateral Collateral Ligament
MCL	Medial Collateral Ligament
MSC	Mesenchymal Stem Cell
μ-CT	Micro-Computed Tomography
NDGA	Di-catechol nordihydroguaiaretic acid
PCL	Posterior Cruciate Ligament
PCL	Poly-caprolactone
PDL	Periodontal Ligament
PDGF	Platelet-Derived Growth Factor
PDGFR	Platelet-Derived Growth Factor-Receptor

PEM	Polyelectrolyte multilayer
PEGDA	Polyethylene Glycol Diacrylate
PET	Polyethylene Terephthalate
PGA	Polyglycolic Acid
PLLA	Polylactic Acid
PLL	Poly (L-lysine)
PLGA	Poly (DL-lactide-co-glycolide)
PLLA	Poly (L-lactic Acid)
PLCL	Poly-(L-lactide-co-ε-caprolactone)
PRP	Platelet Rich Plasma
PL	Platelet Lysate
PLAGA	Polylactic-co-glycolic Acid
PTFE	Polytetrafluoroethylene
PU	Polyurethane
PVA	Poly (vinyl acetate)
RS	Red Sirus
Scx	Scleraxis
SEM	Scanning Electronic Microscopy
SIS	Small Intestinal Submucosal
TNC	Tenascin-C
TNMD	Tenomodulin
TGF-β1	Transforming Growth Factor β1

UTS	Ultimate Tensile Stress
WJ	Wharton's Jelly
2D	Two-dimensional
3D	Three-dimensional

1. Chapter I: State of art

1.1 General Introduction

Ligaments are the most frequently injured tissue within joints, which could cause disruptions in the balance between joint mobility and joint stability. Many researches and efforts have been made to resolve this problem. Unfortunately, there has been not yet an effective method till now. This study is based on the proposition of ligament tissue engineering as an approach for tissue regeneration. In order to well develop a neoligament by tissue engineering, the first section provide a description of the characteristics of ligament (structure, composition, function), the nature healing process and the current strategies for ligament injuries to get a knowledge of nature ligament. The second section focus on three elements of ligament tissue engineering, relating cell sources, scaffolds and mechanical or biochemical stimulation.

1.2 Ligament structure

1.2.1   Gross structure

Ligaments are bounds of dense connective tissue, which play an essential role in supporting internal organs and ensuring bone-to-bone in order to restrict excessive motion within joints (Chiras 2005; G. Yang, Rothrauff, and Tuan 2013). They vary in size, shape, location and orientation (C. B. Frank 2004a). Anatomically, it includes articular ligament, peritoneal ligament, fetal remnant ligament and periodontal ligament (Reviews 2016). There are for instance broad, ribbon-shaped medial collateral

ligaments (MCL) within knee, or some complex structures consisting in two bands bearing differential tensions adapted to the knee movement in the case of anterior cruciate ligament (ACL) (Savio L-Y. Woo et al. 1999). The surface of ligament is covered by a vascular overlying layer called "epiligament", which is indistinguished from ligament and merges into the periosteum of bones at the attachment sites (Hauser et al. 2013; C. B. Frank 2004a). Epiligament is more vascularized and cellularized than ligament (Masoud et al. 2014; Hauser et al. 2013). The bony attachment of ligament is called "enthesis" or insertion site and is associated with stress concentration at the hard-soft tissue interface. Consequently, entheses are vulnerable to acute or overuse injuries in sports (Benjamin et al. 2006). Such insertions may be classified into direct and indirect insertions: in the case of direct insertion, fibers attach directly into bone and the force transmission occurring in four zones: ligament, fibrocartilage, mineralized fibroblast and bone (S. L. Woo et al. 1987), while superficial fibers anchored to periosteum and deeper fibers are attached to bone directly in the case of indirect insertion (S. L. Woo et al. 1987).

1.2.2 Microscopic organization

In a microscopic level, complex ligament structure mainly consists of collagen fibers and fibroblasts. Ligament fibroblasts are mainly responsible for the matrix synthesis; however, they are relatively few in number and appear functionally or physically isolated. Fibroblasts communicate by means of cytoplasmic extension and anchored to the cytoplasmic extension of adjacent cells, forming a three-dimensional structure

(Birch 2007). Gap junctions is also detected and supposed to facilitate fibroblast-fibroblast communication and coordinate cellular and metabolic responses throughout the tissue (C. B. Frank 2004b).

1.3 Ligament composition

Ligaments are mainly composed of cells and extracellular matrix (ECM) (C. B. Frank 2004b; Birch, Thorpe, and Rumian 2013) (Figure 1). Fibroblasts are the main cellular component (Zhao 2008; Nau and Teuschl 2015), and ECM is composed of collagen, proteoglycans, tenascin-C (TNC), elastin, water etc. (Birch, Thorpe, and Rumian 2013). ECM takes account for 80% of tissue volume and fibroblasts make up the remaining 20%. In the composite of wet ligament tissue, water accounts for about 70% of the weight, collagen type I (Col I) takes up approximately 20%, and other ECM represent about 10% (Lujan et al. 2009; Rathbone and Cartmell 2011) (Table 1). In the dry composition of ACL ligament, the ratio of Col I and collagen type III (Col III) is 9:1 (Rathbone and Cartmell 2011). The role and particularities of these components are described in the following sections.
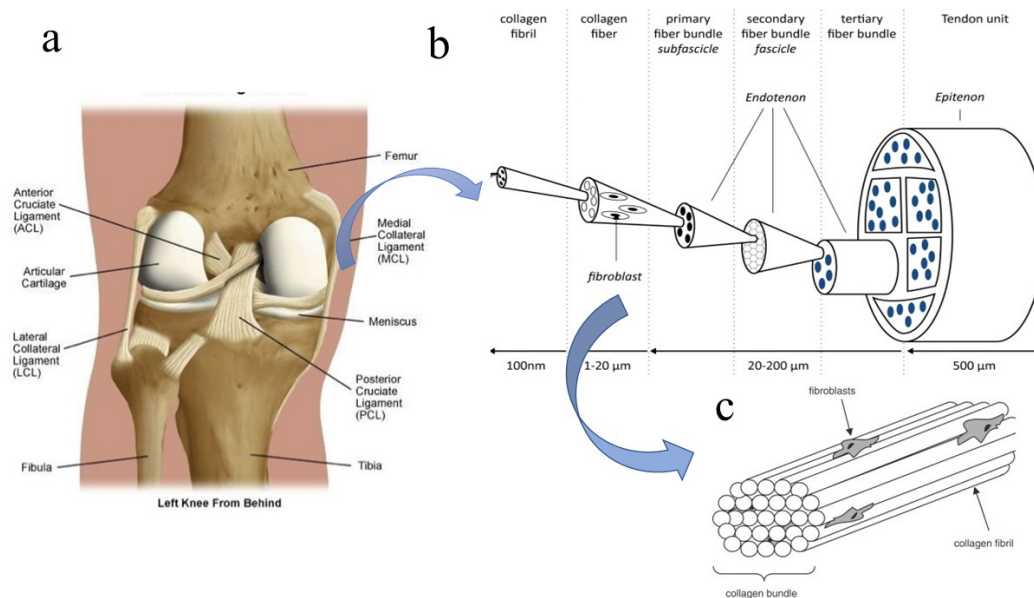
Figure 1 The anatomic diagram of knee joint (a), a schematic drawing of tendon/ligament as a multi-unit hierarchical structure (b) (Barfod 2014), relationship between a collagen bundle and fibroblasts (c) (Doroski, Brink, and Temenoff 2007)

Table 1 The biochemical constituents of wet ligament tissue (Rathbone and Cartmell 2011).

Tissue type (wet weight)	Collagen type I (%)	Other collagens such as type III, V, VI (%)	Elastin (%)	Fibronectin and other glycoproteins (%)	Proteoglycans (%)	Water (%)	Author
Ligament (general)	20	3-5	1-2	1-2	<1	70	(Einhorn, O'Keefe et al. 2007)

1.3.1   Cellular component

The majority of cells in ligament tissue are fibroblasts, which present a spindled shape

and locate in the longitudinal direction of collagen bundles (Doroski, Brink, and Temenoff 2007). The quantity of fibroblasts is quite few and constitute small volume of ligament (LEE 2005). Fibroblasts are mainly responsible for ECM synthesis (Mackey et al. 2008). Due to a relatively low blood supply and the few cellular compositions, ligament has a poor self-repair or self-regenerate ability.

1.3.2 Molecular components

1.3.2.1 Collagen

Collagen is the most abundant protein of ligament ECM (LEE 2005). Various kinds of collagen are present in ligament tissue. Col I accounts for approximately 70-80% of the dry weight of ligament tissue, Col III and collagen type V (Col V) make up 8-10%, 10-12% respectively (Sensini and Cristofolini 2018).

According to the structure and molecular composition (Shoulders and Raines 2009), collagens are classified into fibril-forming collagens (type I, II, III, V, XI), basement membrane collagens (type IV), microfibrillar collagens (type VI), anchoring fibrils (type VII), hexagonal network-forming collagens (type VIII, X), Fibril Associated Collagen with Interrupted Triple helixes (FACIT) collagen (type IX, XII, XIV, XIX, XX, XXI), transmembrane collagens (type XIII, XVII), and multiplexins collagens (type XV, XVI, XVIII) (Gelse, Pöschl, and Aigner 2003). The majority of collagen families is fibril-forming collagen, which accounts for approximately 90% of all the collagens, and is also mainly constitution of ligament ECM (Gelse, Pöschl, and Aigner

2003).

The ability of collagen to provide mechanical support is mainly related to its molecular structure. Moreover, molecular crosslinking also contributes to enhance mechanical properties (Doroski, Brink, and Temenoff 2007). Collagen is characterized with a right-hand superhelix structure composited with three α-chains. Col I is composed of two identical α1 chains and one α2 chain. It provides tensile strength, and is mainly located in bone, tendon, ligament, dermis, etc. (Cai et al. 2013). Col III is made of three α1 chains and usually contributes to fibrils together with Col I. Collagen type II (Col II) is also formed by three α1 chains and constitutes the characteristic protein in cartilage, which is supposed to limit the diameter of fibrils diameter (J. H. Yoon and Halper 2005).

In Col I and Col III, these superhelices form long fibers and their alignment and diameter affect the tissue strength and stiffness. The subunit of superhelix include 3 right-hand helices, which contribute to the high tensile strength with the respect to their rigidity and relative inelasticity. The basic sequence of helices is a repeated unit "Glycine-X-Y", where X and Y represent proline and hydroxyproline (HP) relatively (Shoulders and Raines 2009). The structure of polypeptide and the repeated sequence together influence the tensile strength of tissue. Cross-links play a role in stabilizing collagen and enhancing tensile strength of ligament tissue. The most common crosslinking types are hydroxulysinonorleucine (HLNL), dihydroxulysinonorleucine (DHLNL), and histidinohydroxymerodesmosine (HHMD) (Ge et al. 2006).

1.3.2.2 Non-collagenous components

Non-collagenous components of ligament ECM mainly include glycoproteins and proteoglycans. Glycoproteins are proteins containing oligosaccharide chain covalently attached to amino acid chain of polypeptide, including TNC and tenomodulin (TNMD) (Malmström et al. 2012). Proteoglycans are heavily glycosylated proteins, which consists of a core protein providing attachment sites for one or more glycosaminoglycans, such as decorin, biglycans, versican, etc. (J. H. Yoon and Halper 2005). The structures and functions of non-collagenous proteins are described in the following sections.

1.3.2.2.1   Glycoproteins

TNC is a typically hexabrachion-shaped extracellular matrix glycoprotein (Stamenkovic et al. 2017), and constitutes a member of tenascin proteins family. Tenascin proteins are characterized with a similar module organization include heptad repeats, EGF-like repeats, fibronectin type III domains, and a C-terminal globular domain shared with fibrinogens (Halper and Kjaer 2014). Physiologically, TNC exists in nerve tissue and connective tissue such as bones, tendons, ligaments and except dermis to undertake high tensile stress (Stamenkovic et al. 2017). TNC is limitedly expressed in healthy musculoskeletal tissue, and has been reported to provide elasticity to musculoskeletal tissues by promoting cell adhesion and migration (Järvinen et al. 2000). The expression of TNC has been also detected under mechanical stimulation, or

exposure to appropriate growth factors, hormones, and transcription factors (Chiquet 1999; Imanaka-Yoshida and Aoki 2014). What's more, TNC is markedly expressed during the embryogenesis, and pathological process such as injury, inflammation, regeneration, and cancer (Wong, Gurtner, and Longaker 2013).

TNMD The glycoprotein tenomodulin is a type II transmembrane protein, which is predominantly expressed in ligament, tendon and eyes (Brandau et al. 2001), while less gene expression was detected in muscle, thymus, heart, liver, lunge, cartilage, and spleen (Brandau et al. 2001; Shukunami, Oshima, and Hiraki 2001). Chondromodulin-1 is the homologue of TNMD, and it mainly exists in cartilage (Shukunami, Oshima, and Hiraki 2001; Brandau et al. 2001). They share the same hydrophobic domains consisting of BRICHOS and a C-terminal cysteine-rich domain (Docheva et al. 2005).

In a tenomodulin-deficient mice model, the tenocyte proliferation was reduced at a new born stage, less tenocyte density was observed in adult tendon, the collagen fiber structure was changed, suggesting that TNMD plays a role in the regulation of tenocyte proliferation and collagen fibril alignment and organization (Docheva et al. 2005). It is reported that elongated tenocytes are usually located in thick mature collagen fibers in tendon, while oval tenocytes are randomly distributed in the interlaminar spaces. TNMD was usually detected in tendon tissue with elongated fibroblasts but not in tissue with oval tenocyte (Shukunami et al. 2006) and the expression of TNMD enhanced the periodontal ligament cell attachment (Komiyama et al. 2013), indicating that TNMD is

involved in the tendon and ligament maturation and maintenance (Shukunami et al. 2006). TNMD is also considered as a later marker of tendon/ ligament formation and is positively regulated by scleraxis (Shukunami et al. 2006).

1.3.2.2.2   Proteoglycans

Proteoglycans, located in the tensile region of ligament, belong to small leucine-rich proteoglycans (SLRPS) (Juneja and Veillette 2013), and contribute to the mechanical and viscoelastic properties of tissue (Doroski, Brink, and Temenoff 2007). Decorin is the most abundant proteoglycans found in ligament, making up approximately 90% of proteoglycans in fresh ligament (Ilic et al. 2005). Decorin contributes to the structural integrity by inhibiting the formation and organization of large collagen fibrils (J. H. Yoon and Halper 2005), thus promoting tissue to adapt to the tensile force (J. H. Yoon and Halper 2005; Ilic et al. 2005). Ectopic overexpression of decorin reduces the cell proliferation in periodontal ligament stem cell *in vitro* (Häkkinen et al. 2000).

Biglycans present at a relatively lower level than decorin in tensile region of ligament, as well as the large aggregating proteins (versican, aggrecan) (Ilic et al. 2005) . It also participates in the regulation of tissue integrity together with other proteoglycans (Juneja and Veillette 2013). Versican is the major large aggregating proteoglycan presenting in the tensile region of ligament. Their highly negatively charged glycosaminoglycanes chain develop a "bottlebrush-like" structure, which helps to attract water and acts as lubricant between collagen fibrils in ligament (Doroski, Brink,

and Temenoff 2007).

1.4 Ligament function

In musculoskeletal system, one of the main functions of ligament is to passively stabilize joints, guide joint movement within a physiological range of motion. Another function of ligament is the viscoelasticity, referring to the ability to resist shear stress and also recovery to original state, thus help to keep the joint hemostasis. Ligaments "load relax" (Figure 2 b) means that stress decrease within ligament if they are subject to constant deformations, while Creep (Figure 2a) refers to the deformation/elongation under a constant or cyclically repetitive load. An excessive creep could result in laxity of joint, thus facilitating to predispose ligament to further injury or surgery. The third function refers to joint proprioception. When ligaments are stained, they invoke neurological feedback signals then activate muscular contraction, resulting in adjust joint position sense (C. B. Frank 2004b). The function of ligament varies depending on geometry, shape of the articulating joint surfaces, location and type of insertions to bones.

1.5 Ligament biomechanics

The function of ligament tissue is mainly reflected in its mechanical properties (S. L. Woo et al. 1987; Savio L.-Y. Woo et al. 2006). These mechanical properties depend on the collagen composition, fibers orientation, and the interaction between collagen and non-collagenous matrix (Gelse, Pöschl, and Aigner 2003). Ligament exhibits a

nonlinear anisotropic mechanical behavior, which is commonly represented by a typical J-like stress-strain curve (Figure 2) (Comninou and Yannas 1976). Strain is a parameter to define the deformation per unit length of ligament, and stress is defined as the load per cross-section area of ligament. As shown in Figure 2C, a typical stress-strain curve could be divided into nonlinear toe region and a linear region, in which the slope of this region is termed as Yong's modulus and the stress is linearly proportional to the strain. A ligament with higher collagen density or larger collagen fibers results in a higher modulus.
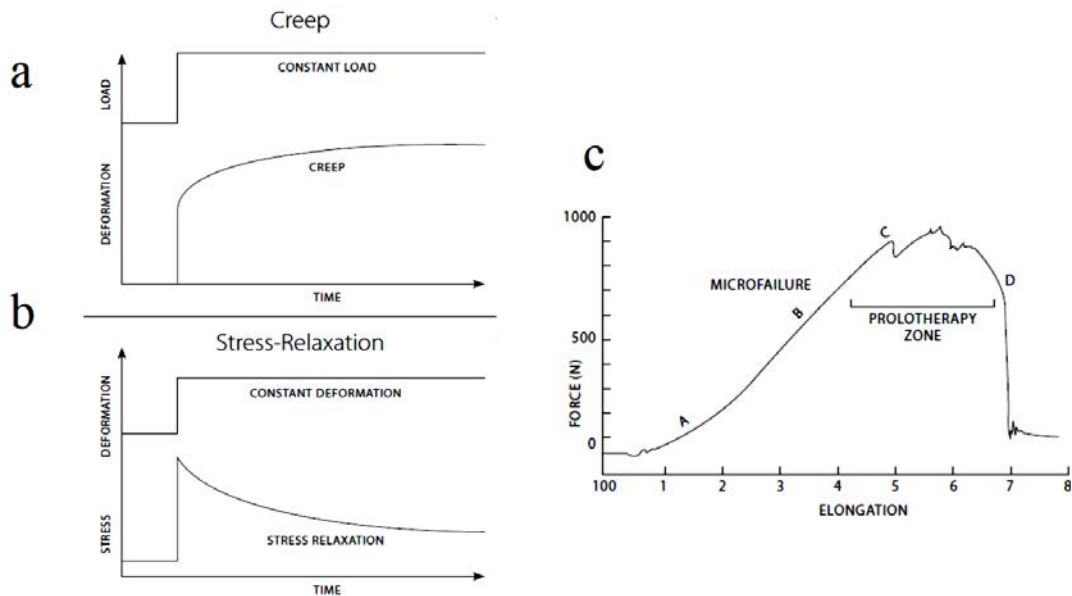
Figure 2 (a) Ligaments, when subjected to a constant stress, display creep behavior (a time-dependent increase in strain), (b)when ligaments are subjected to a constant strain, they exhibit a decrease in the stresses within the material known as stress-relaxation, (c) typical stress-strain curve for ligaments and tendons ('The Ligament Injury-Osteoarthritis Connection: The Role of Prolotherapy in Ligament Repair and the Prevention of Osteoarthritis' 2012)

The biomechanical properties of ligament are also affected by other parameters including age, anatomic location, exercises and immobilization /remobilization (C. B. Frank 2004b). For instance, the stiffness and ultimate load of ACL from young donors (ages 22-35) was reported to be 242 ± 28 N/mm and 2160 ± 157 N, which are three time higher than those of senior donors (ages 60-97) 180 ± 25 N, 658 ± 128 N respectively (Savio L.-Y. Woo et al. 1991). Studies showed that the tensile strength of rat tail tendon increased from puberty to adulthood and then stayed stable till aged (Haut

1983). Experimental exercises in rat results to enhance tensile strength of tendon with the increase of tendon weight, cross-sectional area and collagen content (S. L. Woo et al. 1980; Wren, Beaupré, and Carter 2000). Immobilization could prevent further injury by limiting movement during the early stage of healing. However, it could extend recovery time, synovial adhesions, increased collagen degradation with decreasing collagen synthesis ('Ligament Injury and Healing: An Overview of Current Clinical Concepts' 2012).

1.6 Ligament injuries

1.6.1 Epidemiology of ligament injuries

Ligament injury is among the highest incidence of musculoskeletal disorders, commonly occurring to athletes, elderly people or during accidents. In musculoskeletal system, injuries related to ACL, MCL, Posterior cruciate ligament (PCL) and Lateral collateral ligament (LCL) have been reported frequently. For instance, approximately 90% of knee injuries involves ACL and MCL injuries (Gianotti et al. 2009). Therefore, the following section is focused on these knee ligaments.

ACL is a collagenous connective tissue to anchor femur to tibia and consists of anteromedial and posterolateral bands. ACL injury is a common athletic injury and one of the most commonly treated conditions of knee. Injuries occur frequently in sports like basketball, football, skiing and soccer. It is estimated that between100,000 to 250,000 people suffer ACL injury annually in the United States (Hewett et al. 2016). It

has been reported that the injury risk is 2.4-9.7 times higher for female than male (Gornitzky et al. 2016).

MCL injury is also one of the most frequent knee injuries, especially during sports. It occurs equally for male and female, but more frequently to the aged than young people (Abbott et al. 1944). Among various sports, the ratio of the incidence of MCL injury distributes as the highest in American football (55%) (Meyers and Barnhill 2004), skiing (15% to 20%) (Paletta and Warren 1994), and rugby (29%) (Dallalana et al. 2007). What's more, the MCL may be injured in conjunction with the ACL, PCL, meniscus, bone, and/or lateral complex.

PCL plays a role in preventing posterior translation of the tibia on the femur, controlling and imparting rotational stability to the knee. It is broader and stronger than ACL with a tensile ultimate load of 2000 N (Margheritini et al. 2002). Less frequent injuries occur to PCL than ACL, and PCL injuries often occur under a force to the anterior aspect of the proximal tibia when the knee is flexed. The age- and sex-adjusted annual incidence of PCL injuries has been estimated 2 per 100,000 persons in a retrospective study (Sanders et al. 2017).

LCL is a round ligament that originates close to the lateral epicondyle and inserts onto the fibular head. LCL injuries account for 7.9% of knee injuries, and LCL constitutes therefore the least second commonly injured ligament (Swenson et al. 2013). In a 10-

year study, 48.9% of knee injuries involved LCL injuries, and in most of the cases they were associated with multiple injuries (Majewski, Susanne, and Klaus 2006).

1.6.2   Ligaments response to injury

When ligaments are exposed to excessive loading over the sustain range, tissue fails, leading to partial or complete disruptions. In this case, the body responds by a series of activities to heal injuries. The following process occurring after injury includes three phrases (Figure 3): i) the acute inflammatory phase, ii) the reparative/proliferative phase, iii) tissue remodeling phase (Savio L.-Y. Woo et al. 2006; Hauser et al. 2013). The first phase occurs immediately after injuries and lasts 48 to 72 hours (C. Frank et al. 1983; Weiss et al. 1991). Blood collects at the ligament broken end, platelet cells interact with certain matrix component and activate clots formation. Then platelet-rich fibrin clot release growth factors to promote healing process (Hauser et al. 2013). The second phase activates when immune cells begin to release growth factors and cytokines to promote fibroblasts proliferation and matrix synthesis (Col III and proteoglycans) in order to repair scare. During this stage, the formed scare tissue is quite disordered with more blood vessels, fat cells, fibroblastic, inflammatory cells and loose connective tissue. After 6 weeks, collagen becomes more aligned and Col I and Col V are formed, although the diameter of collagen fibrils is smaller than in normal tissue (Molloy, Wang, and Murrell 2003). Finally, the third phrase of healing process consists in tissue remodeling linked to collagen maturation, lasting from several months to several years. More aligned collagen and maturated collagen matrix are developed

to resemble native tissue, however critical differences in matrix structure and function persist. Major differences between newly formed tissue and native ligament include proteoglycan alternation, failure of collagen crosslink to mature, small diameter of collagen fibril, increased vascularity, abnormal innervation, and the incomplete resolution of matrix flaws (Rathbone and Cartmell 2011).

a

b

	Inflammatory	Proliferative	Remodeling
Effect on blood	Increased blood flow	Formation of new blood vessels	New blood vessels mature
Symptoms	Swelling and pain increase	Swelling and pain subside	If tissue is strong, pain subsides
Physiology	Immune cells, called macrophages, remove damaged tissue	Immune cells, called fibroblasts, form new collagen	Increased density and diameter of collagen fibers occur if healing is not hindered
Length of time	Immediate response occurs for a week	Begins at day 2 or 3 after injury and continues for 6 weeks	Continues from day 42 until 18 months after injury

Figure 3 (a) The healing process following a ligament injury, (b) characteristics of the three stages accompanying a soft tissue injury ('The Ligament Injury-Osteoarthritis Connection: The Role of Prolotherapy in Ligament Repair and the Prevention of Osteoarthritis' 2012)

In the literature, ACL and MCL injuries are the most commonly evaluated models in animal experiments. The remodeled MCL remains ultimately weaker, less stiff, and absorb less energy before failure compared to native tissue (Savio L.-Y. Woo et al. 2006; Niyibizi et al. 2000; Hauser et al. 2013). The viscoelasticity recovers to 10-20% of normal tissue, implying a more pronounced stress relaxation phenomenon in scare

tissue, therefore maintaining a load less efficiently than normal tissue (C. B. Frank 2004b).

1.6.3   Solutions for ligament repair

1.6.3.1 Surgical treatment

Conservative treatments for ligament injuries of children or adolescent were proposed by orthopedic surgeons, including brace and neuromuscular training programs (Stanitski 1995; Frosch et al. 2010). However, these nonoperative treatments are not sufficient for pediatric athletes or severe rupture, and may lead to additional instability episodes, meniscal tears, articular cartilage damage, and early-onset arthritis (Graf et al. 1992; Guzzanti 2003; Lawrence, Argawal, and Ganley 2011). Therefore, a surgical operation including grafts transplantations constitutes a main approach to recovery injured ligament at present.

Grafts for surgical treatment include autografts, allografts and artificial grafts. For instance, ligamentoplasty is a surgical intervention for knee treatment, usually for ACL and PCL injuries, as well as resulting in significant improvement of ligament function for the patients (Texier et al. 2002). The principal technique consists the replacement of impaired ligament with grafts commonly taken from hamstring tendon, patellar tendon, fascia lata or quadriceps derived from patients or donors (Hardy et al. 2017). Patellar tendon constitutes a commonly used graft for ACL repair because of its excellent mechanical properties resembling ACL. The procedure of ligamentoplasty includes the

following steps: i) harvest of a tendon graft, ii) pretreatment by examination of the interior of a joint with a fiber optic arthroscope, iii) establishment of bony tunnels, iv) implantation of the graft and fixation with strips. Surgeries facilitate the increase in knee stability and movement, but clinical complications including donor site morbidity, or limitation of donors may be associated with these techniques (Biau et al. 2009 ; S. Li et al. 2012 ; Hardy et al. 2017 ; S. Li et al. 2012). In addition to these grafts, artificial grafts including Gortex prothesis, the Stryker-Dacon ligament, the Leeds keio artificial ligament, and LARS ligaments have also been used. However, creeping, graft fatigue and limited interaction between graft and host have been observed several years after implantation (Rathbone and Cartmell 2011). The advantages and disadvantages of three types of graft have been summarized and listed in Table 2.

Table 2 The advantage and disadvantage of various types of graft (Rathbone and Cartmell 2011)

	Autograft	Allograft	Artifical graft
Advantages	No rejection No disease transmission No donor scarcity	No donor site morbidity	No donor site morbidity No disease transmission No donor scarcity
Disadvantages	Donor site morbidity Patellar fracture Quadriceps weakness Limited bone integration Mismatch in different tissue properties, causing mechanical failure, creeping, fatigue Recurring injury	Donor scarcity Limited bone integration Tissue rejection Mismatch in different tissue properties, causing mechanical failure, creeping, fatigue Recurring injury	Limited bone integration (weak graft-host tissue interface) Mismatch in different tissue properties, causing mechanical failure, fatigue Creeping(strentching & loosening) Poor long-term instability Fatigue Recurring injury

1.6.3.2 Gene therapy

Gene therapy offers a novel approach for ligament/tendon repair. The introduction of marker genes or therapeutic genes using vectors has been reportedly for ligament healing, and also been used to manipulate the healing environment. Early assays were performed and confirmed the possibility of genes transfer to ligament both *in vivo* and *in vitro* (Kevin A. Hildebrand et al. 1999; Gerich et al. 1996; K. A. Hildebrand, Frank, and Hart 2004). ACL and MCL injuries constitute two classical models to evaluate the feasibility of gene therapy, and a series of issues including the method of vector delivery, either viral or liposomal and the effect of therapeutic genes on the ligament properties are needed to be considered (K. A. Hildebrand, Frank, and Hart 2004). Delivery methods include direct injection of adenovirus in site, direct injection of transduced cells with a BAG retrovirus (K. A. Hildebrand, Frank, and Hart 2004; Kevin A. Hildebrand et al. 1999), intra-articular injection and intra-arterial injection of vectors (N. Nakamura, Timmermann, et al. 1998). Direct injection of vector was reported to be more efficient with longer gene expression *in vivo* (Kevin A. Hildebrand et al. 1999; Menetrey et al. 1999). Nakamura et al firstly reported *in vivo* application of gene therapy based on antisense decorin oligodeoxynucleotides to improve collagen fibrillogenesis during ligament repair process (Norimasa Nakamura et al. 2000). With gene intervention technology, growth factors like Insulin-like growth factor-I (IGF-1), PDGF, and BMP-12 have been reported to be successfully introduced and expressed in ACL and MCL tissues (Yilgor, Yilgor Huri, and Huri 2012). IGF-1 was transferred into

ACL fibroblast and was reported to increase the gel cellularity, promote Col I, Col III, elastin, TNC and vimentin expression to enhance ACL ligament reconstruction (Steinert et al. 2008). PDGF-B was injected directly into the injured patellar ligament, resulting in an enhanced angiogenesis and matrix deposition in wound site (N. Nakamura, Shino, et al. 1998). BMP-12 transferred into mesenchymal progenitor cell promoted tendon-like tissue formation (Lou et al. 1999); BMP-12 transferred chicken tendon cells increased collagen deposition, and resulted in a two-fold increase of tensile strength and stiffness of repaired tendon (Lou et al. 2001). Based on the literature, ligament healing could be manipulated with gene therapy, however, *in vivo* consequences could be more complex than *in vitro*, since one factor modified could have several negative effects on other biological processes. Therefore, more researches need to be done to further study the security of gene therapy for clinical application.

1.6.3.3 Tissue engineering

Recently, tissue engineering has become a novel potential approach to repair or restore ligament tissue (Laurencin and Freeman 2005; Yilgor, Yilgor Huri, and Huri 2012). It refers to a combination of biological, chemical, and engineering knowledge towards the development of substitutes in regenerative medicine (Laurencin and Freeman 2005). Three main elements of tissue engineering include (i) the proposition of a suitable scaffold, (ii) the selection of cell source and (iii) the providing of biochemical/mechanical stimulation (Ge et al. 2006; Tischer et al. 2007). Current advances in these three milestones, constituting the core of the present work, will be

discussed in detail in the following sections.

1.7 Ligament tissue engineering

1.7.1   Requirements for defining scaffolds for ligament tissue engineering

Various kinds of scaffolds have been reported in literature, and may be classified into biological scaffolds (decellularized allograft tissue, protein-based extracellular matrix), natural polymer-based scaffolds (silk, collagen, fibrin or their composite), and synthetic scaffolds (PGA, PLA) (Ge et al. 2006). A suitable scaffold should be biodegradable, biocompatible, processable, and biofunctional (Yang et al. 2001; Yilgor, Yilgor Huri, and Huri 2012). It should also bear the physiological loads or deformations prescribed to the native tissues, and be easy to handle, store and sterilize. Methods to fabricate scaffolds for ligament tissue engineering mainly include braiding, weaving, electrospinning, and freeze-drying (Ge et al. 2006; C. Laurent et al. 2018). Scaffolds in the shape of sponges (H. Liu et al. 2008), nanofiber networks (Rothrauff et al. 2017), knitted fibers (Peh et al. 2007), meshes (Tang et al. 2018), hydrogels (Stoppato, Flotow, and Kuo 2016), and wired yarns (Naghashzargar et al. 2014) have already been reported to mimic ligament in tissue engineering. Despite the benefits of these scaffolds, they also suffer from some drawbacks, such as insufficient mechanical properties, brittle behavior, or lack of functional groups for molecular signaling. In the following sections, the available constitutive biomaterials of scaffolds as well as some mainly reported structures will be detailed.

1.7.2   Biomaterial resources

The selection of biomaterials to enhance or replace impaired tissue has been guided by the willingness to mimic native tissue or to promote new tissue development. The main available materials for ligament tissue engineering could be distinguished into natural-based scaffold, synthetic polymers and decellularized scaffolds (Ge et al. 2006).

1.7.2.1   Natural-based scaffolds

Natural polymers can be classified into proteins (collagen, silk, gelatin, fibrinogen, elastin), polysaccharides (cellulose, amylose, chitin, dextran, glycosaminoglycan starch, chitosan, alginate, hydronic acid) and polynucleotides (DNA, RNA) (Kuo, Marturano, and Tuan 2010; Ge et al. 2006). They possess more biological recognition for cell attachment, better biocompatibility and processing compared to synthetic polymers (Whitlock et al. 2007).

Obviously, the most direct candidate is collagen since it is the main composition of ligament ECM. Additionally, collagen shows a good biocompatibility, low immunogenicity, permeability, and the ability to regulate cell morphology, adhesion, migration and differentiation (Chevallay and Herbage 2000). Unfortunately, the mechanical properties of pure collagen gel can not reach the mechanical requirement of ligament/tendon tissue, therefore limit its application for ligament/tendon tissue engineering (Dong and Lv 2016). Efforts have been made to improve the mechanical properties of collagen gel, such as cross-linking modification, but the introduction of

chemical agents could have a negative effect on cells interactions. Moreover, collagen composites have been investigated to enhance mechanical properties for collagen. For instance, silk (X. Chen et al. 2008; Shen et al. 2012), PLGA fibers (Guoping Chen et al. 2003), polyurethane (Sharifi-Aghdam et al. 2017) and PLA (Dunn et al. 1997) have been reported to enhance collagen and showed improved mechanical properties for ligament tissue engineering. Collagen modified with glycosaminoglycan showed increased mechanical strength adapted to native tendon/ligament tissue and also demonstrated the capacity to promote cell attachment and proliferation for tendon tissue engineering (Caliari, Ramirez, and Harley 2011). Collagen was also reported to be polymerized with the di-catechol nordihydroguaiaretic acid (NDGA) resulting in satisfying mechanical properties, but no biological results was reported (Koob and Hernandez 2002).

Silk is a natural protein fiber, mainly secreted and spun into fiber by silkworm, spider, mites, files and scorpions (Kaplan et al.1994; Altman et al. 2003). It mainly consists of fibroin and sericin (MacIntosh et al. 2008). Silk has been widely used as a promising biomaterial for ligament tissue engineering because of the excellent mechanical properties and biocompatibility.

Indeed, Altman et al (Altman, Horan, et al. 2002) has firstly demonstrated that silk matrix supported cell attachment, expression of TNC, and furthermore proved that the mechanical stimulation could also enhance the ligament differentiation. Numerous silk-

based composites (incorporating collagen, polyurethane, PLGA, RADA16, gelatin, etc.) have been designed for ligament tissue engineering (D. Ma, Wang, and Dai 2018). In the past decades, Ouyang et al (Shen et al. 2014, 2012; X. Chen et al. 2008, 200) had developed a series of knitted silk-collagen sponges and demonstrated their positive effect on musculoskeletal regeneration, including ACL (Shen et al. 2014), Achilles tendon (Shen et al. 2012), MCL (X. Chen et al. 2008) and rotator cuff (Shen et al. 2012). Based on these studies, it may be concluded that this silk/collagen sponges promote ligament healing with more collagen synthesis, increased mechanical properties, more native microstructure regeneration, and the potential to prevent osteoarthritis in the long-term regeneration. However, silk is classified as non-degradable biomaterial by FDA (Ethicon 2000), as no obvious degradation was observed after 18 months post-implantation (Shen et al. 2014). This is one of the points that has been considered to improve in the present study.

1.7.2.2   Synthetic polymeric scaffolds

The advantages of synthetic polymers applied as biomedical constructs are mainly due to their high processability to reach a broad requirement of mechanical properties and degradability. Synthetic prosthetic devices such as polyester polyethylene terephthalate (PET) and polytetrafluoroethylene (PTFE) have been investigated as ligament/tendon tissue substitutes due to their suitable mechanical properties and biologically inert nature (Gao et al. 2010; Paulos et al. 1992; Longo et al. 2010). However, clinical results of these artificial grafts have been associated with graft failure, poor durability, poor

tissue integration, and foreign body synovitis (Glezos et al. 2012). Commonly reported synthetic polymers in literature for ligament tissue engineering include polyesters for instance polylactic acid (PLA) (Ouyang et al. 2002), poly-caprolactone (PCL) (Barber and Click 1992), poly (DL-lactide-co-glycolide) (PLGA) (Ouyang et al. 2002), poly(L-lacticacid) (PLLA) (Lu et al. 2005). An early study concerning cell adhesion and proliferation on various polymers presented that both bMSCs and ACL fibroblasts showed better attachment and proliferation on PLGA (50:50, 75:25) films (Ouyang et al. 2002). Porcine bone marrow stromal cells showed a better cell proliferation and higher expression of Col I, decorin, and biglycan genes on a composite scaffold based on electrospinning PLGA with knitted PLGA than on a knitted PLGA/fibroin scaffold (Sahoo et al. 2006). A braided PLGA scaffold has been showed to result in a strong mechanical strength up to 400 N (Cooper et al. 2005), and PLGA-fibronectin (fn) composites promoted cell attachment and matrix synthesis for ligament tissue engineering (Lu et al. 2005).

1.7.2.3 Decellularized scaffolds

Decellularization is a technique to remove cells from tissue by using detergent, enzyme, or physical methods. Decellularized ECM from intact tissue offers numerous advantages compared to biological-inspired artificial tissues, and has showed a great potential for ligament (Whitlock et al. 2007; Zantop et al. 2006)/ tendon regeneration (S. Wang et al. 2017).

Decellularized ECM from porcine small intestinal submucosa (SIS) and urinary bladder membrane (UBM) have been frequently applied for ligament tissue engineering. RestoreTM, CuffPatchTM, Tissue-MendTM, and PermacolTM are the common commercial products derived from SIS (Zantop et al. 2006). SIS mainly consists of collagen (approximately 90% of dry weight), growth factors and cytokines such as fibroblast growth factor (FGF), transforming growth factor-beta1(TGF-β1), vascular endothelial growth factor (VEGF) (Badylak 1997; Hodde et al. 2001). These bioactive molecules retain most bioactivity during the scaffold processing for clinical application and are beneficial to promote cell migration to scaffold (Savio L.-Y. Woo et al. 2006). The decellularized ECM continues to transmit the mechanical signal to host cells. SIS is a resorbable scaffold and about 40-60% of decellularized ECM scaffold is replaced by new forming ECM within 4 weeks and totally replaced by 3 months after surgery (Zantop et al. 2006). SIS also showed the potential to promote the healing process of MCL with a gap injury in a rabbit model, resulting in improved mechanical properties, histological appearance, and collagen type V/I ratio adapted to normal MCL (Guoping Chen et al. 2003). Moreover, during a long-term study on the effect of SIS on MCL healing, results showed improved mechanical properties, biochemical properties and histological appearance at 26 weeks. A layer SIS could serve to direct neo-ligament formation by inducing better organization and limiting cross-sectional growth of MCL healing (Liang et al. 2006). What's more, further researches need to be done to have a better understanding of the biochemical, cellular and mechanical mechanisms that stimulate the constructive remodeling response.

1.7.3   Scaffold design

A suitable scaffold should mimic the structure and mechanical properties of native tissue. The crosstalk between cells and scaffolds is influenced by the scaffold architecture, mechanical properties and biochemical properties. Mechanical properties are also influenced by material source, structure and porosity of scaffold. In the following sections, the main scaffold structures reported as ligament-tissue constructs that have been proposed are briefly described and compared. Here are examples of scaffold fabricated with various methods for ligament/ tendon regeneration (Figure 4).
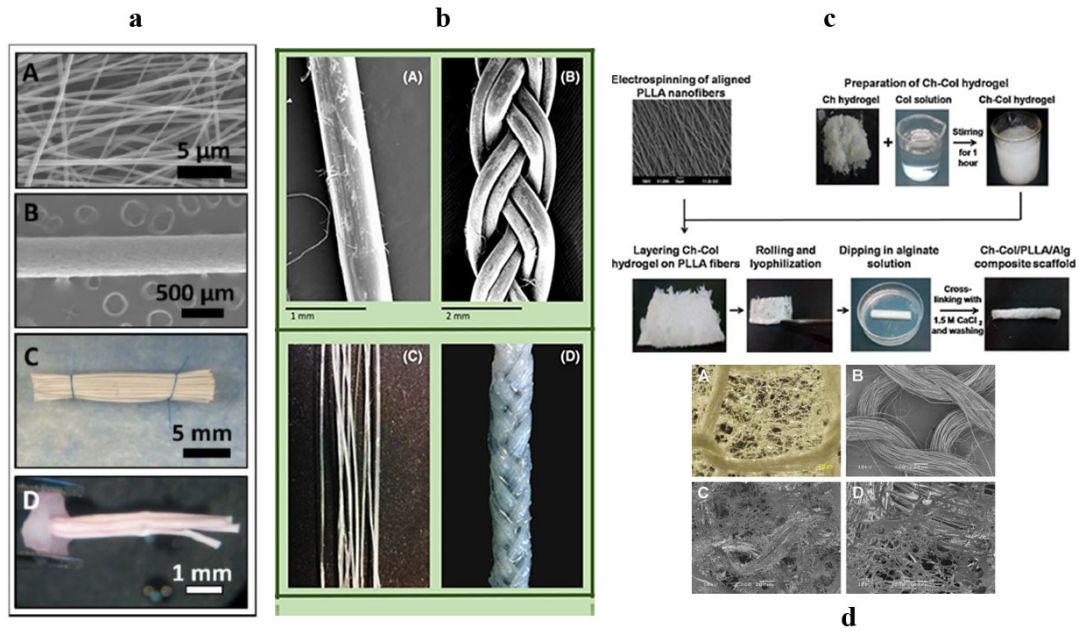
Figure 4 Examples of scaffolds fabricated with various methods for ligament tissue engineering. (a) structured electrospun scaffold (Pauly et al. 2017, 201), (b) silkworm gut fiber braided scaffold (Pagán et al. 2019), (c) Layered chitosan-collagen hydrogel/aligned PLLA nanofiber construct (Deepthi et al. 2016), (d) combined knitted silk scaffold and microporous silk sponge (H. Liu et al. 2008).

1.7.3.1 Hydrogel scaffolds

Hydrogels are three-dimensional networks crosslinked with covalent or noncovalent bonds. The network structure of hydrogel has been proposed to mimic the macromolecular based component in the body. Hydrogel present a rather viscoelastic behavior since water takes account 90-98% of its weight. Hydrogels are favorable for cell migration, nutrient delivery, and angiogenesis (Peppas et al. 2006; Burdick and Prestwich 2011), and they showed potentials to be used for cartilage/bone healing,

wound dress, and drug/bioactive molecular (Baumann et al. 2009; Budama-Kilinc et al. 2017).

A Col I hydrogel has been reported to enhance ligament-specific protein and gene expression by hMSC, while the mechanical strength was too weak to be transplanted *in vivo* (Nöth et al. 2005). A collagen–platelet rich plasma (PRP) hydrogel was reported to enhance primary healing of ACL injury, and results showed significant improvements in load at yield, maximum load, and linear stiffness after 4 weeks compared to intact ACLs suture (Murray et al. 2007). A hydrogel-fibrous composite based on PLLA fibers and polyethylene glycol diacrylate (PEGDA) hydrogel has also been proposed for ACL replacement, and 10% hydrogel-composite showed a similar mechanical behavior as natural ligament, as well as the promotion of fibroblasts growth (Freeman et al. 2011).

1.7.3.2   Braided scaffolds

Braiding is a textile manufacturing process used to make fabrics through intertwining of yarns in a diagonally overlappering manner (Rana and Fangueiro 2015). Braided scaffolds are often characterized by high porosity for cell migration, tissue ingrowth, nutrient diffusion and gas exchange. It has been reported that factors (polymer composition, braided angle, fiber number, fiber diameter) of braided scaffold have an effect on cell behavior. A series of polymers (polyglycolic acid (PGA), poly-L-lactic acid (PLLA), and polylactic-co-glycolic acid 82:18 (PLAGA) have been examined to fabricate braided scaffold for ACL reconstruction, possibly modified with fibronectin

(Lu et al. 2005). Results demonstrated that PLLA based scaffold showed excellent mechanical properties, increased cell attachment and long-term matrix synthesis, thus indicating a strong potential to be used for ACL regeneration (Lu et al. 2005). Scaffold braided with large angle enhanced hiPSC-MSC tenogenic differentiation and showed a spindle shape compared to scaffolds braided with small angles (Czaplewski et al. 2014). A braided scaffold of Col-I/PVA blend fibers was designed for ACL reconstruction in a mini pig model, and it showed good cytobiocompatibility, ligament-specific matrix expression, and the mechanical strength reached 75% of native tissue (Cai et al. 2013). Recently, in our research group, a multi-layer braided PLCL scaffold has been proposed and characterized with satisfying morphological (C. P. Laurent et al. 2011) and mechanical (C. P. Laurent et al. 2012) properties towards ligament tissue engineering.

1.7.3.3 Porous scaffolds

Scaffolds on the form of sponge/foam or meshes possess high porous architecture, which could promote cell interaction, neo-tissue growth, nutrients exchange, and vascularization. A combined knitted silk scaffold and microporous silk sponge was reported to promote hMSC proliferation, function and ligament related-ECM expression (H. Liu et al. 2008). Furthermore, results from *in vivo* implantation into a rabbit model showed that this MSCs/scaffold promoted abundant ligament ECM expression (collagen I, collagen III, and TNC), regeneration of ligament-bone insertion with typical four zones (bone, mineralized fibrocartilage, fibrocartilage, and ligament) and satisfying tensile strength (Fan et al. 2008). A porous PLGA-collagen hybrid mesh

has also been investigated and showed inspiring potentials for ACL tissue engineering. Results showed that a collagen sponge with suitable pore size and increased surface area promoted cell attachment, proliferation and cell ingrowth, while the combination with PLGA improved mechanical strength of collagen scaffold to prevent it from collapse during manipulation and tissue formation (Guoping Chen et al. 2004).

1.7.3.4 Electrospun scaffolds

Fibrous scaffolds have been developed to mimic the native architecture of human tissue and provide a stable structure for cell attachment. Electrospun fibrous scaffold consist of closed-packed fibers and formed interconnecting porous structure. Electrospinning is a fiber manufacturing technology by using electrostatic force where fibers are made from polymer solution. Various parameters links to the properties of electrospun fibers, such as the polymer component, solvent concentration, the form of the collector, conductivity, and displacement (static or rotational) (Z. Li and Wang 2013). The frequent materials used in electrospinning techniques for ligament/tendon engineering include silk, PLLA (Deepthi et al. 2016) (Yin et al. 2010), PLCL (Vaquette et al. 2010), PLGA(Sahoo, Toh, and Goh 2010), PCL(Pauly et al. 2016) and some of their composites (Sahoo, Toh, and Goh 2010).

Fibrous structures obtained by electrospinning are versatile and may take the form of randomly oriented/ aligned structure or two/three-dimensional structures, and the fibers diameter may range from nanoscale to microscale (Erisken et al. 2013). It has been

reported that in a microscale level (small<1 μm, medium (1-2 μm), large >2 μm), the diameter had a more significant effect than alignment on the stem cell proliferation and ligamentous ECM synthesis (Cardwell, Dahlgren, and Goldstein 2014). Compared with randomly oriented nanofibers, aligned nanofibers improved cell attachment, integrin expression, and matrix deposition and increased mechanical properties to mimic native tissue (Moffat et al. 2009; Yin et al. 2010).The pore size depends on the diameter of fibers, which could have an effect on cell infiltration (Jun et al. 2018). The effects of nanofibers and microfibers on the cell behaviors were compared for ligament tissue engineering. Results demonstrated that nanofibers resembled injured tissue and potentially facilitate the repair process, since they promoted cell proliferation as well as total collagen and proteoglycans synthesis. Microfibers represented healthy tissue and stimulated more specific ligament/tendon ECM expression such as Col I, Col III, Col V and TNC (Erisken et al. 2013). While such characteristics of electrospinning are interesting for tissue engineering applications, and due to the micrometer-size of the obtained fibers, its capacity to form 3D structures with a controllable network of large pores and a sufficient mechanical response is still limiting its applications compared to the previously mentioned fabrication methods (P. X. Ma 2004; Barnes et al. 2007).

1.7.4   Cell sources for ligament tissue engineering

An appropriate type of cell sources for ligament tissue engineering or cell-based therapies should possess robust proliferation and strong potential to synthesize organized ECM, which could meet the biological and mechanical requirements

resembling native tissue. In the past decades, fibroblasts and stem cells are the two main cell sources that have been reported in literature for ligament regeneration. The advantages and disadvantages of these two cell sources will be discussed in the following sections.

1.7.4.1 Fibroblasts as a cell source for ligament tissue engineering

Early investigation focused on fibroblasts as the first candidate, given that fibroblasts are the major cells in ligament tissue and possess the phenotypic characteristics towards ligament formation. Cooper et al (Cooper et al. 2006) evaluated the potential of fibroblasts from ACL, MCL, AT, and PT of rabbit as a cell source on 3D PLLA braided scaffolds towards ligament tissue engineering. Cell morphology, proliferation ability and ligamentous gene expression have been evaluated and results suggested that ACL fibroblasts were the most relevant cells for ligament regeneration with the highest ligament-related gene expression. Brune et al (Brune et al. 2007) compared fibroblasts extracted from intact ACL and ruptured ACL on SIS-ECM for ACL regeneration. Both fibroblasts showed similar cell behavior, connective tissue organization and composition, which was concluded that they were both adapted to an application as autologous reparative fibroblasts from ruptured ACL.

Dermal fibroblasts are another accessible fibroblasts that have been reported for ACL regeneration (W. Liu et al. 2006). It is associated with an easy, efficient, cost-effective process to harvest dermal fibroblasts from native tissue through a skin biopsy

(Rodrigues, Reis, and Gomes 2013). Autogenous dermal fibroblasts were injected into allogenous acellularized tendon and showed good cell integration and mechanical strength comparable to native tissue (Tischer et al. 2007). The synovial membrane that surrounds PCL would also be a possible cell source especially for ACL reconstruction. Synovial cells play a role to promote the healing process in an untreated injury by migration and colonization in the injury site (Messenger et al. 2010). Even though some inspiring results have been achieved, fibroblasts are limited by their cell differentiation capacity and cell quantity.

1.7.4.2 Stem cells as a cell source for ligament tissue engineering

Recently, stem cells have been applied for tissue repair and gained an increasing interest in bone, cartilage, cardiovascular and ligament/tendon regeneration. Stem cells are supposed to be a promising cell source for ligament regeneration because of their cell availability, rapid proliferation rate, and differentiation capacities.

Stem cells can be classified into embryonic stem cells and adult stem cells. Embryonic stem cells are obtained from the blastocytes, which possess an unlimited self-renewal ability and can be differentiated to all types of organisms. Adult stem cells are derived from tissues of endodermal, mesodermal or ectodermal lineages, such as hematopoietic stem cells. They may also be obtained from the stroma of other mesodermal tissues such as bone marrow, muscle, adipose tissue, synovium, and periosteum.

1.7.4.2.1 Mesenchymal stem cells (MSCs)

In 1976, Friedenstein and colleagues firstly found that adherent cells in bone marrow (BM) could differentiate towards fibroblasts, bone or cartilage after discarding most of nonadherent hematopoietic cells (Alexander J. Friedenstein 1976). Since then, attempts have been made to study their biological properties and applications for regeneration medicine. Classical methods have been reported, including Colony forming unit-fibroblast (CFU-F), multilineage differentiation potentials and phenotypic expression.

1.7.4.2.2 Characterization of MSCs

CFU-F is one of the primary characteristics to identify MSCs, together with the self-renew ability to generate identical copies of themselves, or multilineage differentiations into bone, cartilage and adipose tissue (Figure 5). Phenotypically, there is no identical mark specific to MSCs. They are reported not to express hematopoietic markers (CD45, CD34, CD14, or CD11) *in vitro*, costimulatory molecules (CD80, CD86, or CD40) or the adhesion molecules (CD31, CD18, or CD56). What's more, they can express markers CD105 (SH2), CD73 (SH3/4), CD44, CD90, CD71, and Stro-1 as well as the adhesion molecules (CD106, CD166), intercellular adhesion molecule ((ICAM)-1, CD29).
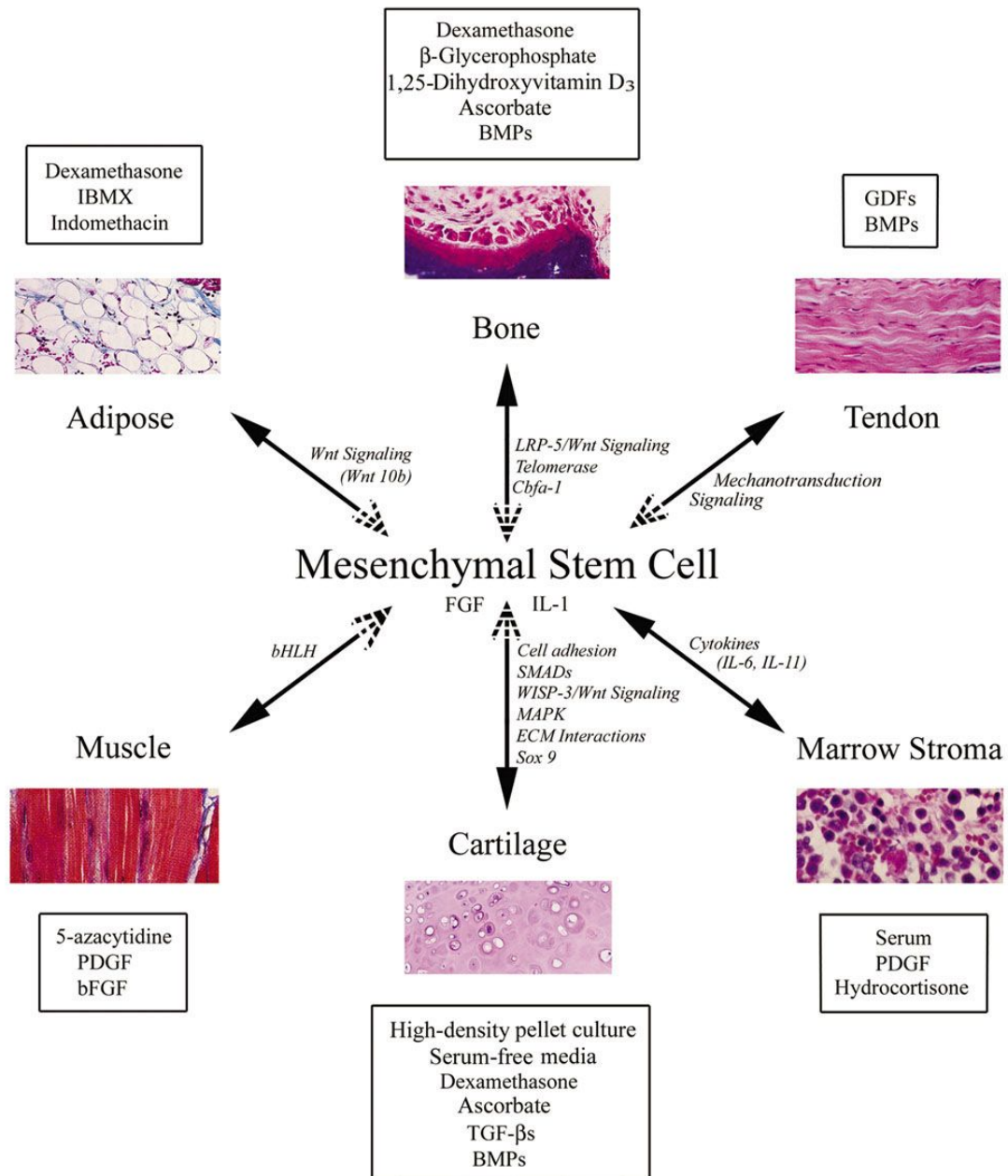
Figure 5 Lineage potential of adult human MSCs (Tuan, Boland, and Tuli 2002)

1.7.4.2.3   MSCs application towards tissue regeneration

MSCs have gained increasing interest for tissue engineering, especially because of their

self-renew and multi-potential differentiation abilities. MSCs could be harvested from

various adult tissues such as peripheral blood, BM, adipose tissue, Wharton's jelly (WJ),

periodontal ligament (PDL), and muscle connective tissue. Sakaguchi et al compared

the properties of MSCs derived from 5 different tissues of 8 donors. It has been shown

that BM-MSCs had better colony-forming ability. Synovium-derived MSCs held better

chondrogenesis and adipogenesis abilities, while adipose-derived MSCs (ADMSCs)

also presented adipogenic potential, and synovium and periosteum-derived MSCs

demonstrated better osteogenic potential (Sakaguchi et al. 2005). In a rat model,

Yoshimura et al (Yoshimura et al. 2007) demonstrated that MSCs from synovium

exhibited the best colony-forming ability, fold increased growth kinetics,

chondrogenesis as well as adipogenicity. ADMSCs showed superior adipogenic

potential, while periosteum and muscle derived MSCs had better osteogenic potential.

In this report, MSCs from solid tissue held better proliferation and differentiation

properties than BM-MSCs. It has been also concluded that the paracrine actions of

MSCs (chemoattraction, angiogenesis, anti-apoptosis, immunomodulation, anti-

scarring) have a greatly therapeutic effect on tissue regeneration (da Silva Meirelles et

al. 2009; Singer and Caplan 2011).

1.7.4.2.3.1   BM-MSCs

There are two kinds of stem cells in BM, including hematopoietic stem cell and MSCs

(S Dhinsa, N Mahapatra, and S Khan 2015). BM-MSCs were the first MSCs initially

discovered by Friedenstein and his colleagues in 1976 (Mafi et al. 2011). MSCs

accounts for a small proportion of bone marrow cells, representing 1/10000 to 1/100000

of nucleated cells in aspirates (Bernardo, Locatelli, and Fibbe 2009). BM-MSCs have

been demonstrated to be capable to form colonies (CFU-F), differentiate into multi-lineages (osteoblasts, adipocytes, and chondrocytes) and hold MSCs typical phenotype (Mafi et al. 2011).

Numerous reports have demonstrated the therapeutic potential of BM-MSCs for tissue repair in various disease models (Phinney and Prockop 2007). BM-MSCs have been investigated to promote healing of tissue injuries by secreting bioactive moleculars like cytokines and adhesion molecules to alter microenvironment rather than MSCs transdifferentiation (Prockop 1997). Further researches investigated the MSCs mechanism of angiogenesis, bone development, vasculogenesis and hematopoiesis (Mafi et al. 2011).

Van Eijk et al reported that BM-MSCs were the best candidate for ACL tissue reconstruction compared with fibroblasts from ACL tissue and skin, regarding to better cell proliferation and collagen production (Van Eijk et al. 2004). In parallel, BM-MSCs and fibroblasts from ACL and MCL tissues have been evaluated for ligament tissue engineering (Ge, Goh, and Lee 2005). Results showed that BM-MSCs tended to be a predominant candidate due to their higher cell proliferation and enhanced collagen secretion capacity. What's more, BM-MSCs could survive for more than 6 weeks in knee joints. It has been also reported that BM-MSCs enhanced ACL regeneration on hamstring tendon autografts in rabbits. Large areas of chondrocytes on the tendon-bone joint were detected at 2 weeks, and a mature zone of cartilage at 8 weeks (Lim et al.

2004). BM-MSCs was evaluated to proliferate profusely on silk scaffold and express fibroblast-like gene in mRNA level *in vitro*. Within a MSCs-seeded scaffold transplanted in a pig model for ACL regeneration, MSCs exhibited fibroblast morphology, expressed ligament-specific matrix, and resulted in an indirect ligament-bone insertion with three zones (bone, Sharpey's fibers, and ligament) at 24 weeks (Fan et al. 2009).

1.7.4.2.3.2   WJ-MSCs

WJ-MSCs are isolated from umbilical cord and have been considered as a promising cell source for regenerative medicine. It possess numerous advantages such as ease of access, low-cost, no donor site morbidity, non-conventroversially ethical issue, immune compatibility and multipotential differentiation (L. Wang et al. 2011). WJ-MSCs had been widely applied for musculoskeletal tissue engineering and showed promising results in bone (Bailey et al. 2007; Baksh, Yao, and Tuan 2007; Sarugaser et al. 2005), cartilage (Bailey et al. 2007; Baksh, Yao, and Tuan 2007; Frank Barry et al. 2001) and muscle tissue engineering (Kocaefe et al. 2010; Vieira et al. 2010). However, only a few studies were performed for ligament/tendon tissue engineering application. Kang et al evaluated the differentiation potential of WJ-MSCs into ligament-like cells under mechanical stimulation (10% strain) and supplied with different mediums (M-DMEM, A-DMEM and DMEM). After 10 days, WJ-MSCs in M-DMEM medium presented elongated ligament-like cell morphology, increased metabolic ability, and ligament-specific gene expression (Col III, α-smooth muscle actin, and TNC) in protein and

mRNA levels, indicating the potentials towards ligament regeneration (Kang et al. 2012).

1.7.4.2.3.3 Adipose derived mesenchymal stem cells (ADMSCs)

Adipose tissue is also an abundant source of adult MSC, which also exhibit self-renew ability, plasticity and multilineage differentiation potential ability. Due to its abundant sources and easy accessibility for cell harvesting, ADMSCs has become an attractive cell source as alternative to BM-MSCs for regenerative medicine (Sterodimas et al. 2010). ADMSCs were seeded on 3D polycaprolactone fumarate (PCLF) and showed increased cell proliferation and expression of a ligamentous matrix (collagen and TNC) by the stimulation of platelet lysate and FGF-2 (E. R. Wagner et al. 2015). The suitability of ADMSCs for ACL tissue engineering under the growth factor treatment was investigated. Results showed that the expressions of Col I, Col III and TNC were increased when exposed to growth factors EGF and bFGF; while no significant difference was observed with TGF-β1 or IGF-1 at 4 weeks (Eagan et al. 2012).

1.7.4.2.3.4 PDL-MSCs

Periodontal ligament is a specialized connective tissue aimed at connecting cementum and alveolar bone to support teeth and maintain the homeostasis. PDL-MSCs were first discovered by Seo et al in 2004 (Seo et al. 2004). It was reported that PDL-MSCs hold better proliferation ability than BM-MSCs: the population doubling of BM-MSCs is 50, while population doubling of PDL-MSC is over 100 (Shi et al. 2005). Previous studies

revealed that PDL-MSCs possessed capacities to differentiate into osteoblast/cementoblast-like cells, osteogenic, adipogenic chondrogenic, neurogenic and angiogenic cells (Seo et al. 2004; Jinping Xu et al. 2008).

The application of PDL-MSCs for regenerative medicine was firstly reported for cementum/PDL-like tissue regeneration (Seo et al. 2004). PDL-MSCs were reported to possess greater potential for tendon regeneration than BM-MSCs and gingival MSCs (GMSCs) *in vivo* and *in vitro* (Moshaverinia et al. 2014). Results from the subcutaneous transplantation of PDL-MSCs encapsulated in TGF-β3-loaded RGD-coupled alginate microspheres into immunocompromised mice showed that PDL-MSCs expressed higher mRNA level of tendon-related gene expression (Scx, Dcn, TNMD, and Bgy) than BM-MSCs after 4 weeks, and *in vivo* histological examination showed the increased expression of tendon-related protein (Moshaverinia et al. 2014). PDL-MSCs exhibited better healing effect on tendon defect than Achilles tendon-derived cells (AT) with similar morphology as AT, advanced tissue maturation, less ectopic fibrocartilage formation, more organized collagen synthesis, and tendon specific matrix expression at 16 weeks after surgery. Thus, it confirmed the feasibility of PDL-MSCs application for tendon/ligament regeneration (Hsieh et al. 2016). Among these promising cell sources for regenerative medicine, WJ-MSCs and BM-MSCs were selected as cell sources for research because of its easy processability and stable donner supply since our lab had a collaboration with CHRU Hospital Nancy.

1.8 Biomechanical/Biochemical stimulation

Ligament reconstruction is a sophisticated and highly-regulated process. In the process of tissue engineering, once an appropriate scaffold and cell source have been selected, tissue regeneration may point to supply biochemical and/or mechanical stimuli to promote ECM synthesis. For the biochemical stimulation, growth factors may be considered to promote tissue regeneration such as Insulin-like Growth Factor-I (IL-1), Vascular Endothelial Growth Factor (VEGF), Platelet-derived Growth Factor (PDGF), basic Fibroblast Growth Factor (bFGF), Transforming Growth Factor-β (TGF-β), and Growth Differentiation Factor 5 (GDF-5). Recently, platelet lysate (PL) consisting in a cocktail of growth factors has gained increased attractions for biomedical and clinical application. For the mechanical stimulation, the item *bioreactor* has been designed to support a mechanical stimulation environment and basically encourage the cells to proliferate and differentiation on the scaffold. These different solutions for providing biochemical and biomechanical stimuli will be detailed in the following sections.

1.8.1   Biochemical stimulation

1.8.1.1 IL-1

IL-1 is a single chain polypeptide with 70 amino acids, which showed the homogenous structure to proinsulin, and it is referred in different processes, such as cell proliferation, migration and nervous system development *in vitro*, as well as metabolic effects and growth effects *in vivo* (Humbel 1990).

IL-1 has been detected in normal and wounded MCL tissues and been demonstrated to facilitate the healing process, especially in early inflammation and also proliferative stages (Sciore, Boykiw, and Hart 1998). IL-1 was reported to reduce functional deficit and accelerate Achilles tendon recovery in a rat model, and it was possible via anti-inflammatory mechanism (Kurtz et al. 1999). The effects of intratendinous injection of IGF-1 on tendon healing have been evaluated in an equine model. Results showed that IGF-I treated tendons promoted cell proliferation, collagen synthesis, and enhanced stiffness, which indicated the potential of IGF for tendon healing (Dahlgren et al. 2002). Collagen hydrogel transduced with IGF-1 gene was reported to augment cells migration from broken ends of ACL and to enhance ligament-specific matrix synthesis (Steinert et al. 2008).

1.8.1.2 TGF-β

TGF-β is a pleiotropic polypeptide and has 3 isoforms expression on mammalian tissues (TGF-β1, TGF-β2, and TGF-β3) (Bennett and Schultz 1993). It is involved in multiple physiological and pathological conditions, including embryonic development, adult stem cell differentiation, inflammation, and tissue healing (Lifshitz and Frenkel 2013). TGF-β plays an important role in tendon/ligament repair process since it promotes cell proliferation, migration, proteinase regulation, and ECM synthesis (Marui et al. 1997).

TGF-β1 was reported to enhance ACL and MCL fibroblasts to synthesize Col I and other collagenous protein, resulting in almost 1.5 times of collagen production

compared to untreated group (Marui et al. 1997). Under the stimulation of rhTGF-β1 (1-10 ng/mL), more collagen was expressed by Human bone marrow stromal cells (BMSCs) on a PLGA scaffold, thus indicating the potential of TGF-β1 to enhance ligament tissue engineering (Jenner et al. 2007). The combination of TGF-β and FGF-2 was reported to promote hAT-MSCs and hiPSC-MSCs differentiation into ligamentous and bone tissue at the central and the end of the scaffold respectively (Kouroupis et al. 2016).

1.8.1.3 VEGF

VEGF is a glycosylated, disulfide-linked homodimeric member of cystine knot growth factor superfamily and is known to regulate angiogenesis (Muller et al. 1997). The isoforms in human includes $VEGF_{121}$, $VEGF_{165}$, $VEGF_{189}$ and $VEGF_{206}$. During tissue healing process, it is expressed in the proliferative stage and especially remolding process, unlike IL-1 and TGF-β that have been observed to be actived immediately after injury and maintained during almost all the process (Molloy, Wang, and Murrell 2003).

VEGF was reported to regulate endothelial cells activation, migration, and proliferation and therefore to promote angiogenesis in tissue remodeling process (Dodge-Khatami et al. 2001). It was proved to decompose easily *in vivo*, and a sodium hyaluronate delivery system was reported to release VEGF for ACL reconstruction in a rabbit model (J. Chen et al. 2012). Results showed that a higher micro vessel density was detected in the graft at 4 and 8 weeks, the stiffness and maximum tensile load were increased under the

VEGF stimulation, which indicated that VEFG could improve the early revascularization and biomechanical properties of grafts after ACL reconstruction (J. Chen et al. 2012). Tohyama et al reported that the application of VEGF promoted the angiogenesis, while reducing the stiffness of the grafted tendon at least temporarily after ACL reconstruction (Tohyama et al. 2009; Yoshikawa et al. 2006). Higher concentrations of VEGF and VEGF receptors were detected in the knee joint fluid after single-bundle anterior cruciate ligament reconstruction (ACLR) than after arthroscopic partial meniscectomy (APM) in the patients, which may indicate that the VEGF and VEGFRs could be considered as tissue healing biomarkers after ACLR (Galliera et al. 2011).

1.8.1.4 PDGF

PDGFs (PDGF-A, -B, -C, and -D) are a kind of polypeptide cytokines, and they share a conserved cystine-knot-fold growth factor domain of ~100 amino acids (aa) (Shim et al. 2010). PDGF regulates cell growth, activation and differentiation. In a wounded tissue, PDGF facilitates the repair process by inducing neutrophils, macrophage and fibroblasts migration into the wounds within the first days after injuries, then activating wound macrophages and fibroblasts in order to secrete endogenous growth factors, promoting ECM synthesis in 2-3 weeks and also participating in remodeling collagen process after 2 weeks till 1 year (Pierce et al. 1991).

In a model of dead space chamber implanted into rats, healing process was accelerated

under the stimulation of PDGF (Marui et al. 1997; Mustoe et al. 1994). Moreover, during *in vivo* assay, PDGF-BB was reported to improve the ultimate load, energy absorbed to failure, and ultimate elongation values of the femur-MCL-tibia complex in a dose-dependent manner. This research also showed that the combination of TGF-β with PDGF-BB did not increase the mechanical properties (Kevin A. Hildebrand et al. 1998). Locally supplied PDGF-BB was reported to alter the mechanical properties of a free tendon graft after ACL reconstruction (Weiler et al. 2004).

1.8.1.5 bFGF

bFGF is widely expressed in cells and tissues and mainly regulates cell migration, proliferation, differentiation, and angiogenesis. Indeed, bFGF has been widely used in tissue reconstruction, including skin (Kawai et al. 2000; J. J. Yoon et al. 2006), muscles (Yablonka-Reuveni, Seger, and Rivera 1999; Doukas et al. 2002), adipose tissue (Tabata et al. 2000; Kimura et al. 2003), cartilage (Chiou, Xu, and Longaker 2006), bone (Tabata et al. 1998; Jeong et al. 2010) and ligament/tendon and nerves (Benoit and Anseth 2005; Gómez-Pinilla, Vu, and Cotman 1995). The effect of different doses of bFGF on BM-MSCs proliferation and differentiation has been investigated. Low-dose (3 ng/mL) bFGF enhanced greatly the BM-MSCs proliferation on day 7, and ligament specific matrix expression increased after 14 and 28 days compared with high-dose bFGF group (30 ng/mL) (Hankemeier et al. 2005). It was suggested that bFGF enhanced healing process by promoting cell proliferation and collagen type III expression in a rat model (Chan et al. 2000). Here is list of effects of growth factors

above on cell response (Table 3).

Table 3 Effect of various growth factors on cell response (Petrigliano, McAllister, and Wu 2006).

Growth Factor	Study	Design	Species	Tissue	Effect
Transforming growth factor (TGF)	Deie, 1997[80]	Ex vivo	Rabbit	MCL	↑ Type 1 collagen synthesis
	DesRosiers, 1996[81]	Ex vivo	Canine	ACL	↑ Collagen and total protoglycan synthesis
	Marui, 1997[82]	Ex vivo	Canine	ACL and MCL cells	↑ Collagen and protein synthesis
	Meaney Murray, 2003[83]	Ex vivo	Human	ACL	↑ Cellular proliferation and collagen synthesis
	Murphy, 1994[84]	Ex vivo	Rabbit	MCL	↑ Collagen synthesis
Platelet-derived growth factor (PDGF)	Spindler, 1996[32]	In vivo	Rabbit	ACL	↑ Cell proliferation
	Batten, 1996[85]	In vivo	Rat	MCL	↑ Structural properties
	DesRosiers, 1996[81]	Ex vivo	Canine	ACL	↑ Cell proliferation
	Hildebrand, 1998[86]	In vivo	Rabbit	MCL	↑ Structural properties
	Kang, 1999[87]	Ex vivo	Rabbit	Flexor tendon	↑ Cell proliferation and matrix synthesis in dose-dependent manner
	Letson, 1994[88]	In vivo	Rabbit	Ligament	↑ Stiffness
	Meaney Murray, 2003[83]	Ex vivo	Human	ACL	↑ Cell proliferation and collagen synthesis
	Scherping, 1997[89]	Ex vivo	Rabbit	ACL and MCL	↑ Cell proliferation
	Spindler, 1996[32]	In vivo	Rabbit	Patellar tendon	↑ Cell proliferation
Epidermal growth factor (EGF)	Marui, 1997[82]	Ex vivo	Canine	ACL and MCL	No effect
	Meaney Murray, 2003[83]	Ex vivo	Human	ACL	No effect
	Scherping, 1997[89]	Ex vivo	Rabbit	ACL and MCL	↑ Cell proliferation
Fibroblast growth factor (FGF)	Hankemeier, 2005[40]	Ex vivo	Human	BMSCs	↑ Cell proliferation and ECM mRNA expression
	Kobayashi, 1997[90]	In vivo	Canine	ACL	↑ Neovascularization
	Letson, 1994[88]	In vivo	Rabbit	Ligament	↑ Ligament stiffness
	Meaney Murray, 2003[83]	Ex vivo	Human	ACL	↑ Cell proliferation
	Scherping, 1997[89]	Ex vivo	Rabbit	ACL and MCL	↑ Cell proliferation
Insulin-like growth factor (IGF)	Abrahamsson, 1996[91]	Ex vivo	Rabbit	Tendon	↑ Matrix synthesis
	Kang, 1999[87]	Ex vivo	Rabbit	Tendon	↑ Matrix synthesis and cell proliferation
Growth and differentiation factor (GDF)	Aspenberg, 1999[92]	In vivo	Rat	Achilles tendon	↑ Tensile strength of tendon
	Koch, 2004[93]	Ex vivo	Human	BMSCs	↑ Collagen and Runx2 expression
	Wolfman, 1997[94]	In vivo	Rat	Ectopic sites	Induced ectopic ligament formation

1.8.1.6 PL

PL is a generated mechanical disruption of platelet concentrates via repeated freezing and thawing. It constitutes a rich cocktail of bioactive molecules including growth factors (TGF-β1, IGF-1, VEGF, PDGF and bFGF), cytokines, chemokines, etc. (Schallmoser et al. 2007; Strandberg et al. 2017; Shanskii et al. 2013). Recently,

researches have suggested the replacement of FBS with human PL for clinical-grade cell culture for regenerative medicine, since FBS is associated with risks of contamination, disease transmission and immune reaction (Dimasi 2011). Bernardi et al developed a ultrasound method to get PL, which showed an accelerate BM-MSCs proliferation rate compared with FBS, and the differentiation potential and immunosuppressive effect were maintained when co-cultured with T cells (Bernardi et al. 2013).

Barsotti M et al reported that PL facilitates the wound healing process during different stages including inflammatory phase, angiogenesis, extracellular matrix secretion and epithelialization (Chiara Barsotti et al. 2013). Effects of PL on cells (endothelial cells, monocytes, fibroblasts and keratinocytes) in wound healing process have been showed to be associated with cell proliferation, migration, angiogenesis and tissue repair pathway activation. Results showed that cell behaviors were enhanced with PL supply (10% and 20%), while only in PL (20%), angiogenic activity was significantly activated (Chiara Barsotti et al. 2013). ADMSC were seeded on 3D PCLF scaffold and supplied with 5% PL in a bioreactor. In the presence of PL, increased AMDSC proliferation rate, lower expression of alkaline phosphatase (ALP), GAG, and higher expression of collagen have been detected, emphasizing the potential of PL application for the stem cells mediated ligament /tendon reconstruction (E. R. Wagner et al. 2015).

1.8.2　Biomechanical stimulation with bioreactors

Bioreactors aim at providing a controllable environment to direct cell proliferation, differentiation, and neo-tissue formation towards a specific tissue (T. Wang et al. 2012). For ligament/tendon tissue engineering, a bioreactor should not only play a role of traditional incubator by supplying an appropriate environment (temperature, humidity, waste removal), a suited biochemical environment (pH, pO_2, concentrations of nutrients and growth factors) to support cell proliferation and matrix deposition, but should also provide scaffolds with the regulation of mechanical stimulation to promote ligament differentiation (Altman, Lu, et al. 2002). The stimulation of scaffolds within dynamic bioreactors mimicking the native physiological environment of the tissue may also permit to draw conclusions concerning the evolution of the properties of the construct when subject to loading, without demanding *in vivo* implantation. First proposed bioreactors provided uniaxial cyclic loading via a piston, and more recent bioreactors are capable of applying multiaxial and cyclic strains, such as 2-dimensional (2D) cyclic mechanical strain bioreactor, 3-dimensional (3D) dynamic shear and compression bioreactor. Recently, commercial ligament/tendon bioreactors as the Bose® ElectroForce® BioDynamicsy® system and the LigaGen system (Figure 6) were developed and expected to provide more accurate and complex environment for tissue regeneration (T. Wang et al. 2012). However, such bioreactors are limited by the complicated scaffold fixation or the type of mechanical stimulation (T. Wang et al. 2012).
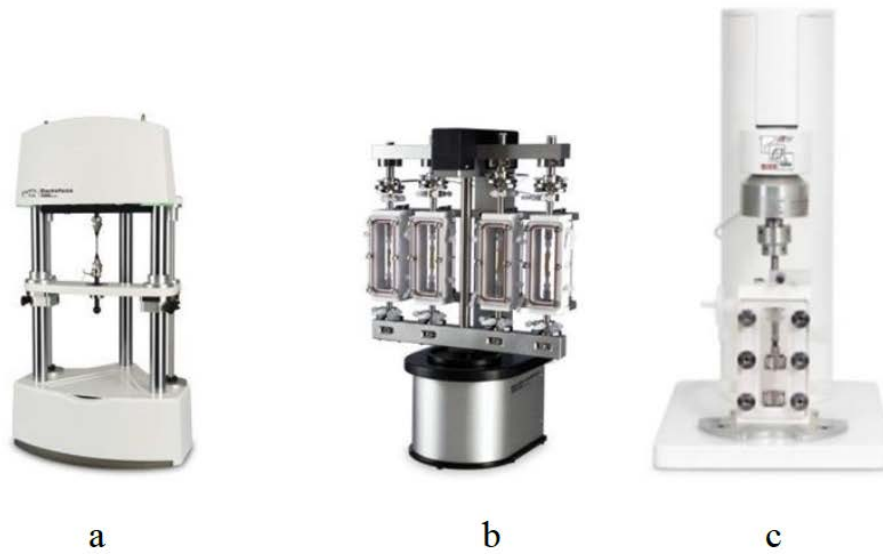
Figure 6 Examples of commercial bioreactors: (a) Bose® ElectroForce®, (b) BioDynamics® system and (c) LigaGen system.

Mechanical stress plays a pivotal role in tissue repair and regeneration. In the literature, mechanical signals were applied on scaffolds on the form of shear stress generated by fluid flow, hydrodynamic pressure or direct mechanical stress. Mechanical stimulations were reported to enhance cell proliferation, regulate cell morphology, cell alignment, and ECM synthesis. The expression of Col I, Col III, TNC, and elastin was increased by MSCs in the presence of mechanical loading. The first 3D bioreactor for ligament/tendon tissue engineering was developed by Altman et al. It has demonstrated that this system could promote hBMSC proliferation and differentiation towards ligamentous tissue on silk matrix (Altman, Lu, et al. 2002). The ultimate tensile stress (UTS) and elastic modulus (EM) of a tenocytes seeded tendon construct was increased when cultured in a bioreactor (Saber et al. 2010). Recently, various bioreactors were

designed to promote ligament/tendon regeneration. In a previous study performed by our research group, a multi-chamber, tension-torsion bioreactor was developed (C. P. Laurent et al. 2014b). Compared with static culture, a higher cell adhesion, proliferation and ECM synthesis were observed for cell-scaffold in bioreactor (C. P. Laurent et al. 2014b).

1.9 Conclusion

1.9.1 Summary, issues and hypothesis

In this chapter, the characteristics of native ligament tissue including the structure, composition and functions have been described to guide ligament repair or regeneration. It has been emphasized that ligament injuries were among the highest musculoskeletal disorders, especially in knee, and that ligament had poor self-repair or regeneration capacities due to its hypovascular and hypocellular nature. Currently, solutions for ligament repair or regeneration are limited to conservative treatment and surgical operation. Consequences occurring after ligament injuries may have a seriously detrimental effect on daily life. The current surgical strategies improve joint stability and patient's movement, however, a number of remaining issues such as the availability of graft sources, the risk of disease transmission and post-transplant graft failure greatly limits its application. Ligament tissue engineering constitutes therefore a potential alternative method to regenerate ligament tissue. Three main elements in the core of the approach of ligament tissue engineering have been detailed, namely: i) scaffold characteristics including biomaterial sources (natural, synthetic or biological),

physiochemical properties (mechanical properties, degradability, processability, etc.) and structure (hydrogel, sponge, electrospun fibers, braided fibers etc.) ii) cell sources including fibroblasts and stem cells, iii) microenvironment effect, including biochemical and biomechanical stimulations.

Such a tissue engineering approach has been raised as a novel potential solution to treat injured ligament. So far, even though progress has been achieved to recover injured ligament from the tissue regeneration process, there is no consensus concerning the most suited cell-scaffold construct which could replace injured tissue or realize its function. A suited scaffold should possess satisfying mechanically strength, biodegradability, biocompatibility and should morphologically mimic native tissue. A satisfying candidate cell should offer differentiation capacities towards target tissue. The most suited microenvironment (including biochemical or biomechanical stimulations) for the promotion of cell-source differentiation towards ligament tissue also constitutes an issue to be addressed in the current state of art.

Objective and content of the thesis

This work aims to develop a tissue-engineered construct for ligament repair or regeneration by studying suited cell source, scaffold and biomechanical stimulation. Based on the knowledge acquired from the state of art described in the previous chapter, criteria to develop an effective tissue engineering system for ligament may be identified and will be briefly addressed in the following chapters.

- In the chapter II, the materials and methods used to carry out every study reported in the manuscript are firstly described in detail.

- Chapter III focuses on the selection of cell sources, WJ-MSCs and BM-MSCs being selected as candidate cells. The evaluations related to "stemness' and cell quality are performed before cells interact with scaffold. Cell behaviors including cell attachment, proliferation, migration and ECM synthesis are also studied.

- In the chapter IV, a Poly-(L-lactide-co-ε-caprolactone) (PLCL) multi-layer braided scaffold with or without Layer-by-Layer (LBL) modification is proposed, and its interaction with WJ-MSCs and BM-MSCs towards ligament tissue engineering has been studied. This study is performed as a result of a previous study performed by our team, in which PLCL has been used to develop a multi-layer braided scaffold. The biocompatibility has been confirmed *in vivo* and *in vitro* assays, but cells did not show homogeneous distribution on scaffold. Therefore, poly-L-

lysine/hyaluronic acid (PLL/HA) LBL modification have been introduced on PLCL scaffold in order to improve cell homogeneous distribution.

- In the chapter V, silk and silk/PLCL braided scaffolds are proposed, and their interaction with WJ-MSCs and BM-MSCs towards ligament tissue engineering are studied. This study is performed as a result of a previous study performed by our team, in which a brittle behavior of PLCL fibers after two months of degradation has been observed. Silk is thus used to develop silk and silk/PLCL scaffolds in order to enhance mechanical properties of scaffolds and expect to adjust the degradation rate. The physiochemical properties and biocompatibilities of PLCL scaffolds, silk scaffolds and silk/PLCL composite scaffolds are investigated.

- In the chapter VI, the results of a preliminary study relating the mechanical stimulation on WJ-MSCs and BM-MSCs differentiation towards ligament tissue engineering are reported. This study follows a previous work carried out in our team, in which a dedicated traction-torsion bioreactor for ligament tissue engineering has been developed.

Finally, the obtained results in the present work are discussed in chapter VII, while the last chapter VIII is dedicated to the main conclusions, limitations and perspectives of this work.

2 Chapter II : Materials and methods

In the present chapter, the material and methods used for the forthcoming chapters are gathered and described all together. This choice aims at clarifying and easing the reading of the forthcoming chapters, in which we will refer to the current chapter as far as the methodological aspects will be concerned.

2.1 Biological study of MSCs

2.1.1 Isolation and expansion of BM-MSCs and WJ-MSCs

2.1.1.1 BM-MSCs

Human bone marrow was harvested from patient's femoral head during surgery and supplied by Orthopedic Surgery and traumatology center of CHRU Hospital (Nancy, France) with the informed consent of patients. Firstly, 25 mL α-MEM (Lonza, BE12-169F) complete medium contained 10% Fetal bovine serum (FBS) (Dominique Dutscher), 2 mM L-glutamine (Sigma, A-4034), 100 U/mL penicillin /streptomycin (Gibco, 15140-122) and 1μg/mL amphoterin B (Gibco, 15290-026) was added to 20 mL BM, and then centrifuged at 300 g for 5 min. The supernatant was removed, and 20 mL α-MEM complete medium was added, aspirated and blowed. 10 μL cell suspension was mixed with190 μL leucoplate for 3 min, red blood cells were lysed, and BM-MSCs were counted. Cells were seeded on tissue culture plates at the density of 50000 cells/cm^2, then incubated in 37□, 5% CO_2, 90% humidity for 3 days. The culture medium was changed twice a week.

The primary culture BM-MSCs were washed with HBSS, and detached with 3 mL 2.5% trypsin (Gibco, 25300-054) when cells reached 70%-80% confluence. Cells were then seeded on the tissue culture plate at the density of 1000 cells/cm^2 and supplied with α-MEM complete medium. The culture medium was changed twice a week.

2.1.1.2 WJ-MSCs

Human umbilical cords were supplied by maternity hospital (Nancy, France) with the informed consent of patients. Method#1: firstly, the cord was washed with 75 % ethanol to remove the blood and blood clot on the surface, then cut into small pieces of 3-4 cm in the HBSS buffer. The cord was opened to peel off the 2 arteries and 1 vein, with a particular attention not to damage the blood vessels in order to avoid the contamination of endothelial fibroblasts. WJ was exposed, and the jelly was torn off from cordon into the HBSS buffer. The jelly was cut into fine pieces and transferred to 6-well plates, and cultured at 37°C, 5% CO_2 and 90% humidity. After 7 days, the jelly was removed, the culture medium was changed twice a week. Method #2, umbilical cord was firstly washed with 75% ethanol and then PBS. The two ends (1 cm) of cord were discarded, and then the veins were syringed with PBS. The cord was cut into 5 cm pieces, and the veins were washed again with PBS. The surface of cord was then scratched with a blade along the longitudinal direction of the cord. The cord was cut into 1 cm pieces and put into a Petri dish with the transverse side attached on the Petri dish. Cords attached on the dish after a rest time of 10min, 30 mL of a-MEM complete medium was then added

and cultured for 10 days. Cords were washed with PBS and cells observed on the dishes by microscopy. Finally, the cords were discarded, and cells were washed with PBS, before adding 20 mL of a-MEM complete medium and being cultured in the incubator.

WJ-MSCs detachment was realized as described for BM-MSCs.

2.1.2　Colony Forming Unit-fibroblast (CFU-F)

MSCs were detached from culture flask and seeded on petri dishes at 100 cells/ dish, then cultured in an incubator at 37°C, 5% CO_2 and 90% humidity. MSCs were supplied with α-MEM complete medium for 14 days. At the end of day 14, 3 mL crystal violet was added to each petri dish and stained for 15 min, then dishes were washed with distilled water. The colonies petri dishes were recorded with a scanner (Scanner GS-800, BIORAD).

2.1.3　Phenotype characters

The typical cell surface epitope markers on MSCs at passage 2 (P2) were determined by flow cytometer (Beckman Coulter, Gallios AN24085). MSC (P2) were defreezed in 5 mL α-MEM complete medium, centrifuged at 400 rmp/min for 5 min, and then resuspended in 5 mL 0.5% PBS-BSA. Isotype FITC /PE were used as negative control, classical markers like CD 146, CD106, CD200, CD90, CD34, HLA-DR, CD73, CD45, CD166, CD44, and CD105 were detected. The antibodies related were shown in Table 4.

Table 4 Details related to antibodies for MSCs phenotype characterization

Antigen	clone	Conjugation	Isotype	Reference
Isotype		PE	Mouse IgG1	Dako X0928
Isotype	MIB-1	FITC	Mouse IgG1	Dako X0927
CD106		PE	Mouse IgG1	BD 555647
CD146	F4-35H7	PE	Mouse IgG1	Biocytex 5050-PE-100T
CD200		PE	Mouse IgG1	BD 552475
CD90		FITC	Mouse IgG1	BC PNIM1839V
CD34	8G12	PE	Mouse IgG1	BD 555822
HLA-DR	B8.12.2	FITC	Mouse IgG1	BC IM0463U
CD73	AD2	PE	Mouse IgG1	BD 550257
CD45	T29/33	FITC	Mouse IgG1	Dako 0861
CD106		PE	Mouse IgG1	BC-PNA 22361
CD44	J173	FITC	Mouse IgG1	BC PNIM1219V
CD105	1G2	PE	Mouse IgG1	BC PNA07414

2.1.4 Differentiation

2.1.4.1 Adipose differentiation

MSCs were detached and seeded on a 48-well plate at the density 21000 cells/cm^2 until cells reached 70% - 80% confluence in 5 days. For differentiation group, cells were washed with PBS and supplied with induction culture medium for 3 days, then changed to supply maintenance culture medium for the next 3 days. This process was repeated 3 times, then supplied with maintenance culture medium for 7 days. The negative control was supplied with the maintenance medium when cells reached 70%-80% confluence. The medium was changed twice a week.

2.1.4.2 Adipored staining

Live cells were firstly incubated with DAPI (1/40) for 1 h at 37°C, then gently washed with PBS twice. 12 μL adipored was diluted to 400 μL PBS, then added to each well for 15 min. Adipocytes were observed and recorded under fluorescent microscopy.

2.1.4.3 Osteocyte differentiation

MSCs were seeded on 48-well plate at a density of 310 cells/cm^2 and supplied with α-MEM complete medium. For the differentiational group, after 24 h cell attachment, MSCs was supplied with induction medium for 21 days. The negative control was supplied with α-MEM complete medium for 21 days. The culture medium was changed twice a week. Cells were finally fixed with 1% paraformaldehyde and stained with alizarin red.

2.1.4.4 Alizarin red s (ARS) staining

ARS solution was prepared at concentration of 40 mM and adjust pH to 4.1. ARS solution was filtered each time before staining. Cells were then washed with distilled water twice and add 125 µL ARS solution for 20 min in gentle shaker. Extra coloration solution was then removed, and the resulting solution was dried overnight.

2.1.4.5 Chondrocyte differentiation

MSCs were detached and 3.75×10^5 cells were selected for both BM-MSCs and WJ-MSCs. Each cell source was distributed equally into 3 polypropylene culture tubes (15 mL), centrifuge at 150 g for 5 min. One tube constituted the control group and was supplied with α-MEM medium and another 2 tubes were supplied with induction medium. The induction tubes were resuspended in induction medium twice. All cell tubes were then centrifuged at 150 g for 5 min to develop a pellet, then cultured for 21-28 days. Pellets were fixed with 1% paraformaldehyde, and paraffin embedded for histological processing.

MSC pellets were dehydrated and embedded in paraffin, then cut into 5 µm by microtome and collected on slides. The slides were stained with alcein blue and observe under microscopy.

2.1.5   Senescence

MSCs were detached and seeded on 24-well plate at the density of 1000 cells/cm^2. After 2 days, remove culture medium, add 0.5 mL α-MEM medium with EdU (1/1000). On the third day, cells were fixed with 1% paraformaldehyde, and senescence test was performed with a Senescence β-Galactosidase staining kit (Cell Signaling, 9680), then incubated 37°C for 24 h. The cells were then washed with PBS, and cells were stained with EdU kit. Cell nuclei were stained with DAPI (1/1500) for 15min at room temperature. Cells were washed with PBS 3 times and observed by fluorescence microscopy to count the number of senescent cells.

2.2 Scaffold fabrication

2.2.1   PLCL multilayer braided scaffolds

2.2.1.1 Fiber processing

Raw PLCL (Purac Biomaterials) with a lactic acid/ε-caprolactone proportion of 85/15, was stored under 20□, then taken out to room temperature before usage. A mini-extruder machine (C. P. Laurent et al. 2011) was used together with a Zwick tensile machine used to prescribe the extruding force. 2 g of raw material powder was added to a chamber heated at 180°C. The polymer was then pushed through a die to form fibers. Constant compaction of raw material was required in order to obtain homogeneous fibers. Fibers were then rolled around bobbins and stored in a dry environment. The rolling speed of the bobbin was set such as the final fiber diameter is around 170µm (C. P. Laurent et al. 2011).

2.2.1.2 Scaffold processing

16 homogeneous bobbins were formed, then installed on a custom braiding machine (Composite & Wire machinery, United States). The speed of bobbins and braid rolling during the process were optimized to have a homogeneous scaffold. 6 concentric layers were successively built on each other as shown in Figure 7. Scaffolds were then divided into small pieces with a length of 1cm for static culture.
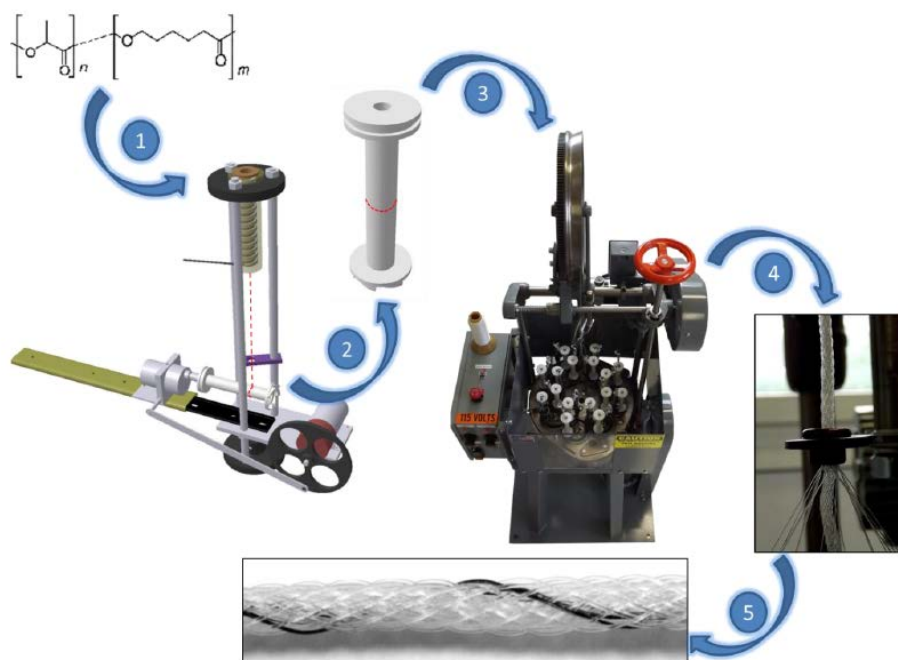
Figure 7 The processure of 6-layer PLCL braided scaffold fabrication.

2.2.2 Silk and silk/PLCL multilayer braided scaffolds

2.2.2.1 Sericin removing from silk

Raw silk fibers (Bombyx mori, 20/22D) were supplied by Trudel Limited (Zurich, Switzerland). Prior to fabricate scaffold, silk was firstly collected on the bobbins, and

boiled in 0.02 M Na_2CO_3 solution at 100 □ for more than 1.5 h to remove sericin. Silk was then rinsed under running water overnight and finally washed with distilled water for 3 times.

2.2.2.2 Scaffold fabrication

16 bobbins of silk fibers were installed on the custom braided machine described previously to fabricate one-layer silk braided scaffold (S1), two-layers silk braided scaffold (S2), three-layers silk braided scaffold (S3) and Silk-Polymer (SP) three-layer composite scaffold made of a layer of PLCL between two layers of silk, with optimized and consistent speed. The ends of the scaffold were fixed with silk fiber and cut into 1 cm for the following study.

2.3 Scaffold modification with Layer-By-Layer (LBL) technology

2.3.1   Scaffold with PLL/HA modification

Firstly, NaCl-Tris buffer (0.9% w/v NaCl in 10 mM Tris buffer) was prepared at pH 6.0-6.5 and pH 7.4 respectively. PLL (Sigma, P2636-1G) and HA (ACROS, 251770250) were dissolved in the NaCl-Tris buffer at the concentration of 1mg/mL. The scaffold pieces were firstly immersed in PLL solutions for 7 min, then gently rinsed in NaCl-Tris buffer for 1 min. They were subsequently introduced into HA solution for 7min and then rinsed in NaCl-Tris buffer for 1 min. This process was repeated (n=1, 3, 5) at the 2 different pH conditions, then ended with PLL solution to get scaffold-(PLL-HA)$_n$-PLL (n refers to the number of bilayers "PLL-HA"). The term scaffold-blank (SB)

refers to the scaffold without LBL modification, and scaffold-PLL refers to scaffold modified only by PLL solution. The names of all the scaffolds in this study are listed in Table 5.

Table 5 List of scaffolds named in the study

Name	Scaffold
SB	PLCL scaffold blank
SP	PLCL scaffold with PLL modification
S1L	PLCL scaffold with PLL/HA/PLL modification
S1	One-layer silk scaffold
S2	Two-layer silk scaffold
S3	Three-layer silk scaffold
SP	Silk/PLCL/silk composite scaffold

2.3.2 Fibers modification with PLL-FITC/HA

PLCL fibers were cut into pieces at the length of 1 cm, PLL-FITC (Sigma, P3096) was dissolved in NaCl-tris buffer at pH 6.3 and pH 7.4 with the concentration of 1mg/mL. Fibers were immersed in PLL-FITC solution for 7 min, then washed with NaCl-tris buffer for 1 min. Fibers were kept in PBS for observing.

2.4 Scaffold characterization

2.4.1 Structure by Fourier transform infrared spectroscopy (FTIR)

PLCL fibers were vacuum-dried at 60°C for 24 h and cut into fine powders for FTIR measurement. The dry powders were respectively mixed with KBr, and spectra were recorded on an FTIR spectrometer (TNZ1−5700, Nicolet, USA) over the wavenumber range from 4000 to 600 cm^{-1}.

2.4.2 Morphology by Scanning Electronic microscopy (SEM)

The multi-layer braided structure was observed by SEM. Scaffold were firstly dehydrated with a series of gradient alcohol solution (50°, 10 min; 70°, 10 min; 90°, 10 min; and 100°, 10 min for 2 times). Scaffolds were then coated with gold and viewed with SEM (JEOL 5400 LV).

2.4.3 Morphology by confocal laser macroscopy (CLSM)

PLCL fibers were cut into 1 cm-long pieces, PLL-FITC (Sigma, P3096) was dissolved in NaCl-tris buffer at pH 6.3 with the concentration of 1mg/mL. Fibers were then immersed in PLL-FITC/HA solution as described above, with the replacement of PLL with PLL-FITC solution, then washed with NaCl-tris buffer. Finally, fibers were observed with CLSM.

2.4.4 Topology by atomic force microscopy (AFM)

The surface of modified fibers was observed using AFM (MFP-3D Infinity, Oxford instruments). PLCL fibers were cut into 1cm and maintained on a glass slide. Surface topology was observed using contact mode, and images were taken at sizes of 40 µm×40 µm and 5 µm×5 µm for both fibers treated with PLL (SP) and with one-layer PLL/HA/PLL (S1L).

2.4.5 Mechanical properties

2.4.5.1 Mechanical properties of isolated fibers

The mechanical properties of PLCL fibers were assessed using tensile tests. These tests were performed using a Zwick Roell 2.5 device (Zwick, Germany) equipped with a 2.5 kN cell force, at a tensile speed of $0.1 mm.s^{-1}$. 60 cm-long fibers were rolled up and then fixed around cylindrical parts, in such a way that 6 fibers were tested in parallel. Four different tests were performed for SB, SP and S1L, and stress and strains were computed from measured displacements and forces. The initial length of scaffolds between grips were initially measured, and the following loading cycle was prescribed (1) 1% strain then unloading (2) 3% strain then unloading (3) increasing strain up to failure. Forces and displacements were recorded and then manually post-treated, Young's modulus was measured for each sample from the slope of the stress-strain curve just after the first unloading cycle (at 1% of strain).

2.4.5.2 Mechanical properties of braided scaffolds

Four different scaffold configurations (S1, S2, S3 and SP) were tested (n=2) in tension in order to assess and compare their tensile mechanical response in a physiological environment. Load-unload cycles with increasing amplitudes were prescribed using a Zwick Roell Z0.50 TN tensile machine equipped with a load cell XforceP of 100 N. Scaffolds were inserted and screwed within custom designed samples bearing immersed into water at 37°C. The initial length of scaffolds between grips were initially measured, and strains corresponding to 1%, 3%, 5% and 10% of this length were successively prescribed at a speed of 0.1 mm/s. Forces and displacements were recorded and then manually post-treated in order to determine scaffold properties (toolbox Scipy. optimize).

2.4.6 Morphology and Porosity by micro computed tomography (µCT)

The four scaffolds (S1, S2, S3 and SP) were scanned within a single acquisition using a nanotomograph (EasyTom, RX Solutions) at a resolution of 4.89 µm/voxels and a custom setup aimed at maintaining the samples during the acquisition. 140 consecutive cross-sections were selected in the middle part of the scaffolds, and subject to standard image processing techniques using custom Matlab routines. The images were firstly binarized, and then an equivalent scaffold diameter was computed for each cross-section. To do so, the center of gravity of the images was firstly computed, and the diameter of the circle (centered at the center of gravity) containing 99% of the non-zero values of the images was defined as the equivalent diameter. The porosity was defined

as the ratio between non-zero and zero values within this circle. Standard watershed algorithms were thus applied to defined pores within this circle, and global pore size distribution was computed. The post-treatment of μ-CT results for silk and silk/PLCL scaffolds has been shown in Figure 8.
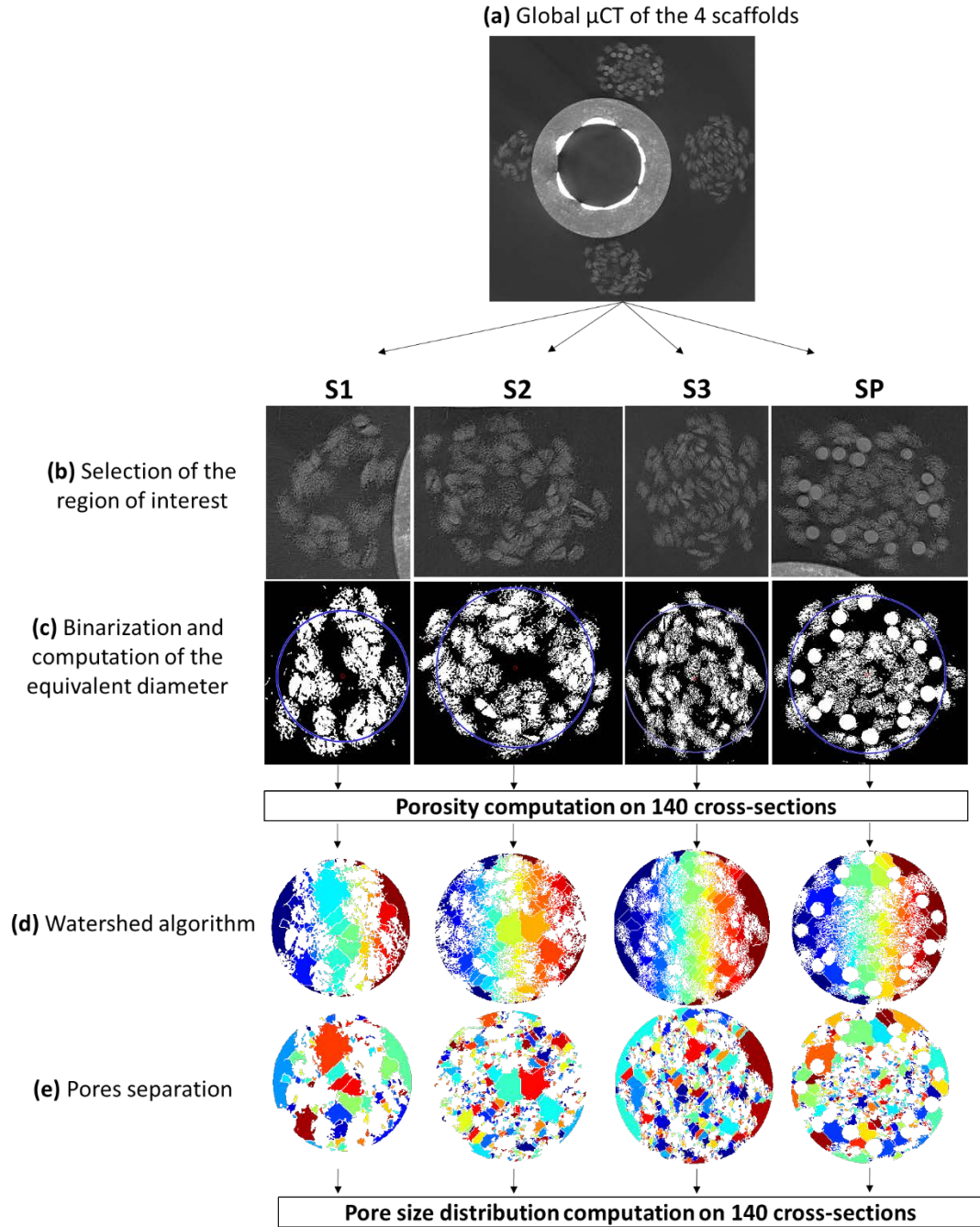
Figure 8 The flow chart of μ-CT results post-treatment for silk and silk/PLCL scaffolds (S1: one-layer silk scaffold; S2: two-layer silk scaffold; S3: three-layer silk scaffold; SP: silk/PLCL composite scaffold)

2.5 Evaluation of biocompatibility of MSCs on scaffolds

2.5.1   Scaffold sterilization

Scaffolds were sterilized by immersion in 70% ethanol for 30 min and subsequently UV-irradiated for 30 min for each side.

2.5.2   Cell seeding on the scaffold

Firstly, the scaffolds were exposed to UV for 15 min each side after LBL modification. MSCs were detached from flask by 0.25% trypsin, 0.05 mL suspensions with 300,000 cells were distributed on the scaffold in each well. Seeded scaffolds were then put in the incubator for 30 min and supplied with 0.95 mL α-MEM complete medium with ascorbic acid (Sigma, A-4034) to get 1mL medium for each well. Cells were cultured for 2 weeks. Alamar Blue (AB) tests were performed after 1 (D1), 3 (D3), 5 (D5), 7 (D7), and 14 (D14) days of culture.

2.5.3   Cell proliferation evaluated by AB test

After cells were seeded on scaffold, AB tests were performed on D1, D3, D5 and D7. Before testing on each time interval, discarded culture medium, and scaffold were washed gently with PBS for 1 time. 1 mL 10% AB work solution (Thermo scientific, 88952) was added to each scaffold, and incubated for 3 h at 37 °C, the solution was then aspired and transferred into 96-well plate (150 µL in each well) to test the optical density at 570 nm and 630 nm. Each well was repeated 3 times. The negative control was AB working solution without cells. Cell-scaffolds were washed gently with PBS, and the absorbance was tested at different time intervals.

To calculate the % Reduction of Alamar Blue Reagent using absorbance reading:

$$\%Reduction\ of\ AB\ reagent = 100 \times \frac{117276 \times A_{570} - 80586 \times A_{600}}{155677 \times C_{600} - 14652 \times C_{570}}$$

Molar extinction coefficient (E) of oxidized Alamar Blue reagent at 600 nm =117216,

E of oxidized AlamarBlue reagent at 570 nm =80586,

E of reduced AlamarBlue at 570nm = 155677,

E of reduced AlamarBlue at 600nm = 14652,

A570=absorbance of test wells at 570 nm,

A600=absorbance of test wells at 600 nm,

C570=absorbance of negative control well (medium AB Reagent, no cells) at 570 nm,

C600=absorbance of negative control well at 600 nm.

2.5.4   Cell location and morphology detection by SEM

MSC-Scaffolds were firstly fixed with 2.5% glutaraldehyde overnight at 4 °C on day 14, then washed with PBS for 3 times. MSC-scaffolds were frozen with liquid nitrogen for 10 min, dried in vacuum oven for 7 h, then coated with gold and observed by SEM (TESCAN, Czech Republic).

2.5.5   Cell morphology observation by CLSM and fluorescent microscopy

First, MSC-scaffolds were fixed with 1% paraformaldehyde for 10 min at room

temperature, and then washed with PBS three times. Permeabilization treatment was performed by adding 1 mL 0.5% triton-PBS to each well for 20 min and washed with PBS for three times. 250 µL Alexa 488 Phalloidin (Life technologies) solution was supplied to each MSC-scaffold for 45 min, then washed with PBS for three times. 200 µL DAPI (1/2000) (Sigma) was added to each scaffold for 15 min and washed with PBS three times. Images were taken by CLSM (Leica SP5-CFS).

Quantification of cell nuclear elongation was performed by Image J software version 1.51 k. The length was defined as the longest distance through nucleus and the width was defined as the distance perpendicular to the length. Cell nuclear aspect ratio was calculated by dividing the length to the width. The area of cell nucleus ($n \geq 100$ from more than three images) was measured by Image J 1.51 k.

2.5.6 Live/dead staining of MSCs on scaffolds

Viable and dead MSCs on scaffold were visualized with a live/dead staining that comprise Calcein AM (Biolegend, 425201) and 2 mM ethidium homodimer-1 (Thermo Fisher Scientific, L3224). Working solution was prepared by adding 5 µL of 2 mM Ethd-1 stock solution to 1 mL α-MEM medium without phenol red, then vortexed homogeneously, and then adding 8 µL of 1 mM Calcein AM. MSCs-scaffolds were washed twice with α-MEM medium without phenol red, then 250 µL staining working solution was added and incubated at 37 °C for 45 min. Live cells were stained green and dead cells were stained red (ex/em Calcein: 494/517 nm; Ethd-1 in the presence of

DNA=528/617 nm).

2.5.7   Detection of Extracellular matrix synthesis by fluorescent microscopy

After 2 weeks, MSC-scaffolds were first fixed with 1% paraformaldehyde for 10 min, and then washed with PBS for three times. 5% PBS-BSA blocking buffer was added to scaffolds for 30 min. The first antibody Col I (CALBIOCHEM), Col III (Sigma), and TNC (Abcam) were added (250 µL) to scaffolds for 1 h, and then washed with PBS for three times. The second antibody anti-rabbit IgG-Alexa488 (1/50) (Life Technologies) and anti-mouse IgG-Alexa488 were distributed (250 µL) to scaffold for 45 min, then washed with PBS three times. 200 µL DAPI (1/2000) was added to each scaffold for 15 min. MSC-scaffolds were washed with PBS for 3 times and observed by fluorescence microscopy. Negative controls were performed as MSCs with only second antibody, and positive controls were tested as fibroblast with antibody Col I, Col III, and TNC and second antibody.

2.5.8   Cell migration stimulated by scaffolds

MSCs migration stimulated by silk and silk/PLCL was performed by Boyden chamber assay. A transwell (Corning® FluoroBlok™) with 0.8 µm pore fluorescence blocking PET track-etched membrane insert was used for migration test according to manufacturer's protocol. 10 mg of silk and silk/PLCL were prepared in powder and sterilized with UV radiation for 30 min. The downside of insert membrane was coated with 100 µL collagen for 30 min.

Both WJ-MSCs and BM-MSCs were starved for 24 h, then a suspension of 1.5×100000 cells (200 µL) in α-MEM medium without FBS was added to each reservoir. 500 µL/well α-MEM medium with FBS was added to silk and silk/PLCL powders in 24-well chamber for 24 h. Cells on the membrane were stained with Calcein-AM (1/1000) for 30 min, MSCs were observed by fluorescence microscopy, and the fluorescence intensity was measured by fluorescence spectrophotometer.

2.5.9 Histology and immunohistochemistry of MSCs on scaffolds

MSCs-scaffolds (n=3) were harvested on day 14. Briefly, MSCs-scaffolds were firstly fixed in 1% paraformaldehyde fix solution, dehydrated and embedded in paraffin. MSCs-scaffolds were cut into 5 µm by microtome and collected on slides. Slides (n=3) were stained Hematoxylin/Eosin/Safran (HES) and Red Sirus (RS) for histological evaluation.

To analyze ligamentous ECM protein expression including Col I, Col III, and TNC, immunohistochemistry (IHC) was performed on slides with Mouse and Rabbit Specific HRP/DAB (ABC) Detection IHC Kit (abcam, ab64264). Briefly, slides were deparaffinized and rehydrated, then places in a wet box. Pepsin was added to cover the sample for 30 min at room temperature and then washed with PBS for 2 times (2×5 min). Next, hydrogen Peroxide was added to block endogenous peroxidase for 10 min then washed with PBS for 2 times. Protein block was performed to block nonspecific

background before incubating with primer antibody. Monoclonal antibodies Col I (ab88147, abcam), Col III (C7805, Sigma), and TNC (ab6393, abcam) were applied according to manufacturer's protocol and washed with PBS for 3 times. Biotinylated Goat Anti-Polyvalent was added and incubated for 10 min at room temperature and washed with PBS for 2 times; followed by incubated with Streptavidin Peroxidase for 10 min.

The slides were washed with PBS for 3 times then washed with distilled water for one time. Add 30 μL DAB (1 drop) to 1.5 mL DAB substrate (50 drops), mix by swirling and apply to tissue with 50 μL to cover the samples. Incubate for 1-10 min and then rinse with distilled water. The counterstain was performed with hematoxylin 1-2 min, then slides were dehydrated by immersing into absolute ethanol for 2 times and then immersing into toluene. Each step lasts for 2-3 min. Then slides were mounted in aqueous mounting media then observed with microscopy.

2.5.10 Bioreactor sterilization and assembly

Firstly, 6 separate chambers were disassembled and each part (namely: chamber, stand, silicone, screw etc.) (Figure 9) were autoclaved. Silk and silk/PLCL scaffolds were sterilized with UV radiation. For the assembly step, chambers were mounted as shown in Figure 9, and two scaffolds per chamber were fixed and prepared for cell seeding.
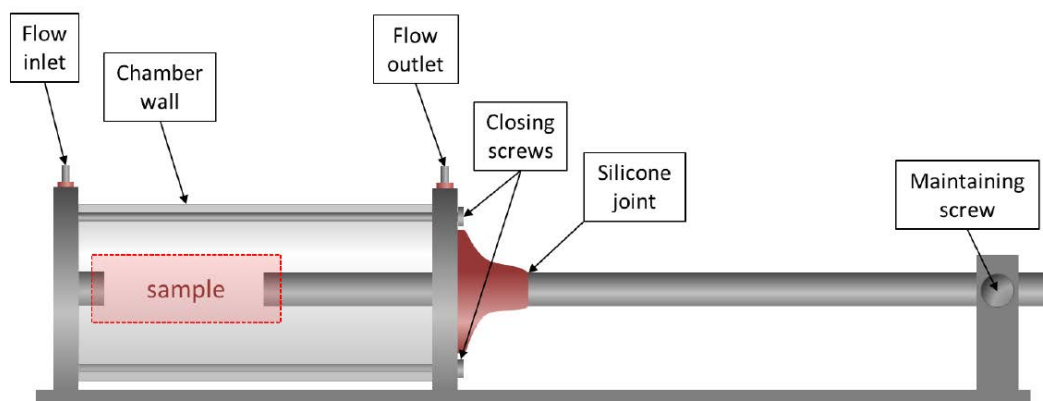
Figure 9 The schematic diagram of chambers from bioreactor.

2.5.11 MSCs seeded on scaffolds with mechanical stimulation and biological evaluation

Both WJ-MSCs and BM-MSCs were detached and seeded on scaffolds with a concentration of 6×10^5 cells/ scaffold and 30 µL/ scaffold. Scaffolds were kept wet with culture medium. MSCs were seeded on scaffolds in the same way as for static conditions. Chambers were closed on the side of flow inlet, and a filter was inserted on the side of flow outlet. They were then put in incubators for 1 h for cell attachment, and then 100 mL medium containing 10% FBS, 1% L-glutamine (2 mM, Sigma, A-4034), 1% penicillin /streptomycin, 1% amphoterin B, 25 mM HEPES buffer, and 100 µg/mL ascorbic acid was added to the chamber content. Chambers were kept in static incubators for 24 h before mechanical loading. There were finally mounted with the bioreactor (Figure 10) and a planned cyclic loading was then applied (2.5% strain, at 1 Hz) during 2 min every 30 min for 8 h. Culture medium was changed every 3 days.

Figure 10 The tension-torsion bioreactor designed by our team.

At D1, D5 and D7, one chamber was unmounted, the two scaffolds were taken out. Scaffolds were washed and kept in separate tubes for AB test. 2 mL of AB working solution was added for each scaffold. After AB assay, cells on the scaffolds were stained with live/dead staining.

2.6 Conclusion of the present chapter

In this chapter, each methodological aspect used in the forthcoming sections have been described. They concern the biological characterizations of cells and cell-scaffold constructs, as well as the processing and imaging of scaffolds, and their morphological and mechanical characterizations. Consequently, we will widely refer to this chapter in the forthcoming sections as far as methodological aspects will be concerned.

3 Chapter III : Biological study of cell sources selected for ligament tissue engineering

3.1 Introduction

WJ-MSCs and BM-MSCs have been selected as cell sources for ligament tissue engineering in the present study. Since they belong to MSCs, they are expected to offer MSCs biological properties such as colony forming properties, phenotypic markers expression and differentiation potentials towards adipocytes, chondrocytes and osteocytes.

The two characteristic features of stem cells are the self-renew ability and multilineage differentiation capacity. Self-renew refers to the process of cell division into one (by asymmetric division) or two (by symmetric division) daughter stem cells, which hold the same potentials than the mother stem cells (Molofsky, Pardal, and Morrison 2004). This phenomenon plays an essential role in the development and maintenance of adult tissue. Differentiational potentials of stem cells are various from totipotent cells of early embryo (fertilized oocyte, zygote, 2-cell,4-cell, 8-cell and morula) to pluripotency of embryonic stem cells, multipotency of MSCs, and lastly to unipotentiality of cells such as epidermal stem cells. The capacity to remain in an undifferentiated state after extended culture is beneficial for therapeutic and research application.

In 1970, Friedenstein et al (A. J. Friedenstein, Chailakhjan, and Lalykina 1970) firstly discovered CFU formed by MSCs *in vitro*, then it was considered as one of universal

criterion to define stem cell by International Society for Cellular Therapy (ISCT). Commonly used surface markers such as CD105, CD73, CD90, Stro-1, CD106, and CD166 were positively expressed on MSCs, while CD45, CD34, CD14 or CD11b, CD79a or CD19, and HLA-DR were negatively expressed. CD73 is an ecto-5'-nucleotidase. In an early report (F. Barry et al. 2001, 3) monoclonal antibodies (SH-3 and SH-4) anti-CD73 were identified and showed specific for mesenchymal tissue-derived cells. CD90 is a cell surface anchored glycoprotein, which plays a role in cell-cell/matrix interaction and cell motility (Rege and Hagood 2006, 1). It was expressed on human MSCs surface and was reported to regulate stem cell proliferation and differentiation (Maleki et al. 2014). CD166 (ALCAM) is an activated leukocyte cell adhesion molecule that binds to cell surfaces (Ohneda et al. 2001). It plays a role in immune response process, nerve system, and also regulate of stem cell differentiation (Fujiwara et al. 2003). CD34 is the primitive marker to identify hematopoietic stem cell (HSC), and is less expressed in human MSCs. CD45 is a marker of all hematopoietic cells. Human leukocyte antigen-DR isotype (HLA-DR) is an MHC class II cell surface receptor and its expression was reported to be lower on MSCs surface.

In the forthcoming sections, we report the differentiation assays that were performed under the induction of commercial differentiation medium. What's more, senescence is also a common parameter to control cell quality and has been evaluated in the current work. In a senescence kit, β-galactosidase is a sensitive enzyme that could be detected during cell senescence. Finally, MSCs were studied to explore whether they still possess

their "stemness" nature, and cell quality was controlled for the following studies.

3.2 Results and discussions

3.2.1 Biological characteristics of WJ-MSCs and BM-MSCs

3.2.1.1 CFU-F

As it is shown in Figure 11a, each point represents a colony and they are generated by heterogeneous cell population. Colonies generated by WJ-MSCs and BM-MSCs are represented, and more colonies were observed for BM-MSCs than for WJ-MSCs.

3.2.1.2 Senescence

The senescent cell nuclei are usually characterized bigger than normal cells, with an irregular morphology and down regulated cell proliferation. At pH 6.0, cells with a high expression of β-galactosidase have been stained as dark blue in cell cytoplasm (Figure 11b), representing senescent cells. EdU is used to label and track MSCs to quantify cell proliferation. Cell nucleus were stained as red by EdU, indicating vibrant cell activity during cell mitotic process. DAPI is used to stain all the cells and combined with staining of x-gal and EdU to recognize senescent cells, blue cells with enlarged nuclear, not stained with EdU correspond to senescent cells. As it is shown in Figure 11b, more senescent cells were present in WJ-MSCs than BM-MSCs, while more BM-MSCs were detected in the cell proliferative process during 24 h.

3.2.1.3 Phenotypic characterization

MSCs were expected to show clonogenicity and tripotency, as well as to form heterogeneous populations with varying proliferation and differentiation potentials. Previous researches have been done to develop a cell-surface antigen profile for the identification and purification of MSCs. The results (Figure 11c) showed that the classical phenotype markers like CD73, CD90, CD166 were positive expressed, and CD34, CD45, HLA-DR were not expressed. And this corresponds to the results in the previous publications (Giai Via, Frizziero, and Oliva 2012; Gecai Chen et al. 2015).
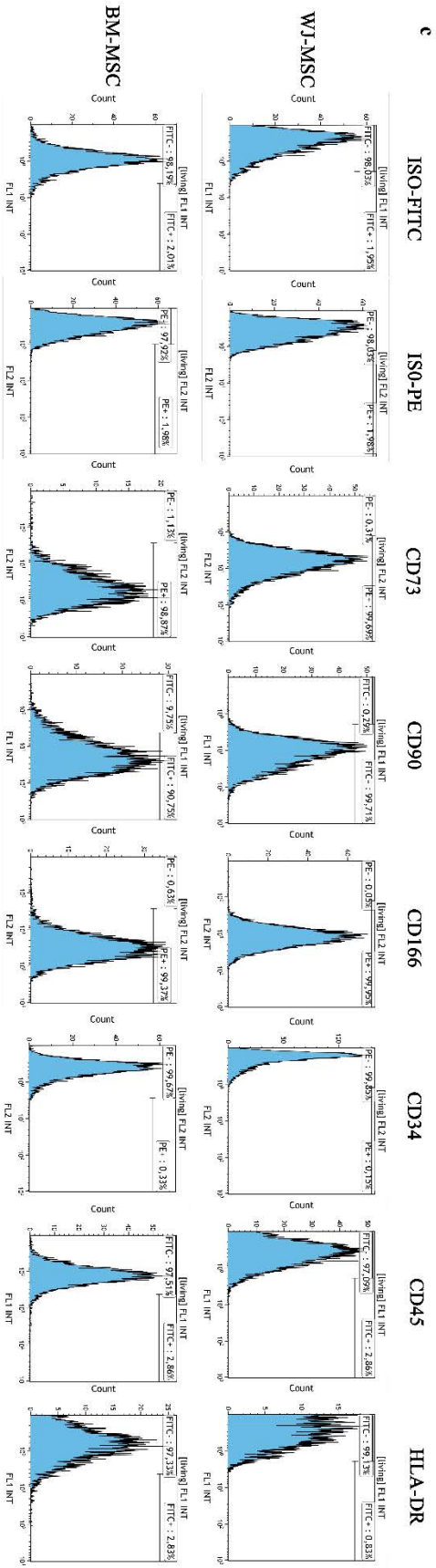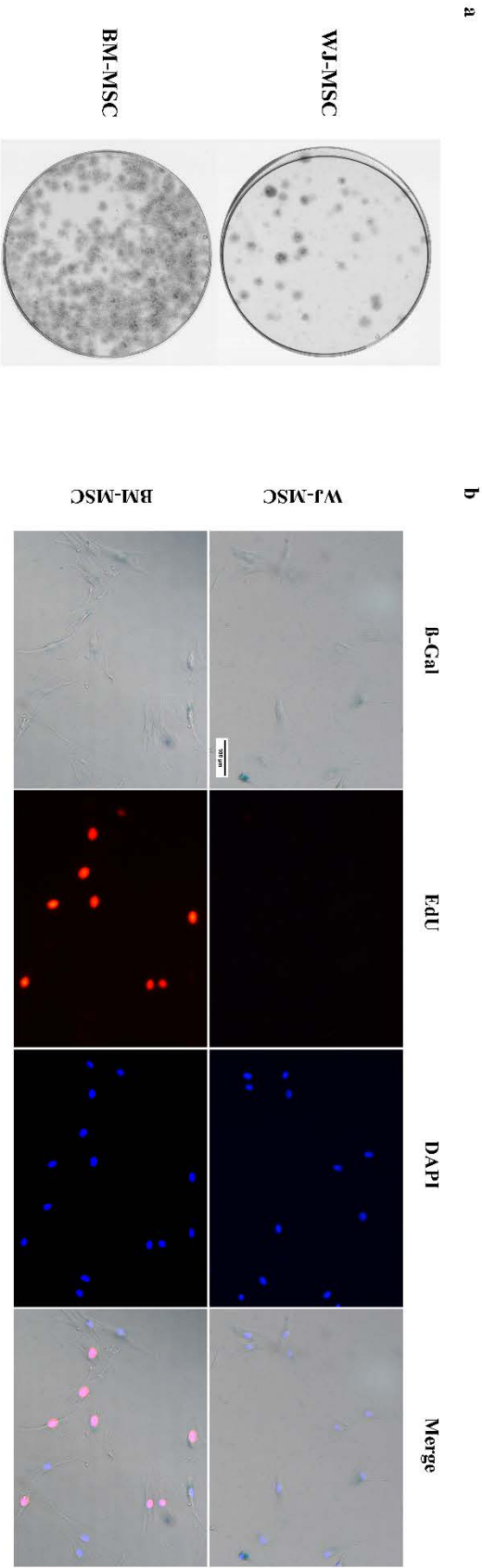
Figure 11CFU formed by WJ-MSC and BM-MSC (a), senescence staining of WJ-MSC and BM-MSC (b), phenotypic expression of WJ-MSCs and BM-MSCs (c).

3.2.1.4 Differentiation capacities

For adipocyte differentiation, MSCs were cultured in a commercial differentiation medium containing dexamethasone, insulin, isobutyl methyl xanthine, and indomethacin for 2-3 weeks. The accumulation of lip vacuoles filled in cells and secreted in medium are shown in Figure 12a. Green vacuoles are the lip-rich drops were stained with oil red. For adipocyte differentiation, more lip drops were developed by BM-MSCs than WJ-MSCs. For osteocyte differentiation, a confluent monolayer WJ-MSCs and BM-MSCs were supplied with induction medium including ascorbic acid, β-glycerophosphate, MCGS and dexamethasone for 2-3 weeks. MSCs aggregated and formed calcium nodules, then they were stained with alizarin red. The red knots (Figure 12b) correspond to calcium accumulation, which indicates both MSC differentiated towards osteocytes *in vitro*. For chondrocyte differentiation, MSCs were centrifuged to form pellets and supplied induction medium with TGF-β3 for 2-3 weeks. Histological analysis (Figure 12c) show glycosaminoglycans staining with alcian blue, which indicates the chondrogenic differentiation.
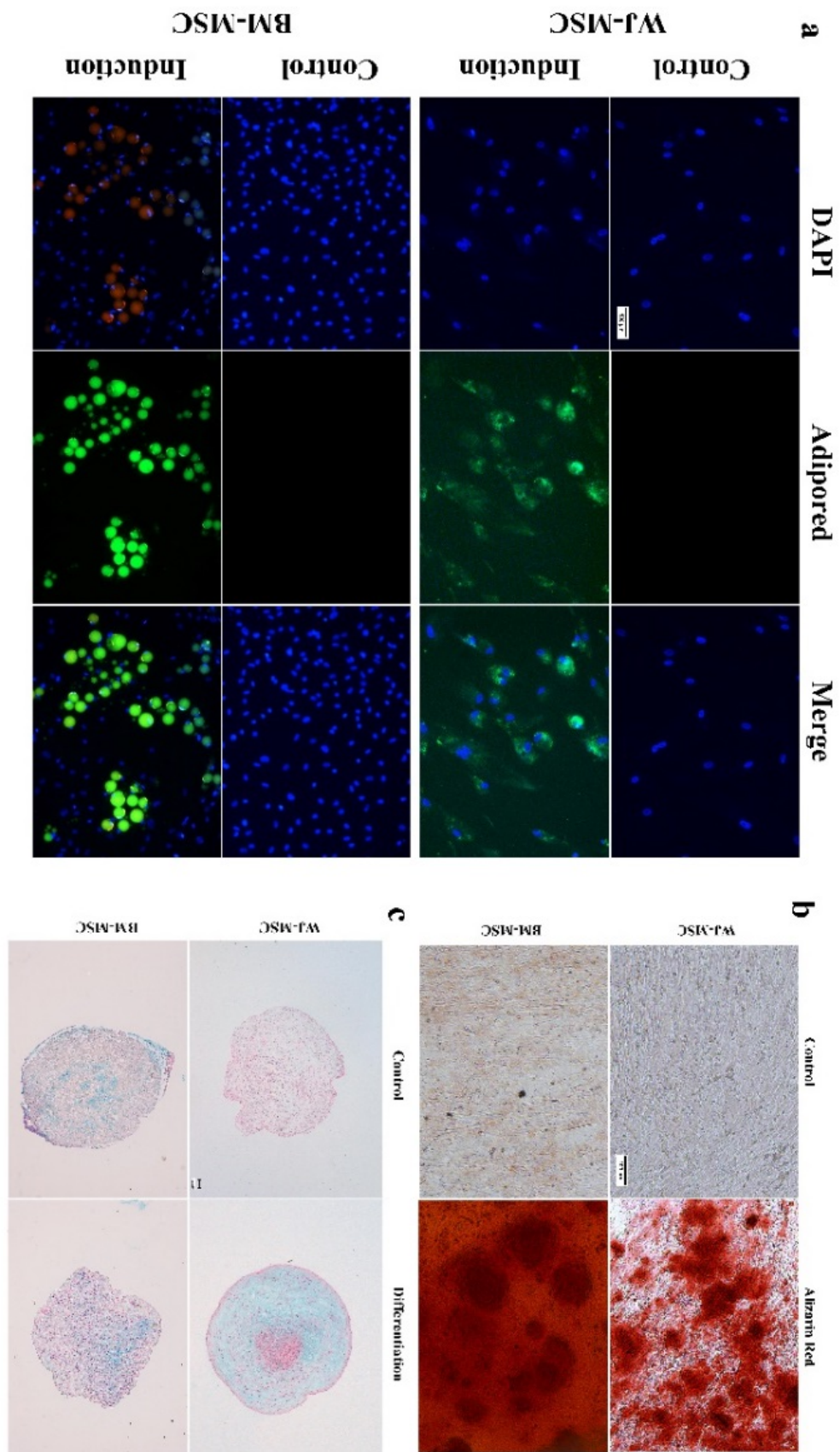
Figure 12 WJ-MSCs and BM-MSCs differentiated towards adipocytes (a); osteocytes

119

(b); and chondrocytes (c).

3.3 Conclusion

As a first conclusion, both cells were therefore identified as MSCs and showed the "stemness" nature and proper quality for the following study.

4 Chapter IV : Surface modification of a braided multilayer PLCL scaffold for ligament tissue engineering

This chapter is based on the article published in 2018 in *Journal of Biomedical material research part A* : Xing Liu, Cédric Laurent, Qiaoyue Du, Laurie Targa, Ghislaine Cauchois, Yun Chen, Xiong Wang, Natalia de Isla "Mesenchymal stem cell interacted with PLCL braided scaffold coated with poly-L-lysine/hyaluronic acid for ligament tissue engineering".

4.1 Introduction

PLCL is a synthetic biodegradable co-polymer with high elasticity consisting of polylactide (PLLA) and polycaprolactone (PCL). It has been demonstrated to possess good cytobiocopatibility and biodegradability with no toxic products in a set time period (S. I. Jeong, Kim, Kim, et al. 2004; Burks et al. 2006; S. I. Jeong, Kim, Kang, et al. 2004). Because of its elasticity and biodegradability, PLCL has been used for artificial vessels (S. I. Jeong et al. 2005; S. I. Jeong, Kim, Kim, et al. 2004), cartilage (Jun Xie et al. 2006; Kroeze et al. 2010), and peripheral nerves (De Groot et al. 1997; Rodríguez et al. 1999). It has also been pointed out to support tendon cell proliferation and also been widely applied in ligament/tendon tissue engineering (Kim et al. 2012). A series of composites based on P(LLA-CL) nanofibers (aligned-, random-, nanoyarn) and collagen I have been designed for tendon regeneration. The physicochemical

properties such as mechanical properties, fiber diameter, porosity and pore size had been optimized. From a biological point of view, electrospun P(LLA-CL)/collagen nanoyarn possess predominant potential for tendon tissue engineering (Y. Xu et al. 2013).

In a previous study performed by our team, PLCL has been used to develop a multilayer braided scaffold (C. P. Laurent et al. 2014b), which presents a porous structure for nutrient exchange, cell and tissue ingrowth. Thanks to the adjustable geometrical parameters of this architecture (e.g. number of layers, fiber diameter, and braiding angle), the mechanical strength could also be adjusted to fulfill requirements of different ligaments (C. P. Laurent et al. 2012, 2011). What's more, it possesses good biocompatibility for MSC attachment and proliferation (C. P. Laurent et al. 2014a). However, results from hMSC-scaffolds culture under mechanical stimulation through a tension-torsion bioreactor showed that, although cells initially presented good attachment and proliferation, they did not distribute homogeneously on the scaffold. This constituted the first issue that has been addressed in the study reported in the present chapter. What's more, as detailed in chapter I on this manuscript, the contribution of certain growth factors for MSCs differentiation have been recognized. Commercial induction medium with growth factors for adipocyte, osteocyte and chondrocyte differentiation have been widely applied in research. In our preliminary study (Appendix Figure 41), growth factors such as TGF-β and FGF-2 have also been evaluated to promote Col I and Col III synthesis. Results showed that TGF-β at

concentration of 1 ng/mL (10% SVF medium) showed best potential for Col I synthesis; and FGF-2 at concentration of 10 ng/mL (10%SVF) greatly promoted Col III synthesis. Since Col I and Col III are the main components of ligament ECM, the application of growth factors drew our attention for ligament regeneration. This constituted the second issue that has been addressed in the study reported in the present chapter.

LBL modification is one of methods to modify scaffold surface and improve cell and scaffold interaction. It is a polyelectrolyte multilayer films (PEM) fabrication process ensured by depositing alternating layers of oppositely charged materials. What's more, LBL has also been applied to develop a more efficient, less-cost and controllable system for growth factors delivery than direct supply. PLL/HA is a classical pair of PEM, which have been widely applied for surface modification. HA, as a component of ECM, plays an important role in improving cell growth, differentiation, and migration, but it has been observed to be non-adhesive to cells (Yamanlar et al. 2011; Hahn and Hoffman 2004). On the contrary, PLL has been shown (Huang et al. 1983; Zhang et al. 2013) to promote cell adhesion and it has widely been used for biomaterial coating and drug delivery. As a consequence, the pair of PLL/HA PEM was expected to be an effective system to improve MSCs behavior on scaffolds.

Prior to any incorporation of growth factors into LBL treated scaffold, it is crucial to study the effect of PLL/HA LBL modification on the behaviors of WJ-MSCs and BM-MSCs on PLCL braided scaffold. Therefore, in the work reported in the present chapter,

the effect of LBL modification on MSCs proliferation, distribution, morphology, collagen synthesis, TNC expression, and migration were evaluated, as well the consequence of this treatment on scaffold topology, and mechanical properties.

4.2 Results and discussion

The methodology concerning the processing and biological, mechanical and morphological characterizations of modified and non-modified PLCL scaffolds are detailed in the sections 2.3 2.4 and 2.5.

4.2.1   Physicochemical properties of PLCL

4.2.1.1 FTIR spectroscopy of PLL/HA LBL modification

PLL/HA is one of classical pairs of LBL PEM for scaffold surface modification in order to improve cell attachment, proliferationn or combine bioactive molecular in a delivery system. The structure of PLCL fiber with/without PLL/HA modification is shown in Figure 13 by FTIR, which demonstrates the development of PLL/HA PEM on PLCL fibers. The spectra at 2990 cm^{-1} (PLLA), 2945 cm^{-1} (PLLA) and 2860 (PCL) cm^{-1} demonstrated (Kalpan et al. 2007) the presence of alkyl group of copolymer PLCL. Bands at 1130 cm^{-1} and 1089 cm^{-1} represented ester backbone of PLA in scaffolds SP and S1L respectively (Jia Xu et al. 2009). The wavelength of PLL in SP was presented as anion group at 1600 cm^{-1}. The wavelength of HA in PLL/HA-PLL was presented as carboxylate anion group (Yamanlar et al. 2011) at 1616 cm^{-1} and 1413 cm^{-1}. The wavelength of amine groups of PLL (Yamanlar et al. 2011) was shown at 1630 cm^{-1} in

PLL/HA-PLL.
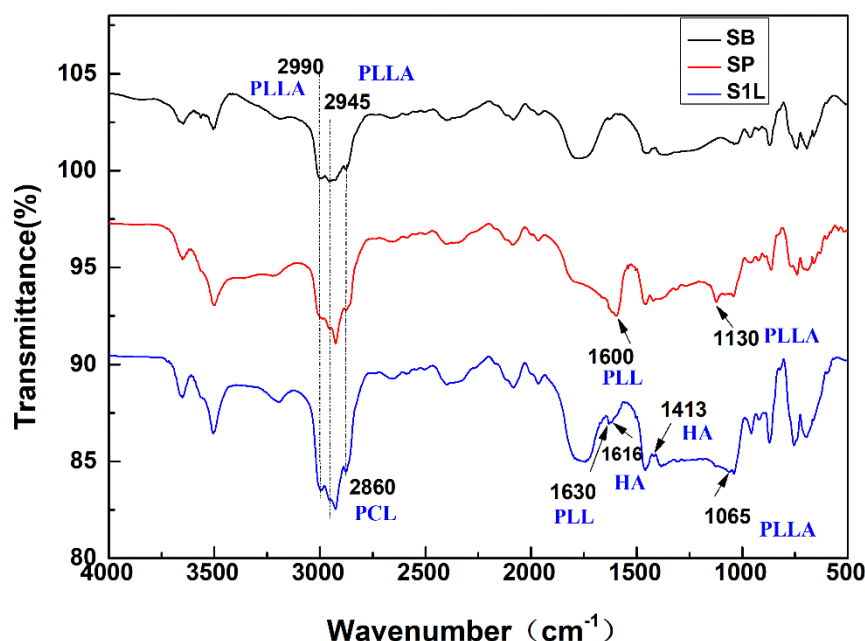
Figure 13 FTIR of PLL/HA modified on PLCL scaffold (SB: PLCL scaffold, blank; SP: PLCL-PLL; S1L: PLCL-PLL/HAPLL).

4.2.1.2 Morphology of PLCL braided scaffold with/without PLL/HA modification

Based on previously encouraging results, this 6-layer braided, porous structure has been conserved. The morphology of PLCL braided scaffold with/without PLL/HA LBL modification was observed by SEM. Scaffold images in Figure 14a & b indicate a porous and braided structure, and this multilayer structure was not influenced by PLL/HA modification. Each scaffold is composed with 6 layers (16 braided fibers in each layer). Based on the analysis of SEM images, the diameter of fiber was about 170 μm, and the diameter of 6-layered scaffold was about 3.73 ± 0.12 mm. For SB without modification, the fibers kept the same texture compared to its original fabrication, while

for SP and S1L the fibers presented a relatively smooth surface after modification. Figure 14b illustrates the global structure of 6-layer braided scaffold, each color representing one layer.
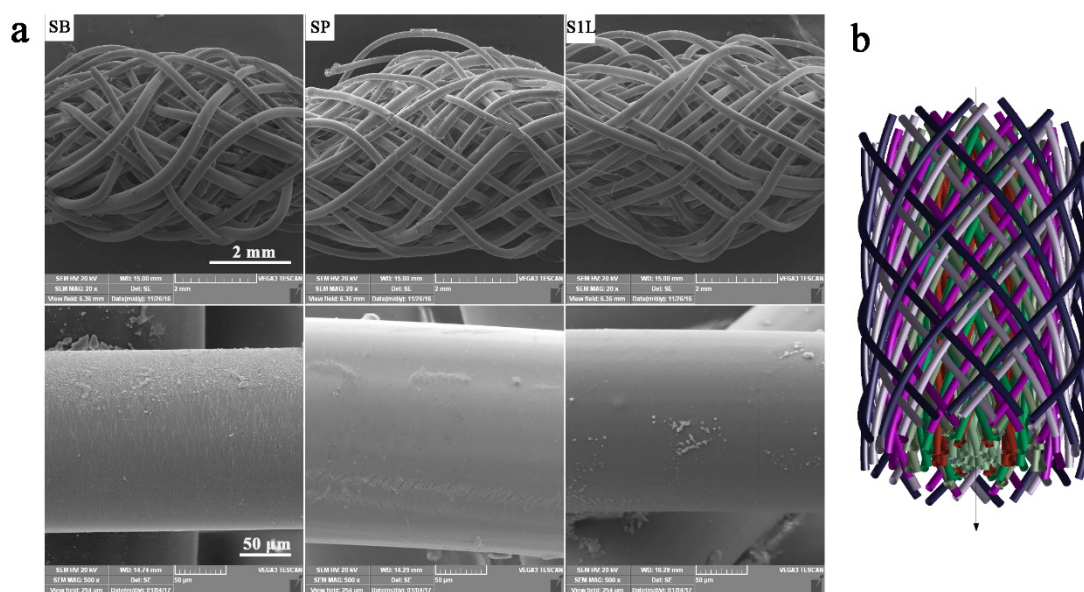
Figure 14 Morphology of PLCL scaffold and PLCL scaffold modified with PLL/HA by SEM (a) (SB: PLCL scaffold blank; SP: PLCL-PLL; S1L: PLCLPLL/HA-PLL). Global structure of the multi-layer braided scaffold. The six different constitutive layers, made of 16 fibers/layer, are represented with different colors (b).

4.2.1.3 Topology of PLL/HA modification on PLCL fibers

The interaction between cells and biomaterials is a complex process. PEM modification could influence the scaffold surface microenvironment as local mechanics, wettability, toughness, thus potentially resulting in an effect on cell attachment and proliferation. The topology of scaffold with/without modification was evaluated by CLSM and AFM

(Figure 15a&b). Firstly, PLL-FITC was used to replace PLL to study PLL/HA LBL modification on fibers, and then was detected to cover the fiber homogeneously by CLSM in Figure 15a, and from SP to S1L the fluorescence intensity was increased. The topology details of the fiber surfaces with/without PLL/HA modification are shown in Figure 15b, where the surface of fibers is globally seen to be flat and smooth. Irregular polygonal structures on the surface of SP were deduced to correspond to PLL molecules, while the "particles" structures on S1L were supposed to be HA molecules.
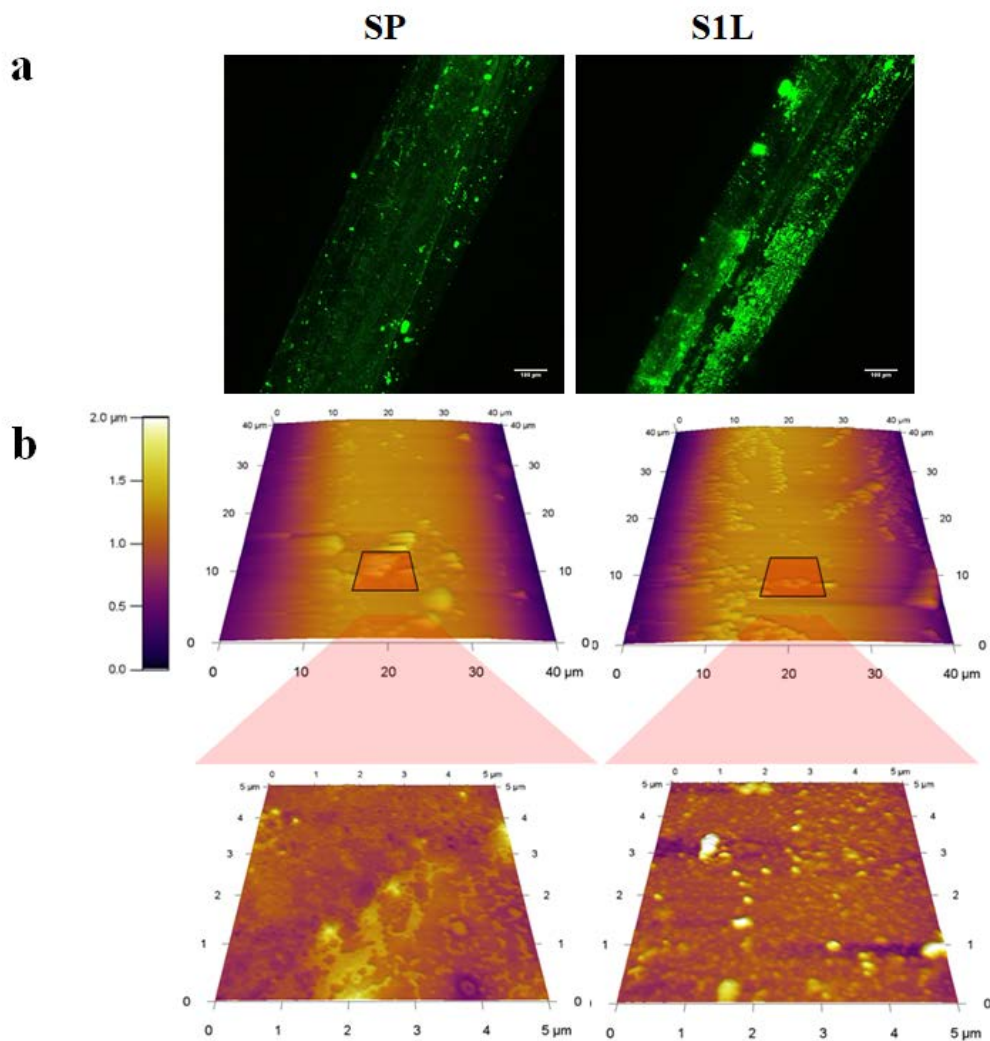
Figure 15 Morphology of PLL-FITC/HA on PLCL fiber by CLSM (a)and topology of PLL/HA on PLCL fiber by AFM (SP: PLCL scaffold-PLL-FITC; S1L: PLCL scaffold-PLL/HA-PLL) (b).

4.2.1.4 Mechanical properties of PLCL fibers with/without PLL/HA modification

Matrix stiffness varies depending on different organs and location in the body. The mechanical behavior is one of the elements to consider when selecting the material to fabricate a scaffold. Mechanical properties of PLCL and the effect of LBL modification on the behavior of isolated fibers mechanical properties were assessed by using tensile

tests (Figure 16). Young's modulus of fibers with no treatment, with a PLL modification and with one PLL/HA layer were respectively 1616 ± 643 MPa, 1608 ± 156 MPa and 1758 ± 470 MPa. No significant changes in Young's modulus were therefore observed. The three types of fibers broke for a strain around 15-25% with no significant effect of surface modification. Typical stress-strain curves as well as Young's modulus evolution obtained from PLCL fibers with/without modification are represented on Figure 16.
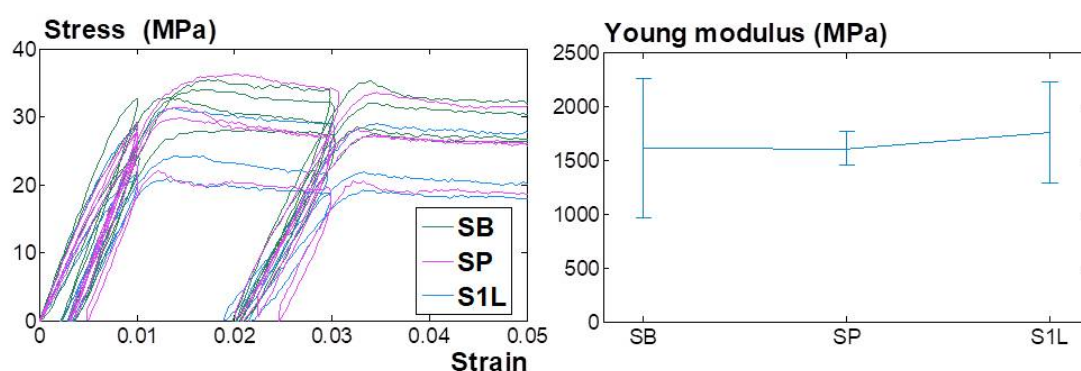
Figure 16 Mechanical testing of PLCL fibers (SB: PLCL fiber blank; SP: PLCL fiber-PLL; S1L: PLCL fiber-PLL/HA-PLL).

4.2.1.5 Effect of pH and PLL/HA layer numbers on WJ-MSC and BM-MSC biocompatibility

PLL/HA polyelectrolyte films have been reported to be a pH responsive PEM (Burke and Barrett 2003), which means that the physicochemical properties (surface friction, wettability) varies with pH adjustment. Both pH 6.0-6.5 and pH 7.4 have been applied for PLL/HA bilayer deposition in the literature (Yamanlar et al. 2011; Burke and Barrett 2003).The effect of PLL/HA PEM developed in different pH on cell attachment and

proliferation have been evaluated and results are shown in Figure 17. For WJ-MSCs, cell metabolic activity increased from pH7.4 to pH6.3; as the layer number increased, the cell metabolic activity decreased from S1L to S5L on pH6.3 and pH 7.4 for one week. For BM-MSCs, the cell metabolic activity also increased from pH7.4 to pH6.3, as the layer number increased more than one layer, cell metabolic activity decreased from day1 to day7 in both pH condition. When layer number increased to 5 layers, no increase of cell metabolic activity was detected. As a result, for both MSCs, cell proliferation did not increase over one-layer modification. Moreover, pH 6.3 for PEM deposition greatly encouraged MSCs metabolic activity, especially for WJ-MSCs. Consequently, in the present contribution, SB, SP and S1L made in pH 6.3 were selected.
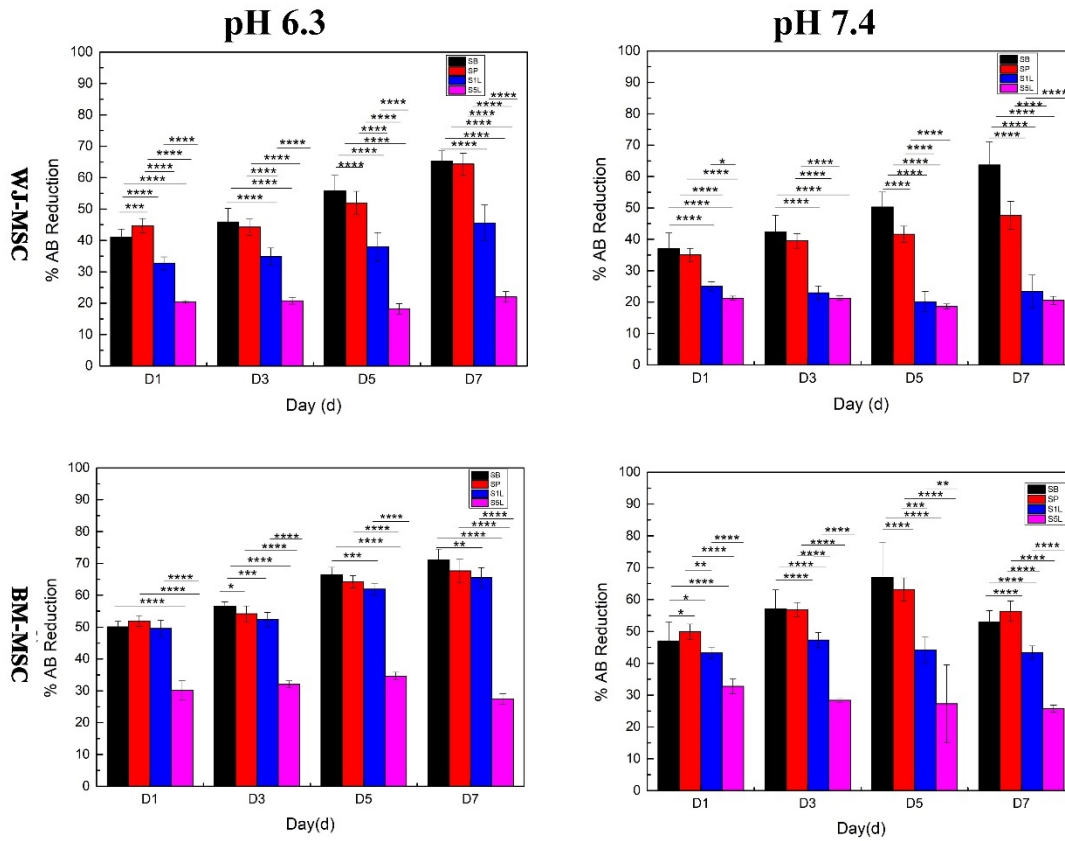
Figure 17 The metabolic activity of WJ-MSC and BM-MSC on SB, SP, S1L, S3L and S5L on day 1, day 3, day 5 and day 7 on pH6.3 and pH7.4 (PLCL scaffold blank, SP: PLCL-PLL, S1L: PLCL-PLL/HA-PLL, S3L: PLCL-(PLL/HA)3-PLL, S5L: PLCL-(PLL/HA)5-PLL, red: n=3 * $p<0.05$, **$p<0.01$, ***$p<0.005$, ****$p<0.001$)

4.2.2 Biocompatibility of MSCs on PLCL scaffold

4.2.2.1 MSCs metabolic activity on scaffold.

Cell metabolic activity on the scaffold was detected and tracked by AB assay from D1 to D7, and results are shown in Figure 18. The metabolic activity of WJ-MSCs on SB, SP and S1L increased 24.2%, 19.64%, and 12.82% respectively from day1 to day7; while for BM-MSCs, increased 21%, 15.77% and 15.95% on SB, SP and S1L from

day1 to day7. Although for WJ-MSCs and BM-MSCs cell metabolic activities were both improved from day1 to day7, while especially for WJ-MSCs, the cell metabolic activities decreased as the surface treatment went from SB to SP and S1L. WJ-MSCs tended to be more sensitive to PLL/HA modification than BM-MSCs, as more difference between SB and S1L were observed. Up to one-layer modification, both WJ-MSCs and BM-MSCs showed good biocompatibility on scaffold.
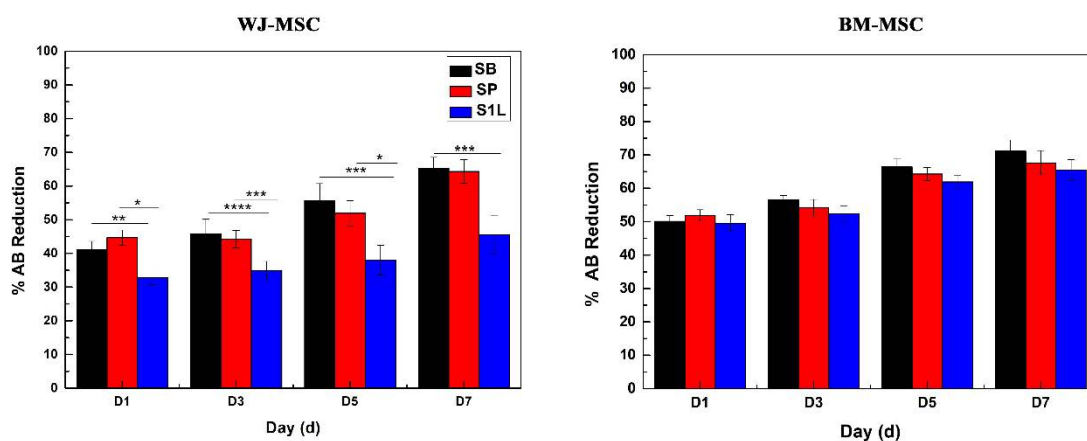
Figure 18 Reduction of AB of WJ-MSCs and BM-MSCs on PLCL scaffold (AB: Alamar Blue; SB: PLCL scaffold blank; SP: PLCL-PLL; S1L: PLCL-PLL/HAPLL) (n = 3,*$p < 0.05$, **$p < 0.01$, ***$p < 0.005$, ****$p < 0.001$).

4.2.2.2 MSCs morphology and location on the scaffold.

The morphology and location of MSCs on the scaffold by SEM (Figure 19) showed that cells gathered to form cell sheets between fibers, and also indicated ECM synthesis. Fluorescent images (Figure 20) displayed details of cytoskeleton and cell nuclei. The spindle and elongated shape of MSCs was observed along the fibers. MSCs tended to

grow along the longitudinal direction of the fiber in a homogeneous manner, migrated and proliferated across fibers to form cell bridges. Quantification of morphological changes of nucleus induced by scaffolds is illustrated in Figure 21. Mean nuclear area of WJ-MSCs (224.7 µm²) was smaller ($p < 0.05$) than BM-MSCs (246.9 µm²) on tissue culture polystyrene (TCPS). For WJ-MSCs, the mean nuclear area did not change between cells on scaffold and cells on TCPS. In contrast, for BM-MSCs, the mean nuclear area decreased for cells on SB and S1L compared to cell nucleus on TCPS. The nuclear aspect ratio (length/width) of cells significantly increased ($p < 0.05$) comparing to cell nucleus on TCPS for both WJ-MSCs and BM-MSCs.

Cell shape is reported to be related to cell fate. It was indeed noted that cell shape changed as a result of surface protein changes (integrins, cadherins and cytoskeletal proteins) during stem cell commitment and differentiation (Gumbiner 1996; Hu, Tontonoz, and Spiegelman 1995). However, not only differentiation leads the cell shape to change, but it was also reported that modifications in cell shape could alter the differentiation of precommitted mesenchymal lineages (Spiegelman and Ginty 1983). Both WJ-MSCs and BM-MSCs tended to exhibit an elongated shape along fiber direction compared with cells on culture plate, which could be helpful to mimic ligament tissue adapted to mechanical tensile loading.
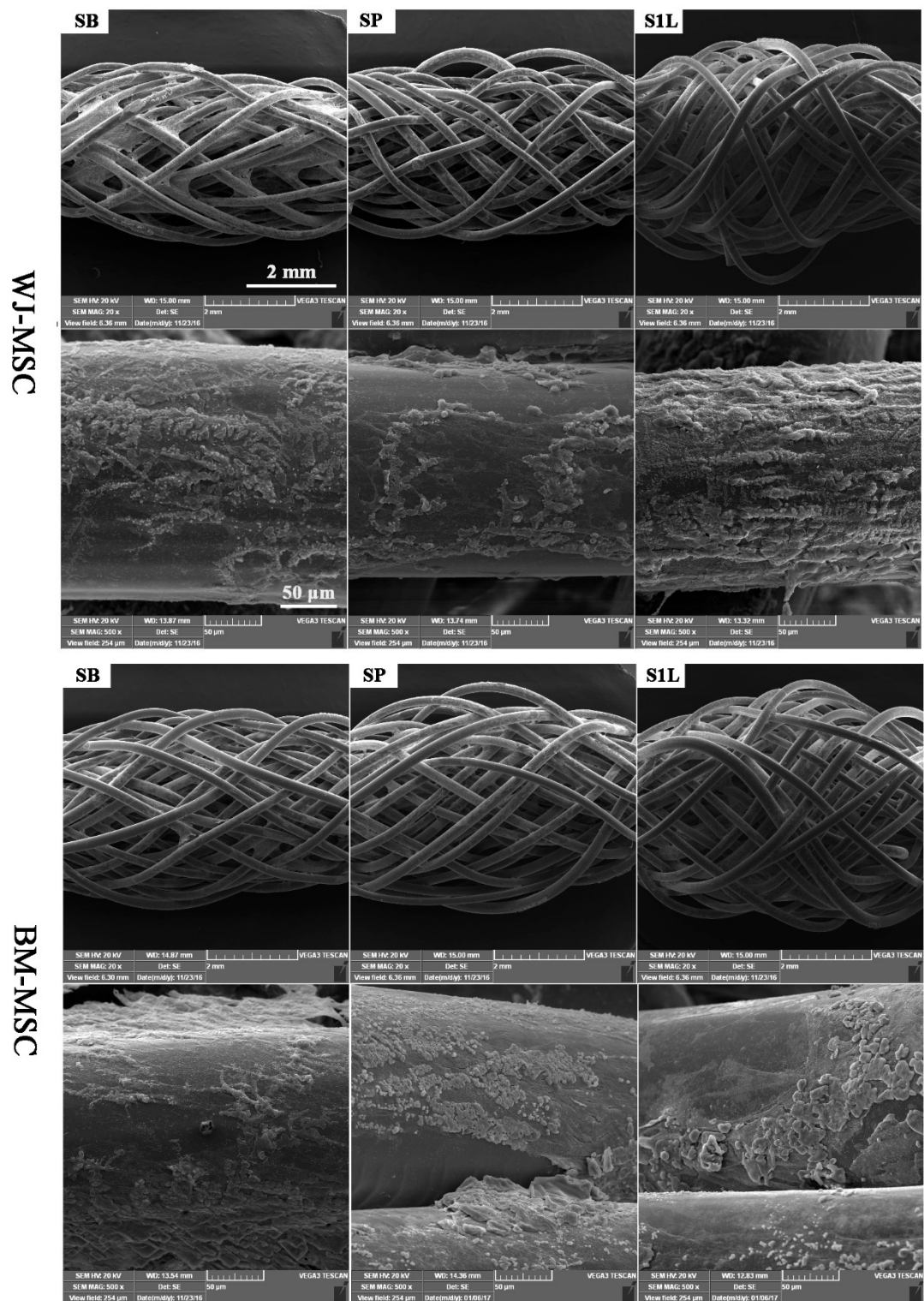
Figure 19 Morphology and distribution of WJ-MSCs and BM-MSCs on scaffolds by

SEM (SB: PLCL scaffold blank; SP: PLCL-PLL; S1L: PLCL-PLL/HA-PLL).
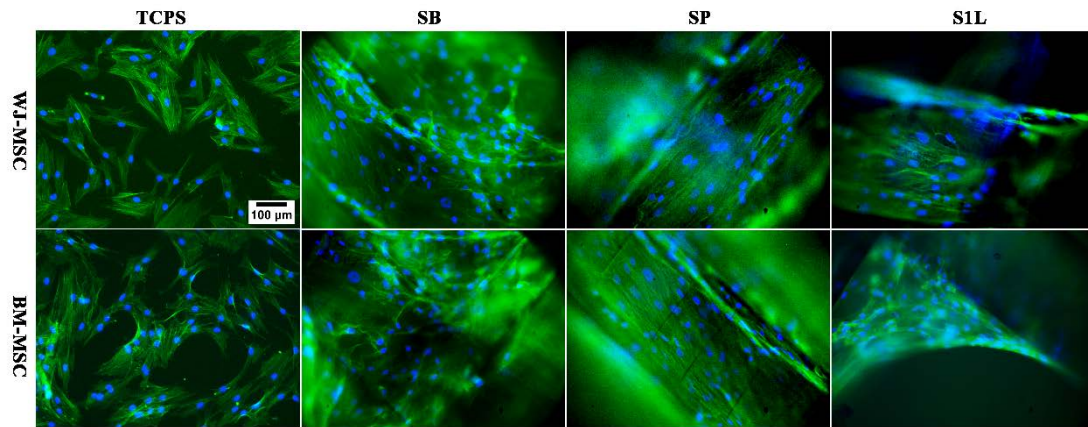
Figure 20 Morphology and distribution of WJ-MSCs and BM-MSCs on scaffolds by

CLSM (SB: PLCL scaffold blank; SP: PLCL-PLL; S1L: PLCL-PLL/HA-PLL; green:

Alex phalloidin 488; blue: DAPI).
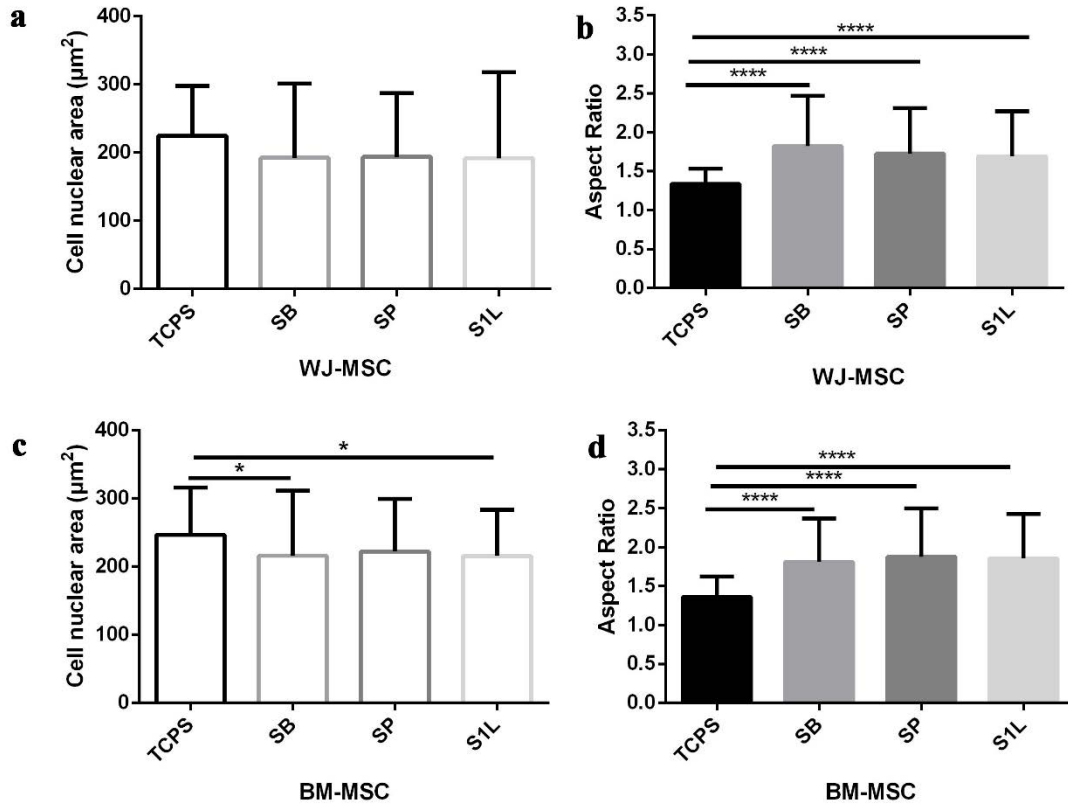
Figure 21 Quantification of cell nucleus elongation. (a) Mean nuclear area of WJ-MSCs; (b) cell nuclear aspect ratio of WJ-MSCs; (c) mean nuclear area of BM-MSCs cell nuclear; (d) cell nuclear aspect ratio of BM-MSCs. SB: PLCL. Scaffold blank; SP: PLCL-PLL; S1L: PLCL-PLL/HA-PLL; TCPS: tissue culture polystyrene (n $\geqslant$ 100 from more than 3 images, *$p < 0.05$, **$p < 0.01$, ***$p < 0.005$, ****$p < 0.001$).

4.2.2.3 ECM expression by MSC on the scaffold.

As reminded in chapter I, the main composition of native ligament ECM includes Col I, Col III, proteoglycans, TNC, water and etc. (LEE 2005; Doroski, Brink, and Temenoff 2007). Results concerning collagen expression in the different treated and non-treated scaffolds are shown in Figure 22. Green points on the scaffolds correspond

to Col I, Col III, and TNC synthesized by WJ-MSCs and BM-MSCs respectively on day 14. It was observed that both types of collagens were substantially secreted, independently of the surface modification. Col I account for almost 80% of nature ligament ECM, and Col III takes up about 10%. TNC is a member of glycoprotein, which makes up very smaller proportion of native ligament tissue. In the present study, fluorescent signal represent Col I was stronger than Col III and TNC, which indicating that MSCs-PLCL constructs are consistent to native ligament tissue.
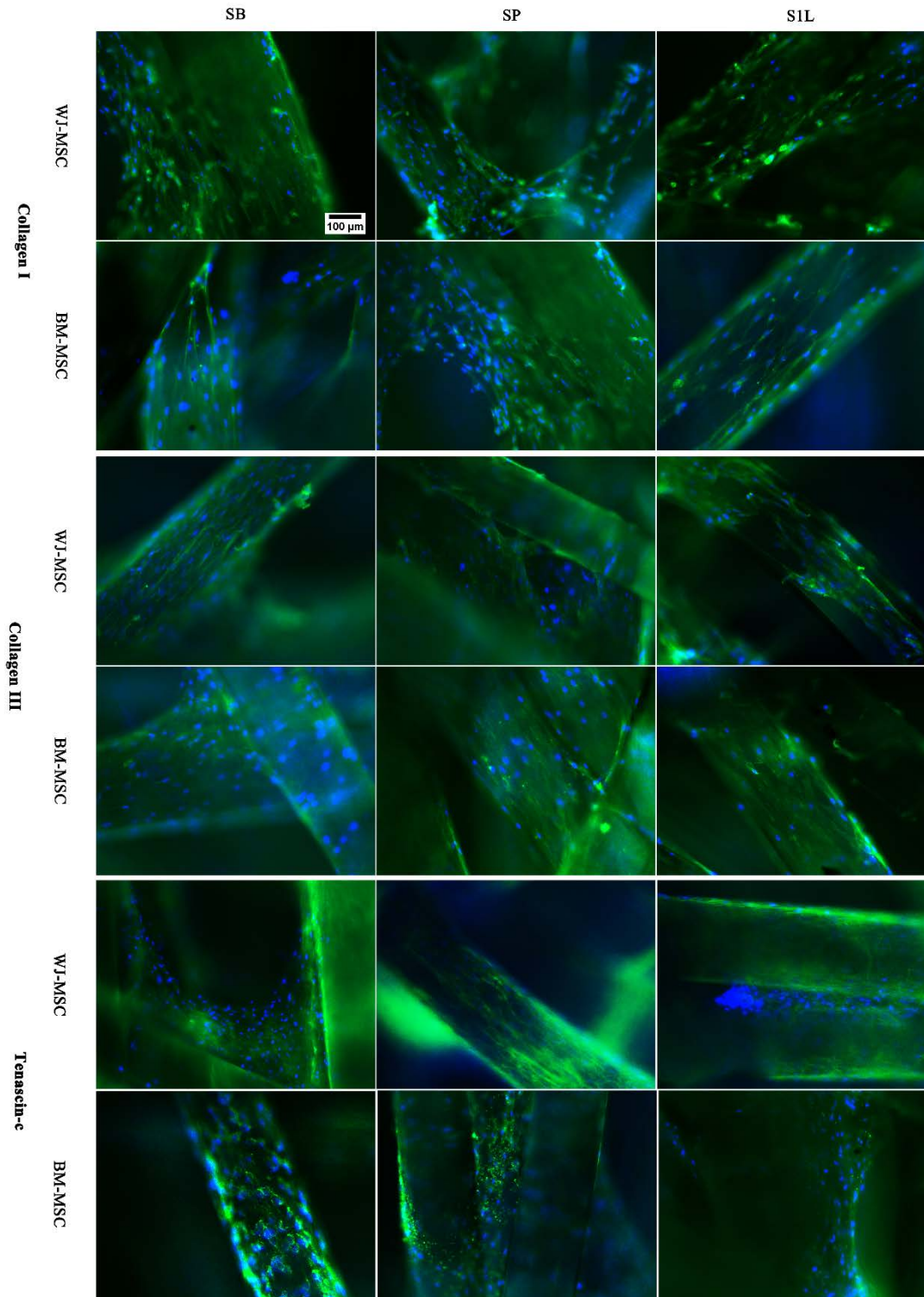
Figure 22 Col I, Col III, and TNC expression by WJ-MSCs and BM-MSCs on PLCL-based scaffolds on day 14 (Blue: DAPI; green: Col I, Col III, and TNC; SB: PLCL scaffold blank; SP: PLCL-PLL; S1L: PLCL-PLL/HA-PLL).

4.2.2.4 Chemotactic properties of scaffold on MSCs

Cell homing and migration is a crucial step in cell-based therapy, as the efficiency of cell therapy mainly depends on MSCs juxtracrine and paracrine to promote regeneration and healing (Sohni and Verfaillie 2013). Therefore, cell migration was assessed to evaluate the effect of scaffold and scaffold modification on MSCs chemotaxis. As fluorescent images show in Figure 23, the number of migrated BM-MSCs tended to be higher than WJ-MSCs induced by SB, SP and S1L and confirmed by fluorescent intensity. It also demonstrated that MSCs chemotaxis was most activated under the stimulation of S1L for WJ-MSCs and BM-MSCs by fluorescent spectrophotometer. Consequently, our results showed that chemotaxis of WJ-MSCs and BM-MSCs was activated by SB, SP, and S1L. This migration was even more pronounced for one-layer scaffold, compared to SB and SP. This may show a possibility to recruit MSC for *in vivo* implantation.
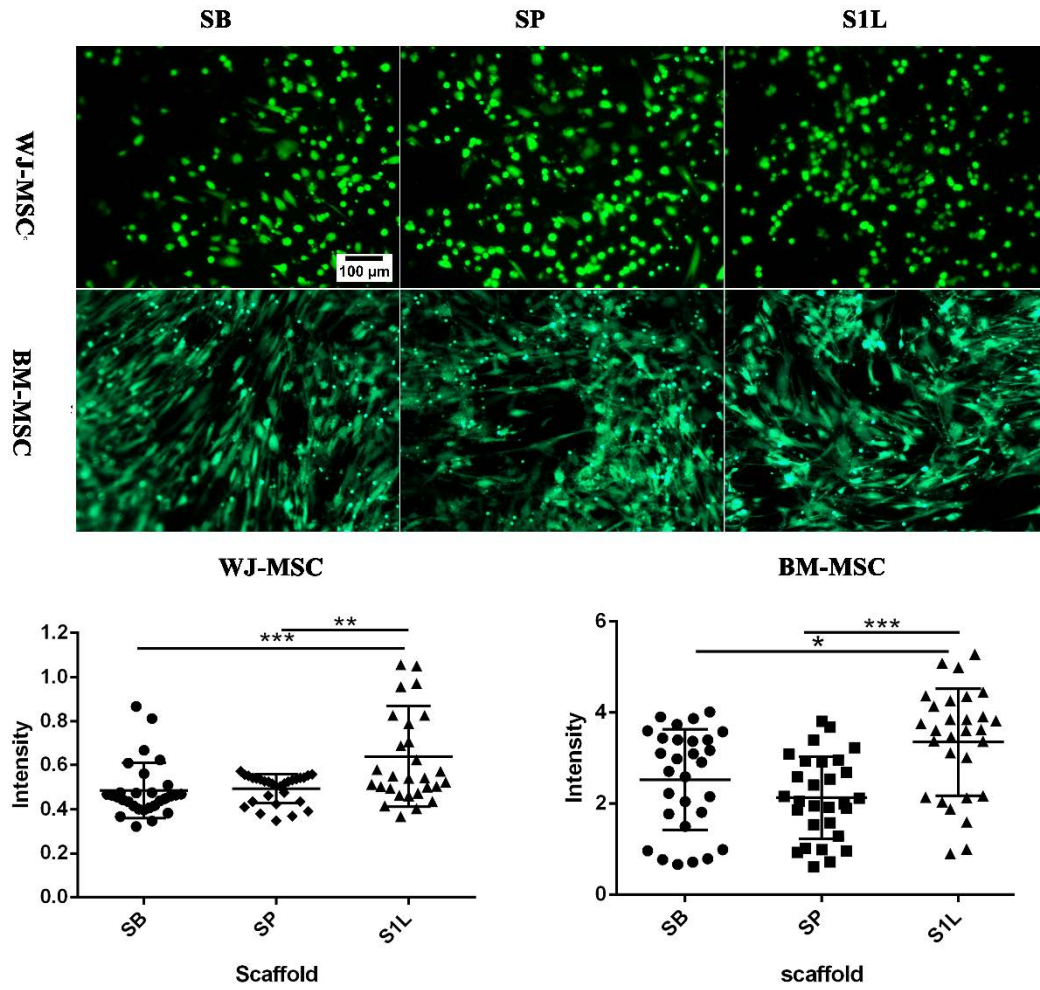
Figure 23 Migration of WJ-MSCs and BM-MSCs induced by PLCL scaffold, scaffold-PLL, and scaffold-PLL/HA-PLL (Green: Calcein AM; SB: PLCL scaffold blank; SP: PLCL-PLL; S1L: PLCL-PLL/HA-PLL; n = 3, *$p < 0.05$, **$p < 0.01$, ***$p < 0.005$).

4.3 Conclusion

PLCL braided scaffolds with/ without PLL/HA modification were developed in the study reported in the present chapter. The mechanical, morphological, and biological results concerning the WJ-MSCs and BM-MSCs behaviors, and the ECM synthesis

showed that such scaffolds may constitute a promising solution for ligament tissue engineering. The incorporation of LBL modification increased cell chemotaxis, which opens interesting perspectives for *in vivo* application. The developed LBL technology may permit to incorporate growth factors on PLCL braided scaffold to encourage tissue growth and the regeneration of a functional ligamentous tissue

5   Chapter V : Proposition of silk and silk/PLCL scaffold for ligament tissue engineering

This chapter is based on an article in preparation. "Characterization of WJ-MSC and BM-MSC response on multilayer braided silk and silk/ PLCL scaffolds for ligament tissue engineering" Xing Liu, Frédéric Velard, Adrien Baldit, Ghislaine Cauchois, Yun Chen, Emilie de Brosses, Xiong Wang, Natalia de Isla, Cédric Laurent.

5.1 Introduction

In last chapter V, PLCL, as a favorable synthetic polymer for biomedicine, has showed excellent mechanical properties and biocompatibility for MSCs attachment, proliferation, migration and extracellular matrix synthesis towards ligament tissue engineering (X. Liu et al. 2018). Moreover, it is known to exhibit a controllable degeneration rate, high flexibility and tunable elasticity, which could be interesting for a potential application in ligament regeneration. However, a recent study performed by our team (C. P. Laurent et al. 2018) has emphasized that PLCL fibers exhibited a brittle behavior after a two-months degradation period, which may indicate that PLCL scaffold could be associated with a premature post-surgery failure risk. This pointed out that it still remains an urgent requirement to seek for a suitable scaffold to fulfill the biological and mechanical requirements for ligament regeneration.

Among the available constitutive materials for scaffolds, silk (D. Ma, Wang, and Dai

2018) is a natural protein-based polymer, which possesses remarkable mechanical properties, excellent biocompatibility, controllable degradability, and low immunogenicity. As already stated in the section 1.7.2.1, researches on silk-based composites have been proved to constitute a promising solution for ligament reconstruction. Besides, silk exhibits high mechanical strength up to 4.8 GPa, good toughness and strain to rupture up to 35% (Altman et al. 2003). However, it has been demonstrated to offer slow degenerate rates since no obvious degradation was observed after 18 months post-implantation *in vivo* (Shen et al. 2014), and it has been classified as "non-degradable" biomaterial by FDA. Considering that the mechanical strength and degradation properties play an essential role for designing a transplantable scaffold towards musculoskeletal tissues, a novel composite scaffold have been fabricated in the study reported in the present chapter. This composite scaffold is based on PLCL associated with silk in the braiding structure presented in the previous chapter. In parallel, a series of multilayered (n=1,2,3) silk scaffolds have also been prepared to be confronted with this new silk/PLCL composite scaffold.

In the study reported in the present chapter, WJ-MSCs and BM-MSCs have been seeded on the different proposed scaffolds. Different cell behaviors, including cell proliferation, cell morphology and location, live/dead cell distribution, cell migration and extracellular matrix synthesis, have been evaluated to assess the potential of such scaffolds to constitute a candidate for ligament tissue engineering.

5.2 Results and discussion

The methodology concerning the processing and biological, mechanical and morphological characterizations of silk and silk/PLCL composite scaffolds are detailed in the sections 2.3, 2.4 and 2.5.

5.2.1 Physiochemical properties of silk-based braided scaffold

5.2.1.1 Morphology of scaffold by SEM

SEM images of silk in different layers (n=1,2,3) and silk/PLCL composite scaffolds are shown in Figure 24. All the scaffolds showed a braided and porous structure, and as the layer number increased, the structure was more compacted, and the diameter of scaffold was enlarged. Based on the SEM images, the diameter of silk yarn was about 281 ± 43 μm, and the diameter of PLCL fiber was about 170 μm. The diameters of S1, S2, S3 and SP were comprised around 2.47 ± 0.14, 3.13 ± 0.12, 3.77 ± 0.66, and 3.3 mm respectively. In the silk/PLCL composite scaffold, the PLCL fiber was twisted and observed to cross between two silk layers. The cross section displayed a bunds of silk fibers and enlarged diameter from S1 to S3. Silk fibers and PLCL fibers were distinguished from cross section images. Porous scaffolds constitute attractive structure for nutrient and gas exchange and cell intergrowth. This multilayer porous braided structure has been confirmed by our previous study (C. P. Laurent et al. 2014a; X. Liu et al. 2018) to support cell attachment and tissue intergrowth; thus it was conserved to fabricate new scaffold based on silk for following study.

Figure 24 The morphology and cross-section of silk and silk/PLCL scaffolds (S1：
one-layer silk scaffold; S2: two-layer silk scaffold; S3: three-layer silk scaffold; SP:
silk/PLCL composite scaffold).

5.2.1.2 Porosity and pore size

Porosity is linked to subtracts exchange and local pH stability, and known to promote
tissue ingrowth and cell signaling (Chang and Wang 2011). Porosity and pore size
distribution were measured and compared for the four scaffolds based on μCT images
as described in the section 2.4.6, and the results are shown in Figure 25. The number of
layers of silk significantly affected the measured porosity (0.85 ± 0.04, 0.77 ± 0.02 and
0.53 ± 0.02 respectively for 1, 2 and 3 layers of silk), since the scaffolds were more and
more compact as the number of silk layers increased. On the contrary, the insertion of
a PLCL layer in the three-layer silk/PLCL scaffold resulted in a higher porosity ($0.74 \pm$

0.02) compared to the three-layers silk scaffold. Pore size distribution detected by watershed algorithms on µCT cross-sections did not result in significant differences between scaffolds. Pore sizes ranged between 20 and 150 µm with a typical Weibull distribution and slight differences between the different scaffolds. Mean computed pore sizes were 29.5 ± 18.2 µm, 28.6 ± 19.2 µm, 30.2 ± 25.5 µm and 28.7 ± 22.1 µm for S1, S2, S3 and SP respectively. Increased pore size lead to the reduction of surface area for whole scaffold, while if pore size is too small, it could limit cell migration. However, the validity of the common watershed algorithm used for µCT image processing is highly debatable in the case of this structure, since pores are largely elongated in the textile structure.

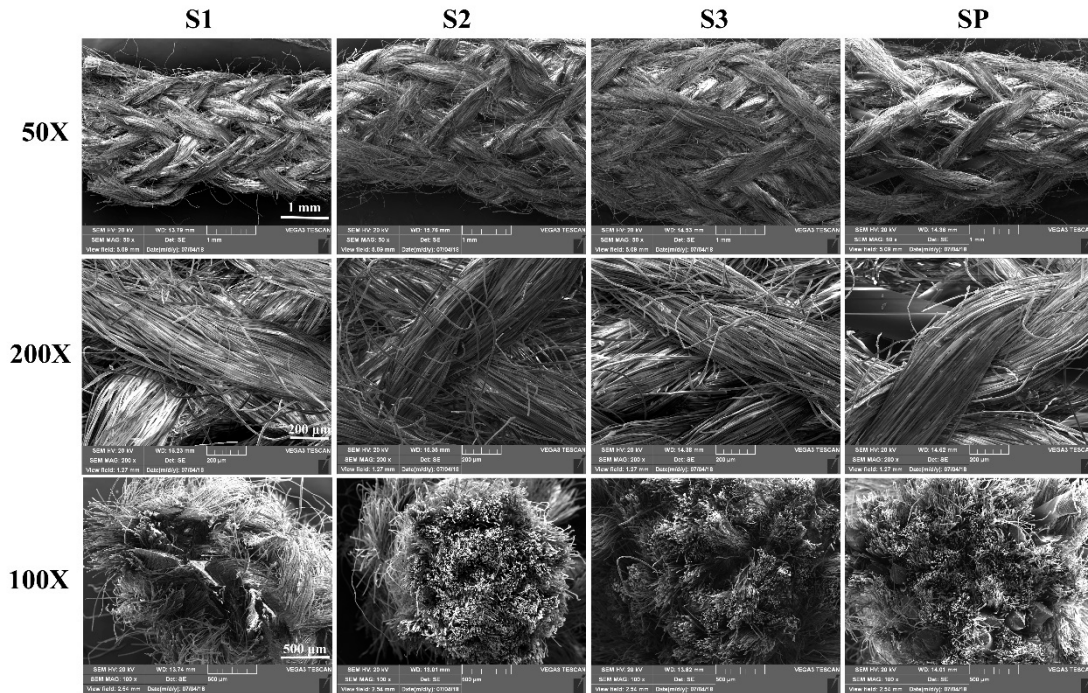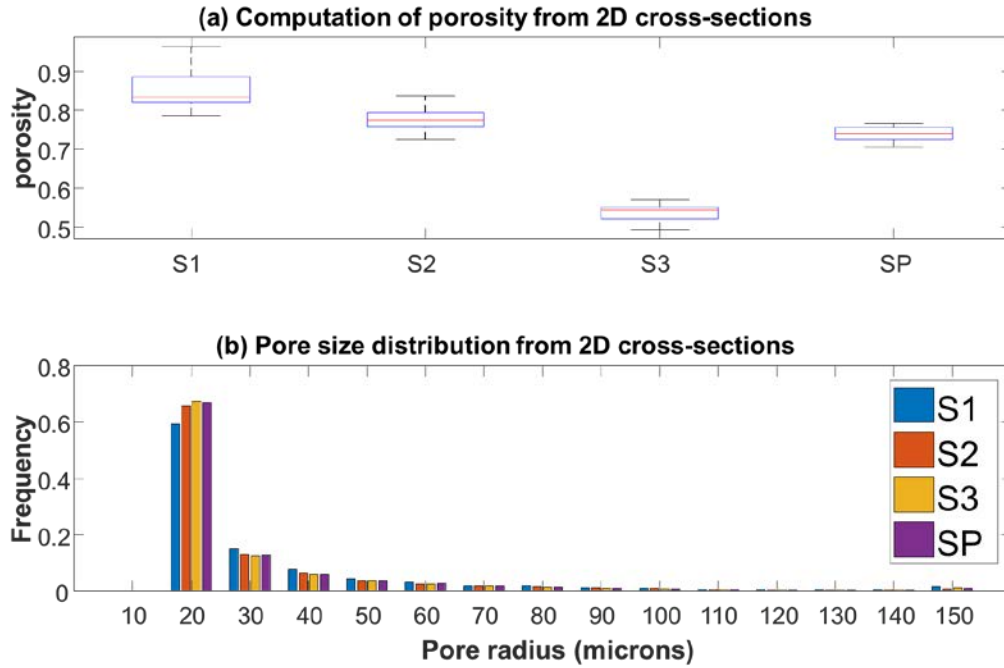Figure 25 Computed porosity and pore size distribution of silk and silk/PLCL scaffolds (S1: one-layer silk scaffold; S2: two-layer silk scaffold; S3: three-layer silk scaffold; SP: silk/PLCL composite scaffold).

5.2.1.3 Mechanical properties

The loading-unloading cycles prescribed to the scaffolds (S1, S2, S3 and SP, n=2) are illustrated in Figure 26, while the corresponding force-strain responses are shown in right image. Scaffolds showed a pronounced J-shape stress-strain response, with tangent apparent modulus increasing with the prescribed strain. The stress-strain responses were used to define "toe" and "heel" tangent moduli at the beginning and the end of each prescribed cycle respectively. The toe tangent modulus decreases for each configuration until reaching a near-zero value as the prescribed strain increases. The "heel" tangent modulus increases as the prescribed strain increases, emphasizing the

well-known non-linear J-response for textile and biological materials. There were no significant differences between the four different scaffold configurations in terms of the two tangent moduli. Values of tangent apparent modulus was in the range 80-115 MPa for the four different scaffolds, which is comparable to a native ligament (Kendoff, Morgan-Jones, and Haddad 2016). Obviously, there is a difference between these different scaffold configurations if we consider the raw force instead of the stress, with mean values of reached forces at 10% equal to 5.2 N, 9.8 N, 10.1 N, and 8.7 N respectively for S1, S2, S3 and SP. It is worthy to note that, when subject to rupture, the SP configuration show very large strain to rupture due to the ductility of PLCL at 37 °C. From a pure mechanical point of view, it seems that S2, S3 and SP may constitute a better choice than S1 due to the higher obtained forces. They also show lower "toe" tangent moduli, which may be indicated to restore native ligament function and flexibility. It is worthy to note that SP may constitute a safer choice since PLCL contributed to scaffold integrity when subject to very large strain.
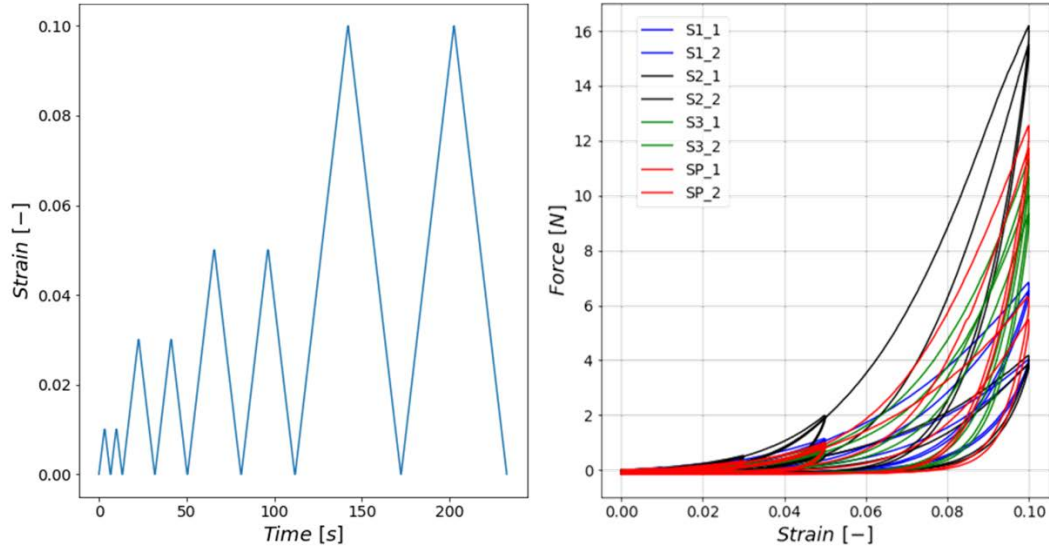
Figure 26 Prescribed loading-unloading cycles (left) corresponding responses (right) (n=2) of the different silk and silk-based/PLCL scaffolds (S1: one-layer silk scaffold; S2: two-layer silk scaffold; S3: three-layer silk scaffold; SP: silk/PLCL braided composite scaffold).

5.2.2 Biological properties of silk-based braided scaffold

5.2.2.1 Metabolic activity of MSCs on scaffolds

The metabolic activities of WJ-MSCs and BM-MSCs on silk-based scaffolds were investigated by the test of AB assay on day 1, 3, 5 and 7. As shown in Figure 27, the metabolic activity of WJ-MSCs on S1, S2, S3 and SP increased from 44.4 ± 4.35%, 40.4 ± 4.41%, 36.3 ± 2.38% and 40.6 ± 4.22% respectively, to 49.5 ± 5.13%, 46.1 ±4.63%, 40.3 ± 4.18% and 44.9 ± 4.85% from day1 to day7. The metabolic activity of BM-MSC on S1, S2, S3 and SP increased from 43.9 ± 6.79%, 44.09 ± 8.26%, 43.76 ± 6.44% and 47.14 ± 7.11% respectively, to 54.4 ± 4.8%, 57.89 ± 5.77%, 51.44 ± 11.26% and 57.13 ± 4.59% from day1 to day7. WJ-MSCs appeared more sensible to the

decrease of porosity than BM-MSCs, since WJ-MSCs metabolic activity decreased as the number of layers increased from S1 to S3 and kept almost the same level for S3 from d1 to d7. For BM-MSCs, cell metabolic activity increased with no significant difference from day1 to day7.

Figure 27 Almar Blue of WJ-MSCs and BM-MSCs on silk and silk/PLCL scaffolds. (S1:one-layer silk scaffold; S2: two-layer silk scaffold; S3: three-layer silk scaffold; SP: silk/PLCL composite scaffold. *$p < 0.05$, **$p < 0.01$, ***$p < 0.005$, ****$p < 0.001$)

5.2.2.2 Morphology of MSCs on scaffolds

5.2.2.2.1   MSCs distribution on scaffold by SEM

The SEM images of WJ-MSCs and BM-MSCs on scaffolds are showed in Figure 28 & Figure 29. MSCs attached and proliferated well on silk-based scaffolds. Cells were gathered together to form cell sheets, and extracellular matrix was observed for both WJ-MSCs and BM-MSCs on S1, S2, S3 and SP. For both WJ-MSCs and BM-MSCs, less cells were located on S3 compared with S1, S2 and SP, while more BM-MSCs were

located on S3 compared with WJ-MSCs.
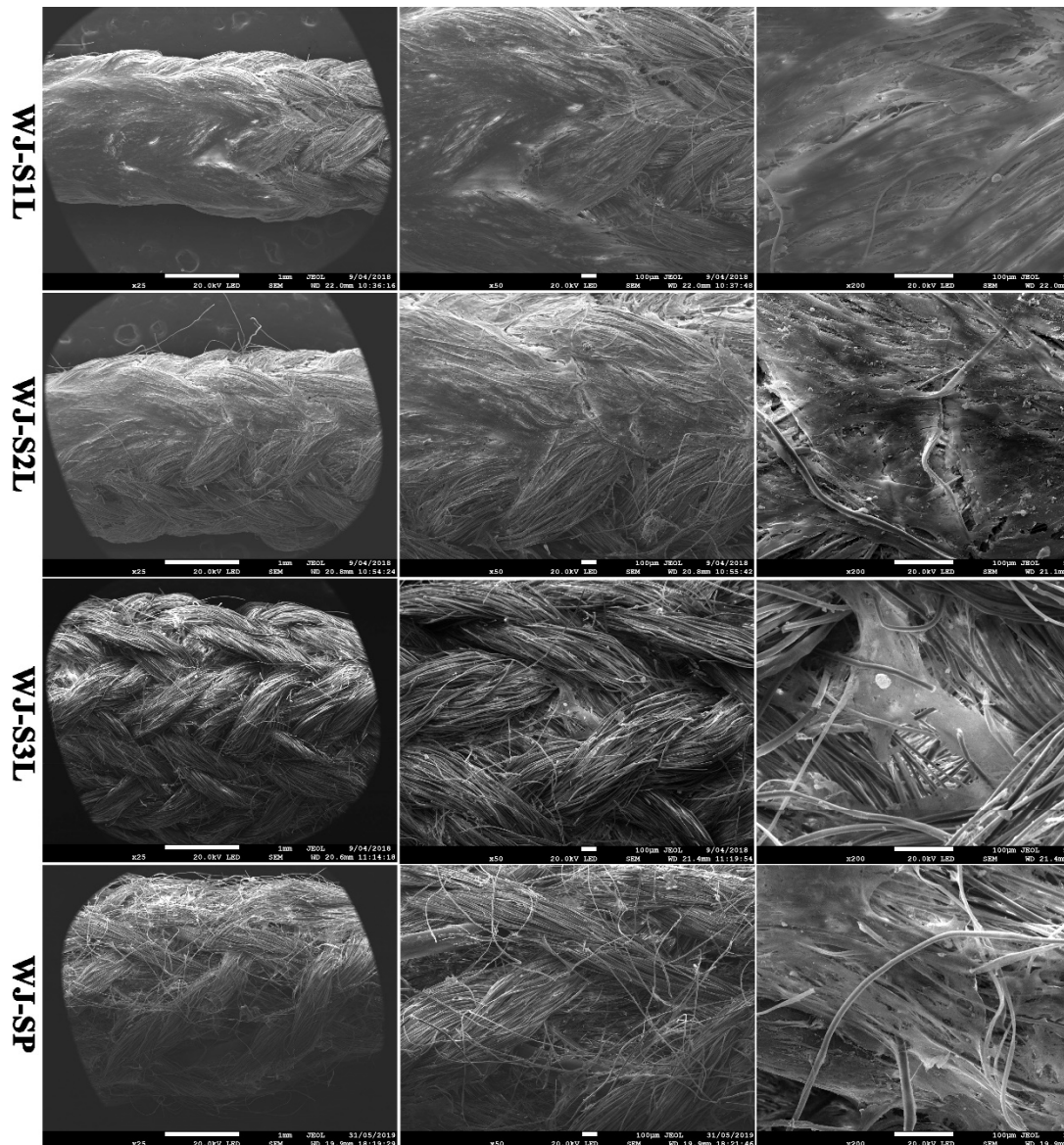
Figure 28 The morphology of WJ-MSCs on silk and silk/PLCL scaffolds imaged by

SEM (S1: one-layer silk scaffold; S2: two-layer silk scaffold; S3: three-layer silk

scaffold; SP: silk/PLCL composite scaffold).
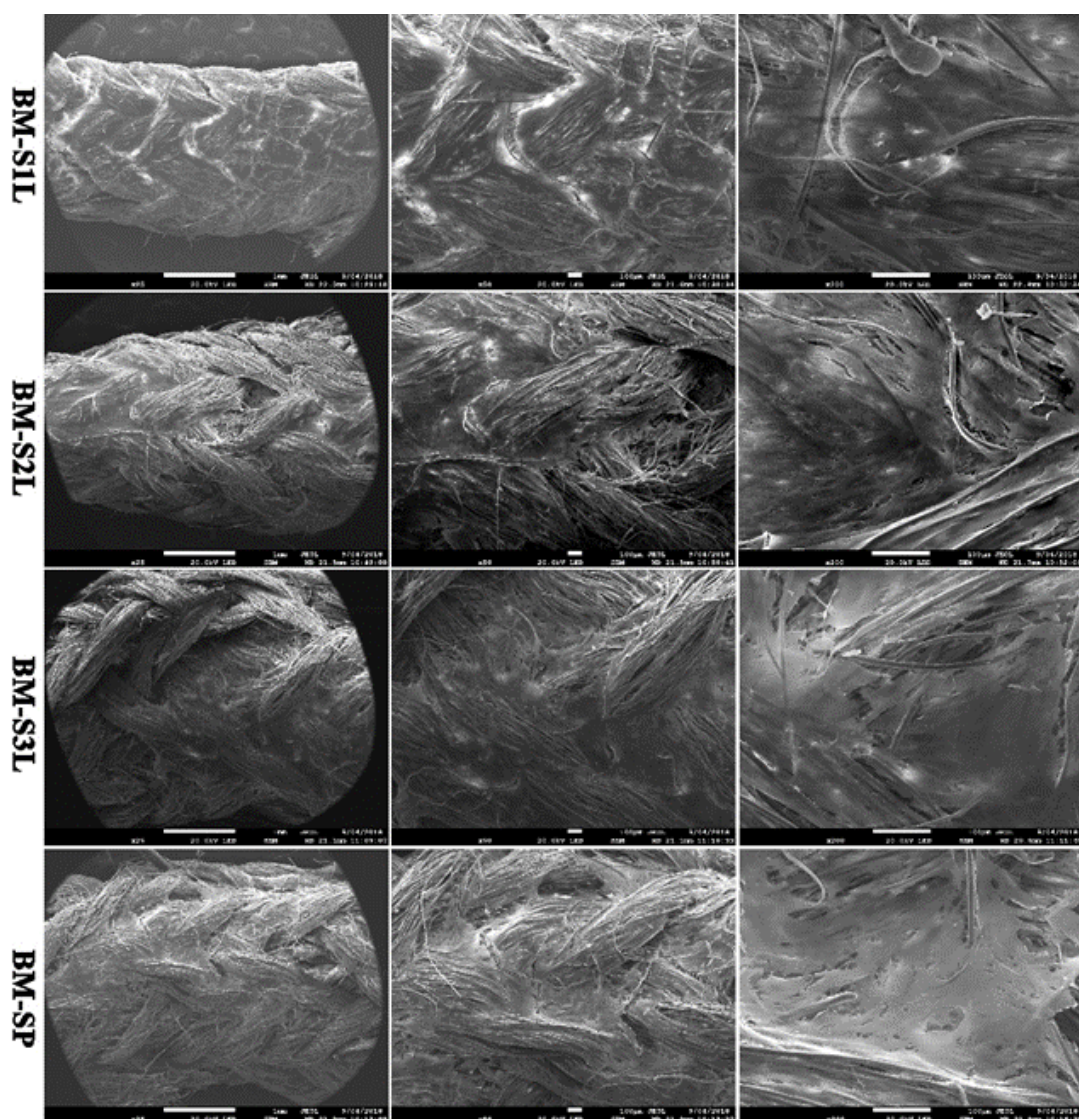
Figure 29 The morphology of BM-MSCs on silk and silk/PLCL scaffolds imaged by
SEM (S1: one-layer silk scaffold; S2: two-layer silk scaffold; S3: three-layer silk
scaffold; SP: silk/PLCL composite scaffold).

5.2.2.2.2   Live/dead staining of MSCs on scaffolds by fluorescence microscopy

Living/dead cells on scaffolds were stained and distinguished with Calcein AM/EthD-
1. Results are presented in Figure 30 & Figure 31, in which green cells represent living
cells stained with Calcein AM, while red cells correspond to dead cells stained with

Ethd-1. MSCs proliferated along the silk fibers longitudinal direction with a spindled shape. They were observed to grow across the silk yarn to form extracellular matrix bridges and were also observed to penetrate and grow between fibers in each silk yarn. For WJ-MSCs (Figure 30), more dead cells were observed on S3 and fewer dead cells were observed on S1, S2 and SP scaffolds, which may be due to the more compacted structure and an associated decreased porosity limiting nutrient supply and cell ingrowth. For BM-MSCs, few dead cells were observed on all the scaffolds compared with WJ-MSCs. BM-MSCs (Figure 31) presented a more uniformly spindle shape and oriented more clearly on the fiber longitudinal direction compared with WJ-MSCs. Except for S3, cells randomly oriented on the silk due to relatively plain surface. BM-MSCs presented a better cell viability than WJ-MSCs since fewer dead cells were observed on BM-MSCs-scaffolds.
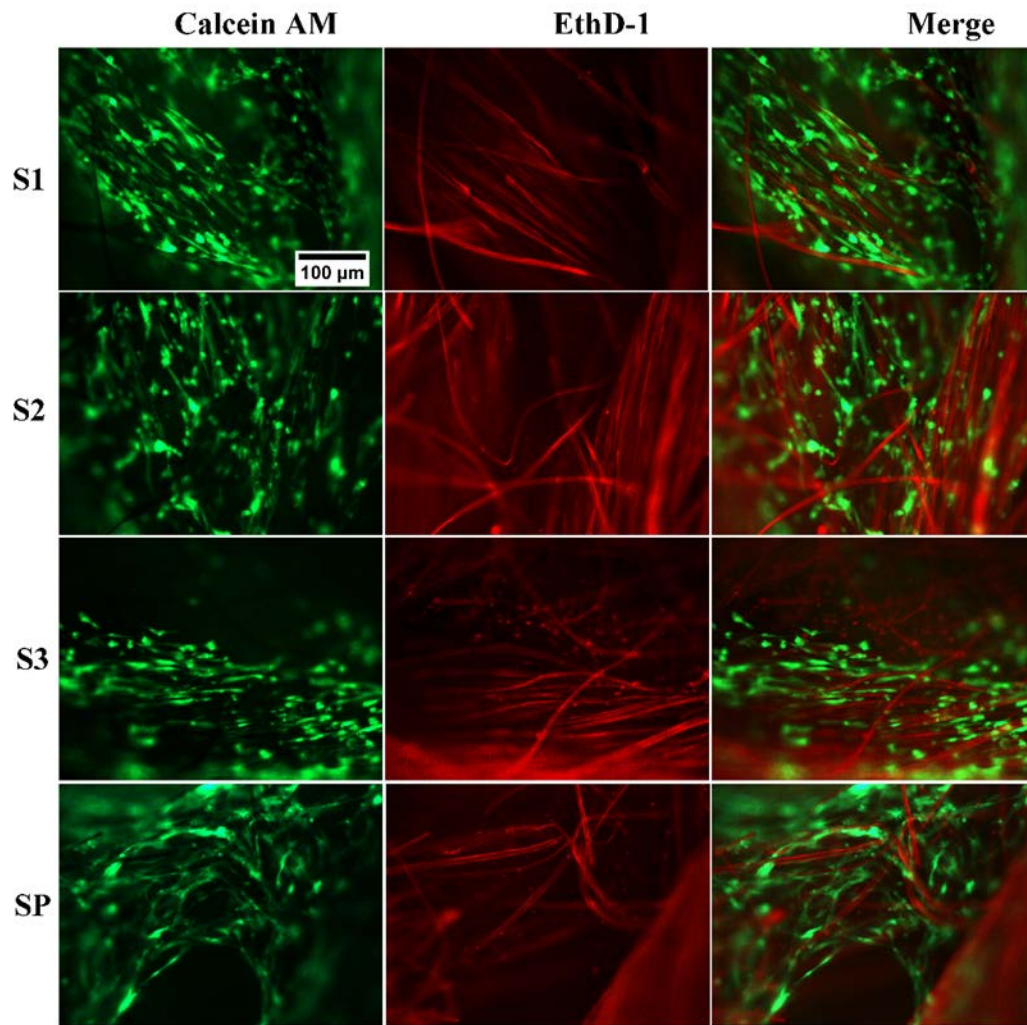
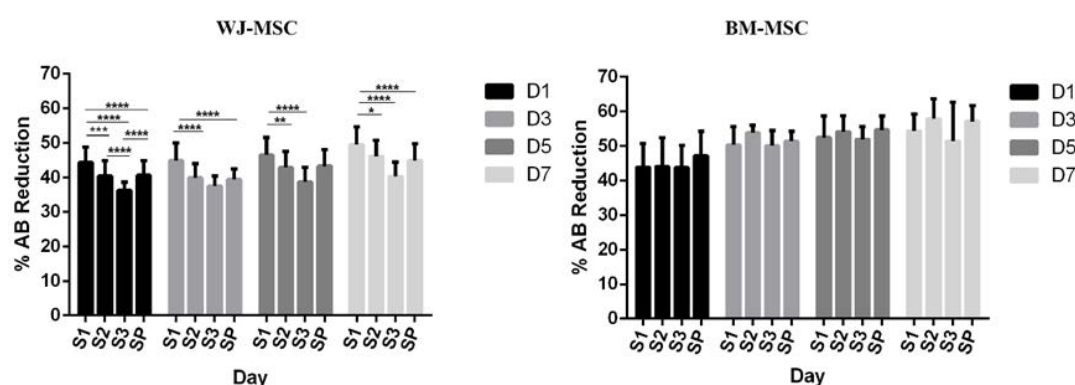Figure 30 The fluorescent images of live/dead staining of WJ-MSCs on silk and silk/PLCL scaffold (S1: one-layer silk scaffold; S2: two-layer silk scaffold; S3: three-layer silk scaffold; SP: silk/PLCL composite scaffold; green: Calceine AM; red: Ethidium homodimer I, dead cells).
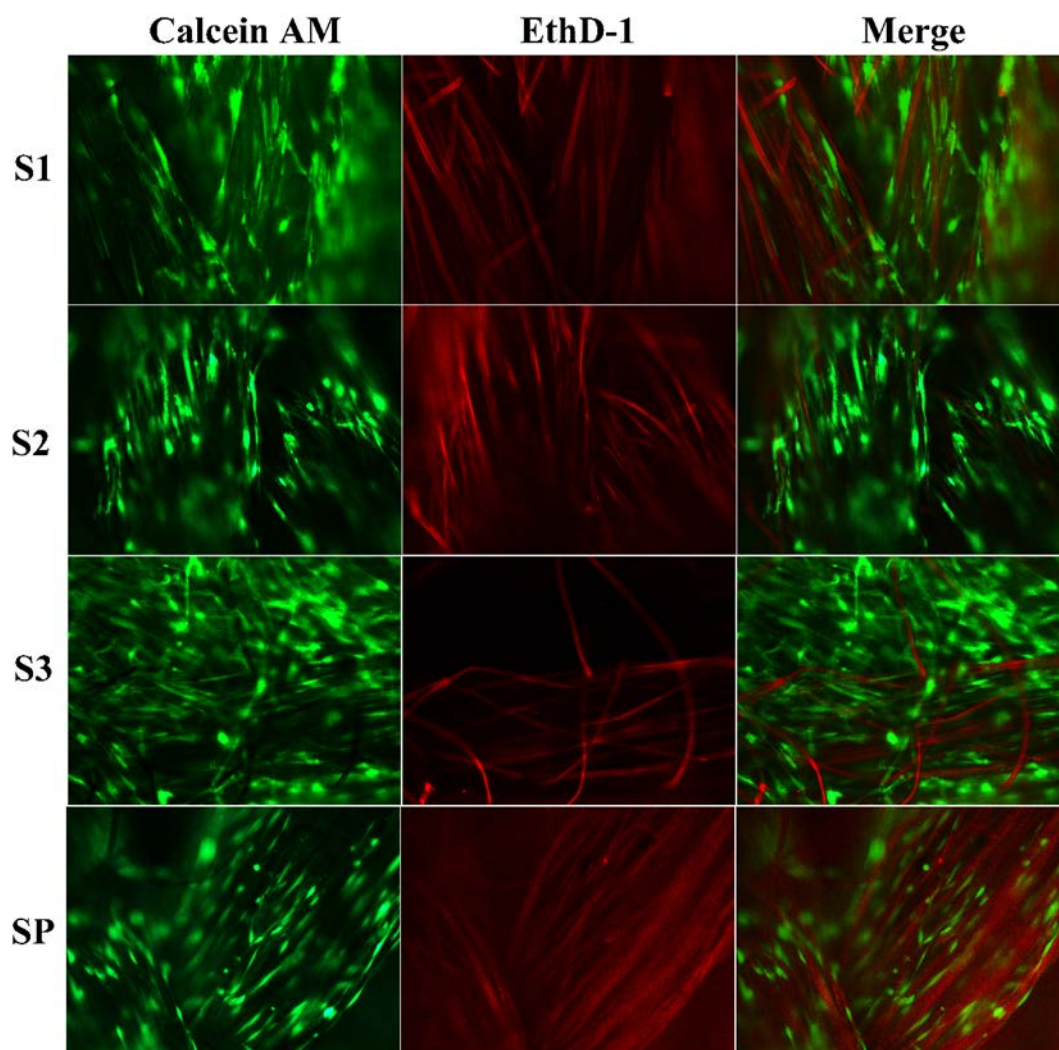
Figure 31 The fluorescent images of live/dead staining of BM-MSCs on silk and silk/PLCL scaffolds (S1: one-layer silk scaffold; S2: two-layer silk scaffold; S3: three-layer silk scaffold; SP: silk/PLCL composite scaffold; green: Calceine AM, living cell; red: Ethidium homodimer I, dead cells).

5.2.2.3 Chemotaxis properties of MSCs

As reminded previously, cell migration is a critical process for wound healing and tissue regeneration. MSCs migrate and proliferate into scaffold to deposit ECM and the

paracrine function of MSCs also facilitate tissue regeneration. MSCs chemotaxis stimulated by scaffolds was evaluated by a transwell migration assay, and results are shown in Figure 32. Under the same stimulation condition, BM-MSCs showed better chemotaxis activity than WJ-MSCs within 24 h, in accordance with our previous study (Liu et al. 2018). For both WJ-MSCs and BM-MSCs, cell migrated more in SP group (silk/PLCL composite scaffolds) than in other groups (silk scaffolds), indicating that combining silk with PLCL is favorable to cells attraction.
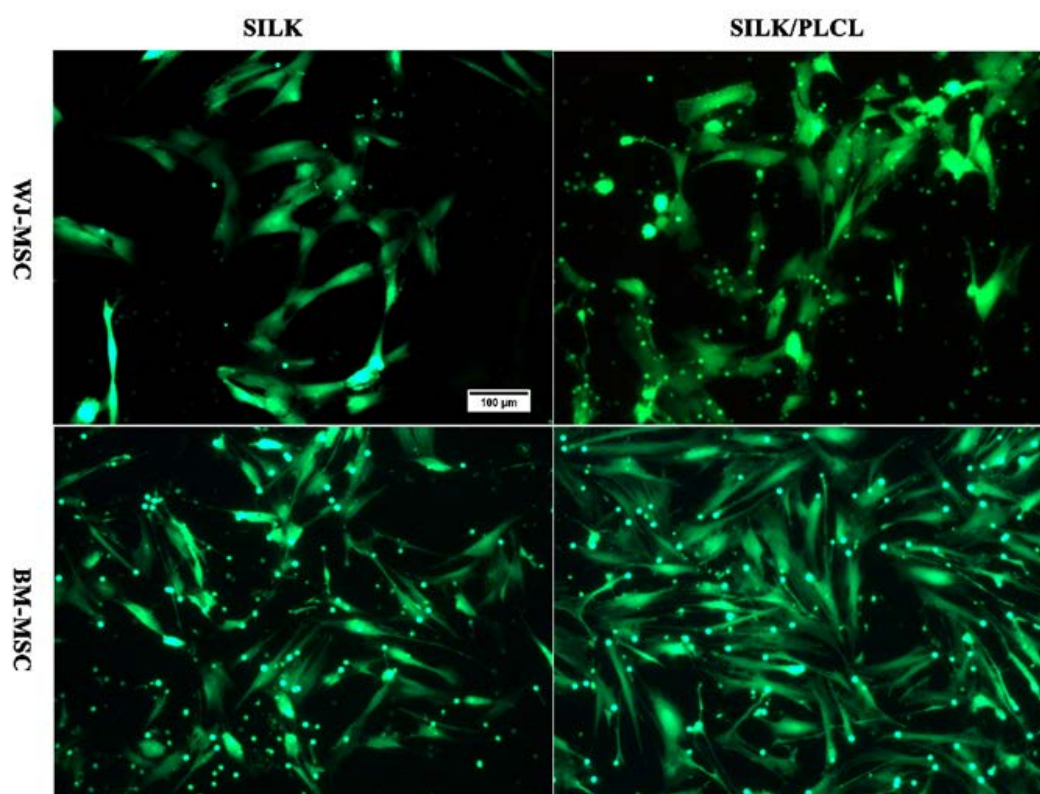
Figure 32 Migration of WJ-MSCs and BM-MSCs under the stimulation of silk and silk/PLCL scaffolds. (S1: one-layer silk scaffold; S2: two-layer silk scaffold; S3: three-layer silk scaffold; SP: silk/PLCL composite scaffold; green: Calceine AM)

5.2.2.4 Histology and immunohistochemistry

Histological examinations were performed by using hematoxylin/eosin/safrene (HES) and Sirius red (RS) and results are shown in Figure 33-36. Cells location and ECM synthesis were revealed with the longitudinal and transverse-section slides. According to HES staining showed in Figure 33 and Figure 34, both images from longitudinal and transverse-section slides have indicated that MSCs formed cell sheets covering the surface of scaffolds, and formed ECM. A pink networked matrix was indeed observed, as well as purple points representing MSCs. ECM was observed among the yarns and also peripheral side of scaffolds. From transverse sections, as silk layer number increased from S1 to SP, less cells were observed to penetrate into yarns especially for S3. From longitudinal slides, cell matrix distributed into the scaffolds and surface for S1, S2 and SP, while less matrix was observed into the scaffolds S3. No difference was obtained between WJ-MSCs and BM-MSCs. Collagen is the most abandon component of ligament tissue. Sirius red is used to stain total collagen in histology as well as distinguish collagen types. Cells were stained in violet and collagen were stained in pink ECM with red Sirius staining. As shown in Figure 35 and Figure 36, more collagen was detected from longitudinal slides for S1 and SP than for S2 and S3 for both WJ-MSCs and BM-MSCs, especially less collagen on S3. It may be concluded that S3 is exceedingly compact to permit the MSCs migration into the silk yarns, resulting in less cells detected between silk fibers, and less matrix formation observed between silk fibers. IHC was used to distinguish the composition of matrix, indicating Col I, Col III and TNC from Figure 37 and Figure 38. From these images, Col I, Col III and TNC

were stained as brown matrix and they were all detected on both MSCs-scaffolds constructs. The expression of Col I was higher than Col III and TNC for both cells, and this was consistent with the results from MSCs-PLCL constructs. More ECM was detected on S1 and SP than S2 and S3 for both cells.

Longitudinal section   **Tranverse section**

WJ-S1

WJ-S2

WJ-S3

WJ-SP
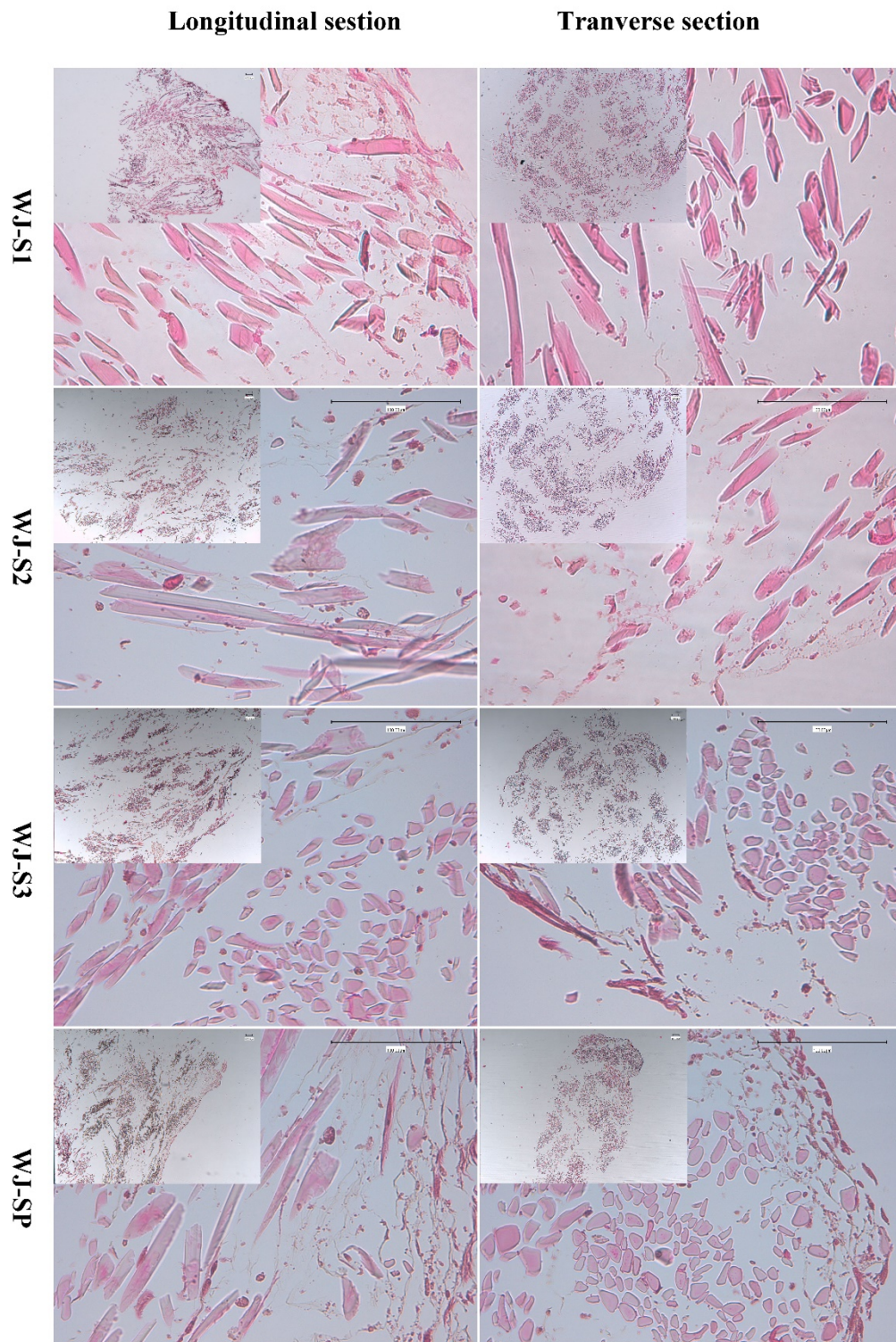
Figure 33 HES images of WJ-MSCs on silk and silk/PLCL scaffolds (S1: one-layer silk scaffold; S2: two-layer silk scaffold; S3: three-layer silk scaffold; SP: silk/PLL composite scaffold).
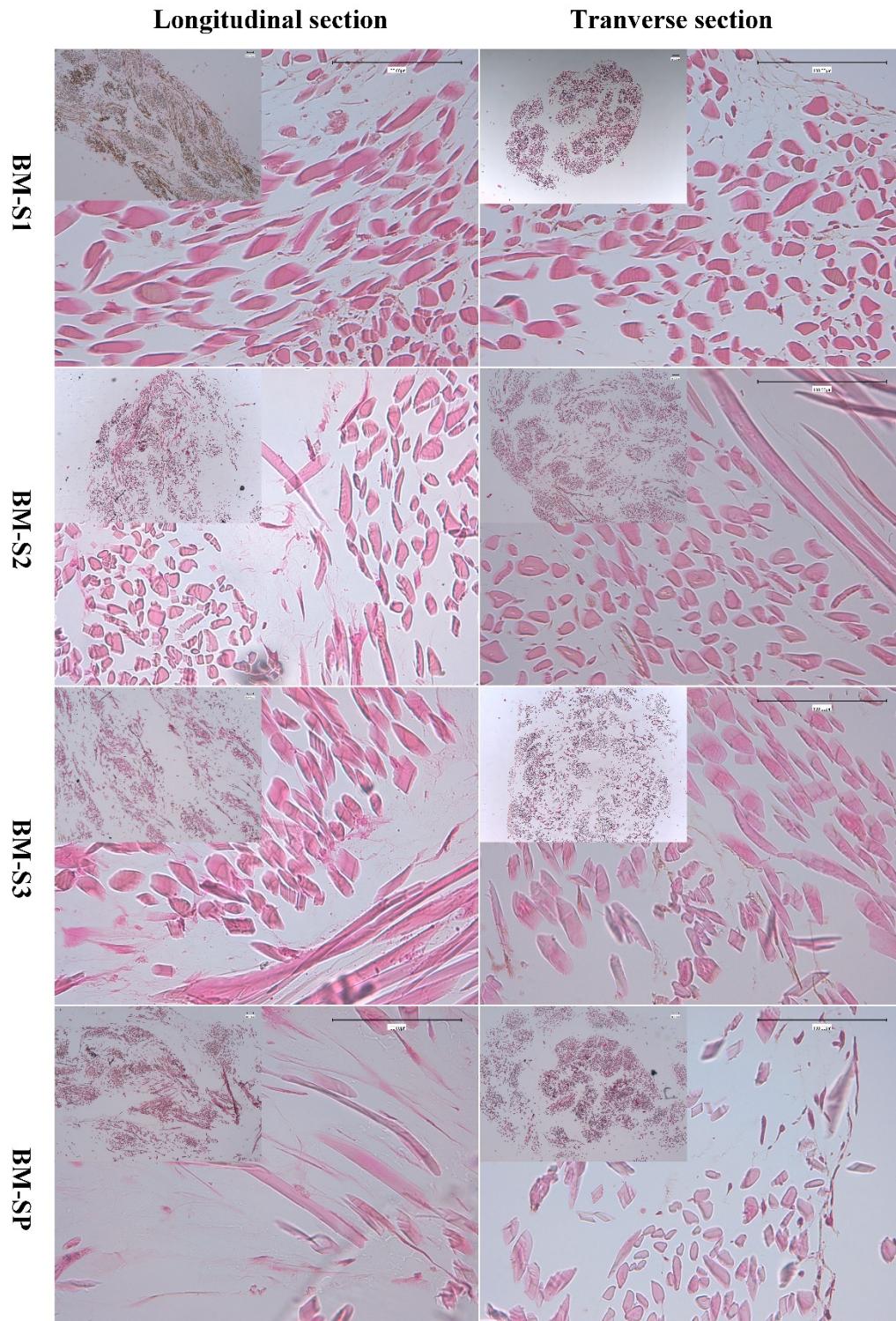
Figure 34 HES images of BM-MSCs on silk and silk/PLCL scaffolds (S1: one-layer

silk scaffold; S2: two-layer silk scaffold; S3: three-layer silk scaffold; SP: silk/PLL

composite scaffold).

Longitudinal section   **Tranverse section**

WJ-S1

WJ-S2

WJ-S3

WJ-SP
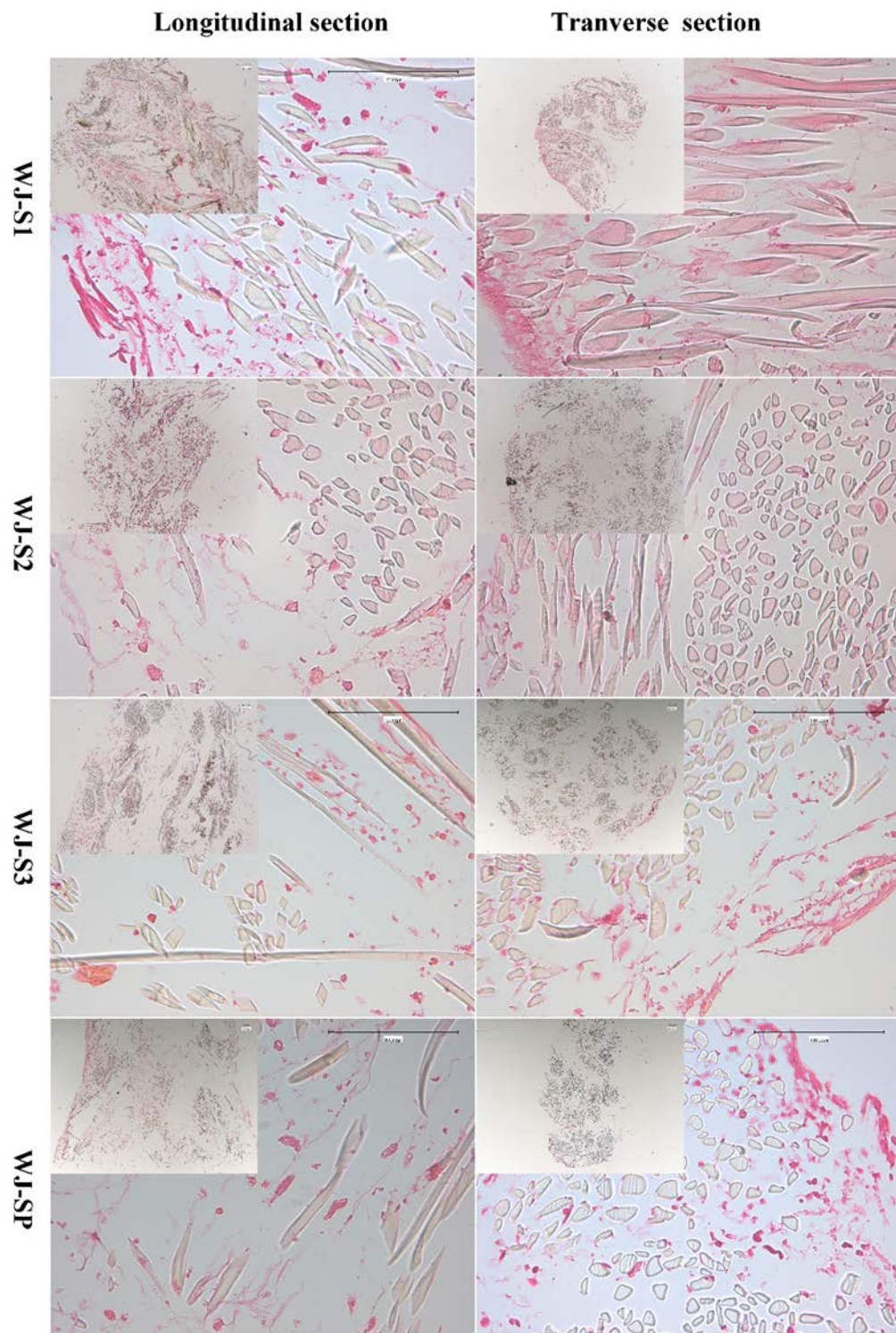
Figure 35 RS images of WJ-MSCs on silk and silk/PLCL scaffolds. (S1: one-layer silk scaffold; S2: two-layer silk scaffold; S3: three-layer silk scaffold; SP: silk/PLL composite scaffold).
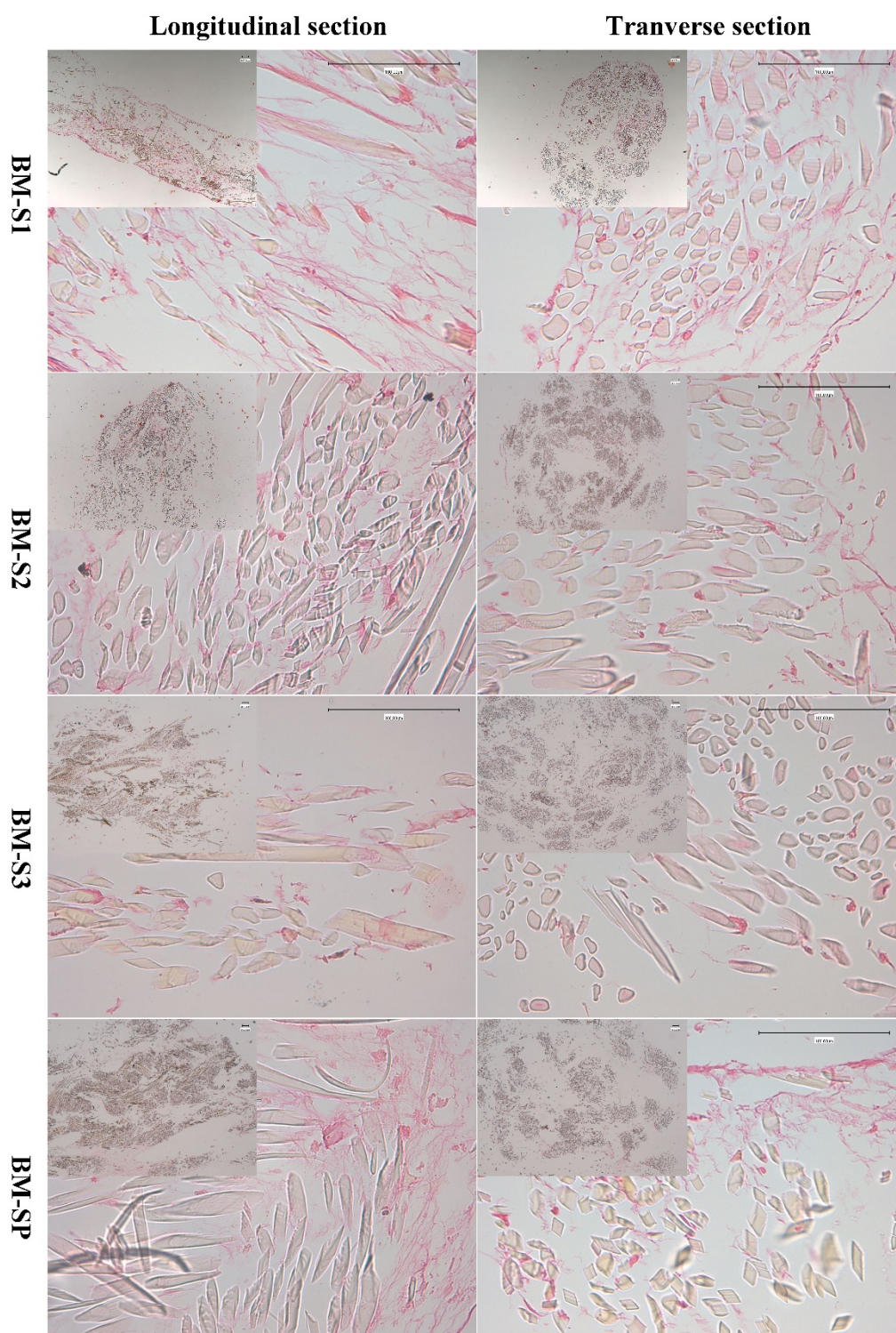
Figure 36 RS images of BM-MSCs on silk and silk/PLCL scaffolds. (S1: one-layer silk scaffold; S2: two-layer silk scaffold; S3: three-layer silk scaffold; SP: silk/PLL composite scaffold).
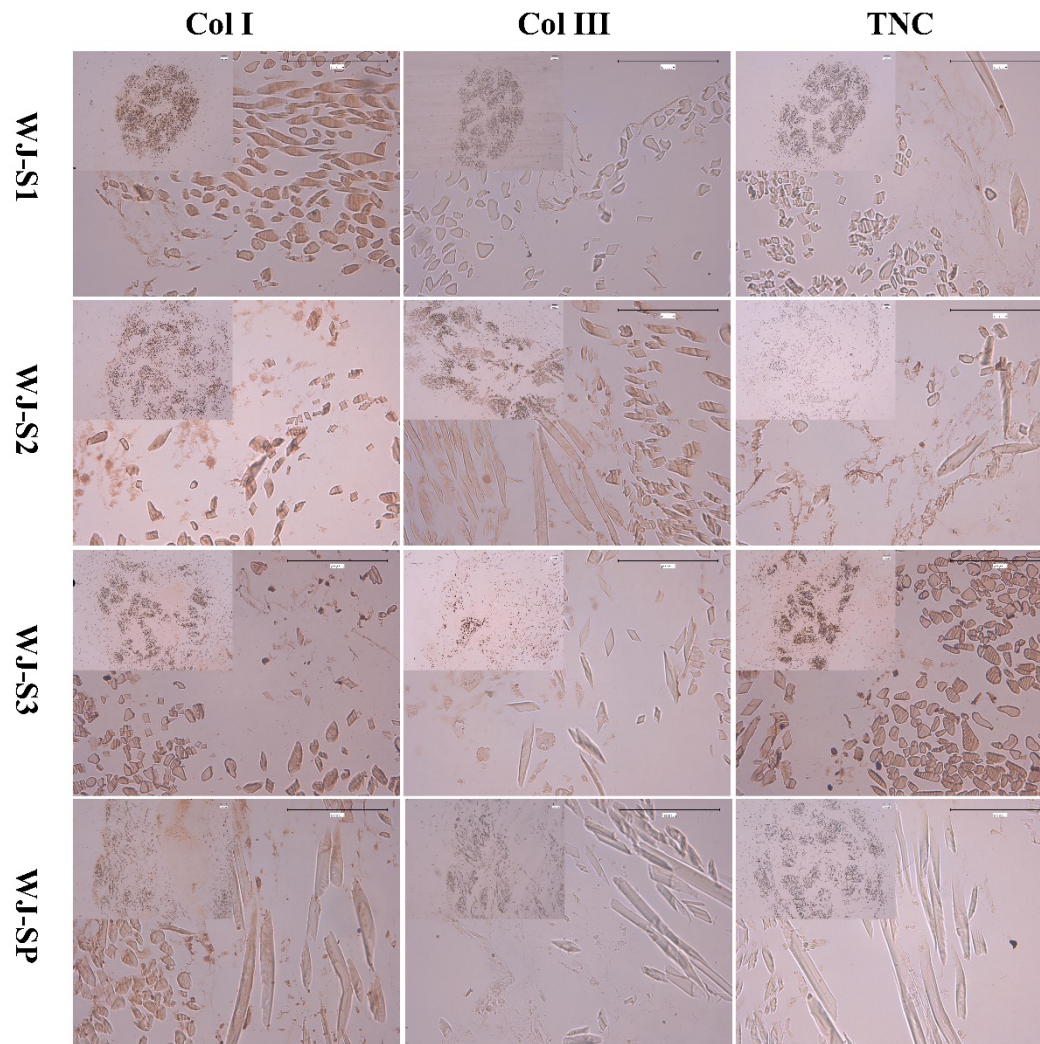
Figure 37 IHC images of WJ-MSCs on silk and silk/PLCL scaffolds. (S1: one-layer silk scaffold; S2: two-layer silk scaffold; S3: three-layer silk scaffold; SP: silk/PLL composite scaffold).
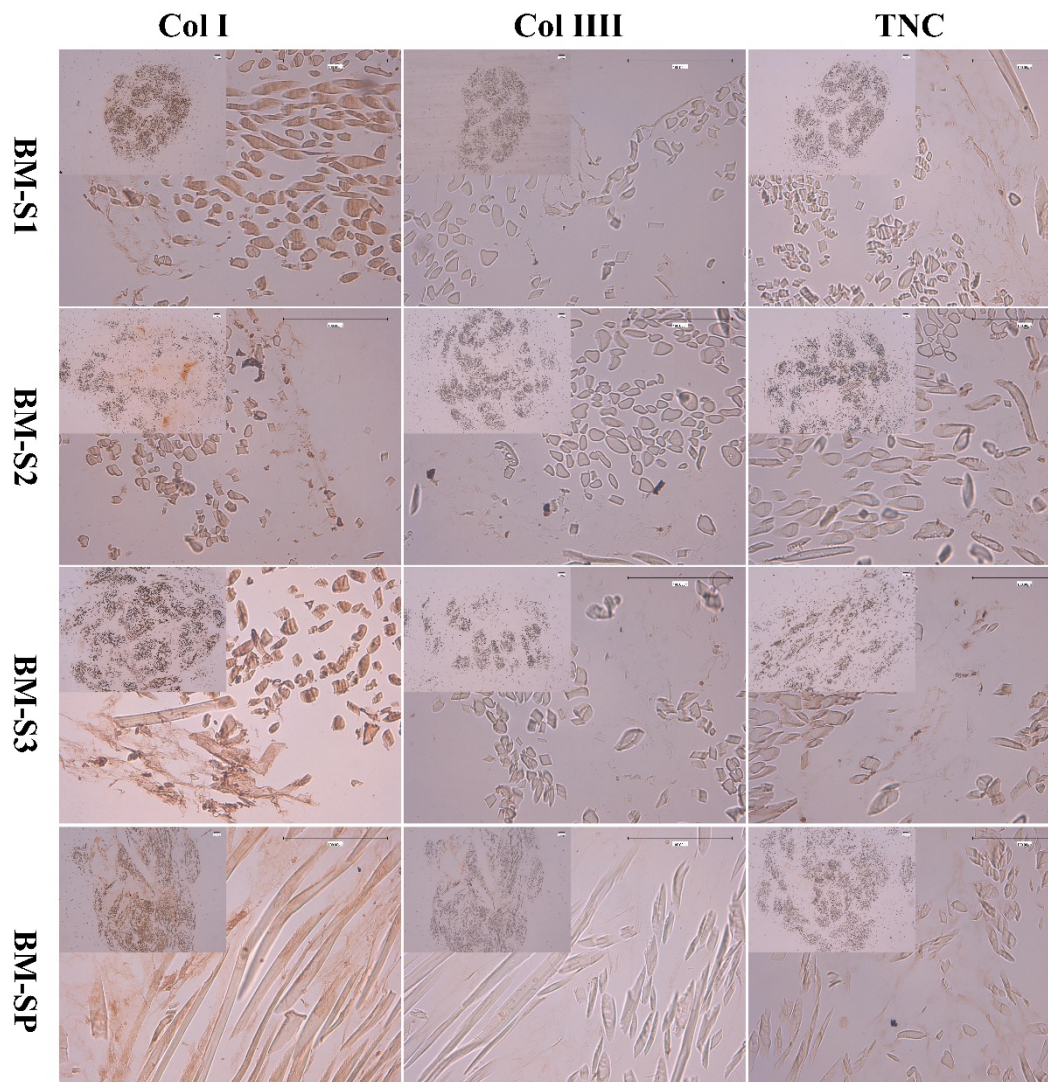
Figure 38 IHC images of BM-MSCs on silk and silk/PLCL scaffolds. (S1: one-layer silk scaffold; S2: two-layer silk scaffold; S3: three-layer silk scaffold; SP: silk/PLL composite scaffold).

5.3 Conclusion

From the present data, considering the mechanical, morphological and biological characterization of the different scaffold configurations, the silk/PLCL composite

scaffold appears to be the most suitable candidate scaffold for ligament tissue engineering application. No distinguished difference of cell behaviors of BM-MSCs and WJ-MSCs were observed from the present study, since they both showed satisfying biocompatibility on this scaffold SP.

6 Chapter VI : An attempt to study effect of dynamic mechanical stimulation on MSCs-construct in a tension-torsion bioreactor

6.1 Introduction

In the last two chapters, studies to optimize scaffolds and cell sources have been carried out. Next focus therefore consisted in improving microenvironment to promote ligament tissue engineering. As mentioned in chapter I, there are two methods to adjust microenvironment, including mechanical and biochemical stimulation. A multi-chamber tension-torsion bioreactor has been previously designed by our group in order to promote cell-scaffolds differentiation towards ligament tissue (C. P. Laurent et al. 2014b). In a previous study, human bMSC with density 200,000 and 600,000 cells were seeded on PLCL scaffold and supplied with cyclic loading (2.5% strain and 10°rotation at 1 Hz) during 2 min every 30 min for 10 h. After 48 h culture, cells satisfyingly adhered to the scaffold, no contamination was observed, and more cells were present on scaffold with high seeding density. However, it has been observed that cells did not homogeneously distribute on the scaffolds (C. P. Laurent et al. 2014b). Since this system to supply mechanical stimulation has been validated, additional work was required to improve homogeneous cell distribution and promote ligamentous ECM synthesis.

As concluded from the chapter V, silk/PLCL composite scaffold has been proved to constitute the most suited scaffold for ligament tissue engineering regarding our criteria.

As a result, silk/PLCL composite scaffolds have been selected to study the effect of dynamic stimulation on MSC-scaffold constructs for ligament tissue engineering. In the present study reported in the present chapter, parameters concerning cyclic loading were set up as 2.5% strain, at 1 Hz during 2 min every 30 min for 8 h per day. Cell behaviors including cell proliferation, morphology and distribution on scaffold have been evaluated.

6.2 Results and discussion

6.2.1   MSCs metabolic activity of MSCs on scaffold

Cell metabolic activities on silk/PLCL scaffold under mechanical stimulation have been investigated with AB assay. As shown in Figure 39, both WJ-MSCs and BM-MSCs showed very low metabolic activity (less than 40%), which is far lower than the results of static culture reported in section 5.2.2.1. For both cells, the metabolic activity decreased as mechanical loading continued to day 7.
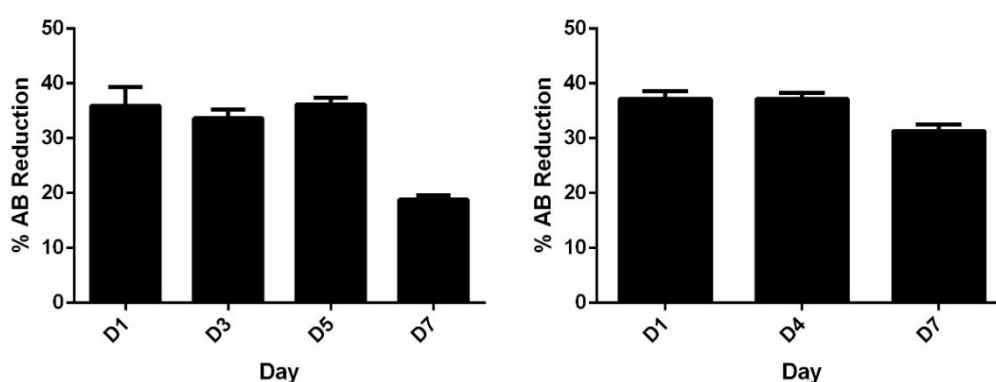
Figure 39 AB assay of WJ-MSCs and BM-MSCs on silk/PLCL scaffolds in bioreactor for 7 days.

6.2.2   MSCs morphology and location on scaffolds

Live/dead BM-MSCs distribution on scaffolds has been shown in Figure 40. Globally, a few cells were detected on fibers after the first 8 h of mechanical stimulation. Afterwards, cells proliferated well on scaffold and more cells were detected with calcein-AM/Ethd-1 staining, which corresponds to AB results. More dead cells were presented in D4 and D7 than at the beginning. MSCs showed an elongated shape and proliferated along the longitudinal direction of silk fibers.

	Calcein-AM	EthD-1	Merge
D1			
D4			
D7			
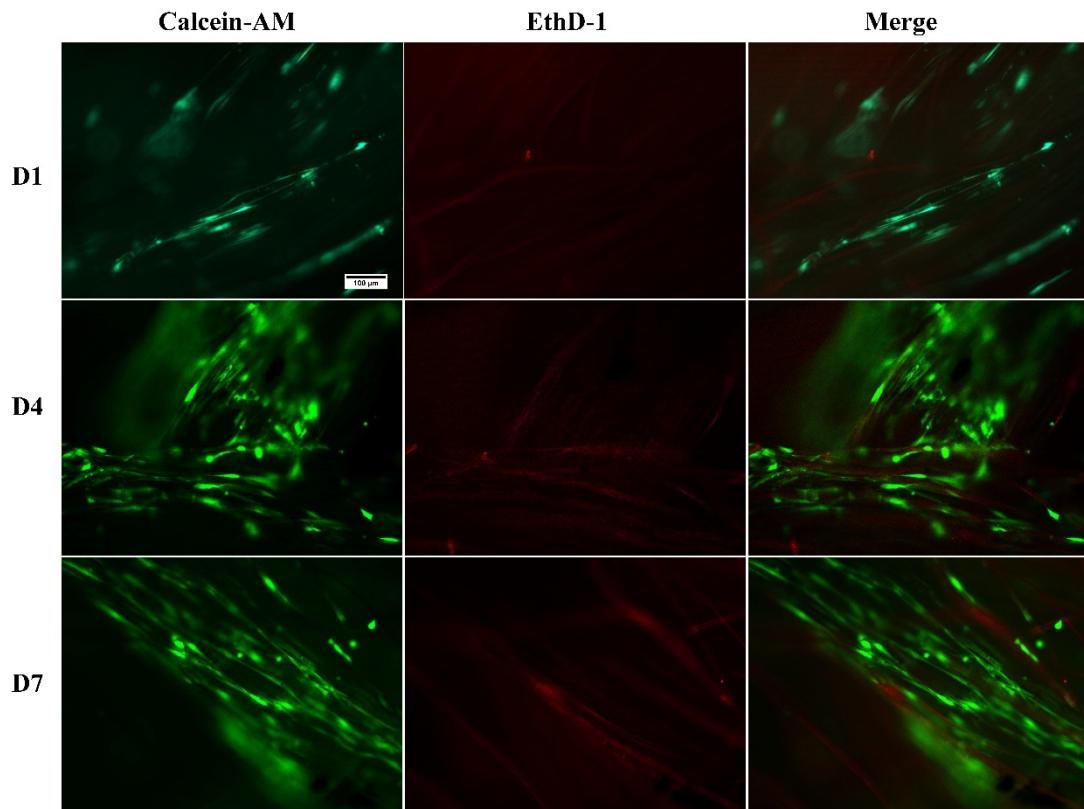
Figure 40 The images of live/dead staining of BM-MSCs on silk/PLCL scaffolds (green: Calceine AM; red: Ethidium homodimer I, dead cells).

6.3 Conclusion

A preliminary evaluation of the effect of dynamic loading on the MSCs-scaffold constructs to differentiate into ligamentous tissue was reported using a tension-torsion bioreactor. Results showed that mechanical stimulation firstly promoted cell proliferation within 4 days, then cell viability decreased for the following days. As a consequence, additional studies need to be performed in order to improve cell attachment, proliferation and ligamentous ECM synthesis, and to understand the underlying mechanisms under cellular response to mechanical loading.

7   Chapter VII: Discussion

In the previous chapters, synthetic polymer PLCL and natural polymer silk have been used to fabricate a series of multi-layer braided scaffold with or without PLL/HA LBL modification. The physiochemical properties (structure, morphology, topology and mechanical properties) and biocompatibility (cell attachment, proliferation, migration, and ECM synthesis) have been evaluated for ligament tissue engineering. Results showed that both PLCL and silk are mechanically suitable for ligament regeneration and biocompatible to support WJ-MSCs and BM-MSCs attachment, proliferation, migration and ligament related ECM synthesis. Silk/PLCL composite showed the most suitable structure with an increased porosity and has been shown to support cell proliferation and exhibit enhanced mechanical properties. We may therefore conclude that this solution may constitute an attractive scaffold candidate for ligament tissue engineering. In the following sections, some of the aspects and limitations related to the initial PLCL braided structure selected at the beginning of this work will be discussed, as well as the silk and silk/PLCL scaffolds that have been proposed.

7.1   Initial PLCL braided scaffold

PLCL is an elastomeric synthetic copolymer made of the two biocompatible, degradable polymers PLLA and PCL. Because of its biocompatibility, biodegradability, and easy processing, PLCL has been widely used in biomedical research, including for artificial vessel (S. I. Jeong et al. 2005; S. I. Jeong, Kim, Kim, et al. 2004), cartilage

(Jun Xie et al. 2006; Kroeze et al. 2010), and peripheral nerves (De Groot et al. 1997; Rodríguez et al. 1999). Applications of PLCL towards ligament/tendon have been reported : for instance, Kim et al showed that PLCL could support tendon cell proliferation (Kim et al. 2012), and Y. Xu et al investigated a series of composite electrospun scaffolds based on collagen/P(LLA-CL) with various structures (aligned-, random-, nanoyarn) for tendon regeneration, emphasizing that nanoyarn scaffolds possessed a wide potential for tendon tissue engineering (Y. Xu et al. 2013). Vuornos et al compared a foamed PLCL (70/30) scaffold with a braided poly (L/D) lactide (PLA, 96 L/4D) scaffold for tendon tissue engineering, and noted that PLCL was excessively elastic to form a braided structure in their study (Vuornos et al. 2016). Braiding is indeed one of the well-established medical textile technology adapted to the development of different medical constructs, especially like suture and stents, and also ligament and tendon tissues (Aibibu, Hild, and Cherif 2016). Braiding can create a three-dimensional fibrous platform to mimic ligament/ tendon structure with the capacities to adapt the porosity and mechanical properties to reach the requirement of target tissue. In previous studies, our team has developed a multi-layered braided scaffold based on elastic PLCL and demonstrated its mechanical and biocompatible potential for ligament regeneration (C. P. Laurent et al. 2012, 2011, 2014a). In these studies, the crucial parameters linked to morphology of the braided scaffold including braiding angle (the pitch length of braid), fiber diameter and layer number were studied and optimized to create a multi-layer braided structure (C. P. Laurent et al. 2011). PLCL with lactic acid/e-caprolactone ratio of 97/3, 85/15 and 70/30 were evaluated by using

a dedicated Finite Element (FE) code. From a mechanical point of view, PLCL in a ratio (85/15) was selected as the most suited candidate material for the following studies (C. P. Laurent et al. 2012). The *in vitro* and *in vivo* biocompatibility of PLCL has been investigated (C. P. Laurent et al. 2014a, 2018), bMSC from Merino sheep had been seeded on 6 layer braided PLCL scaffold for 4 weeks in static culture, and hBMSC from human have been seeded on scaffold and cultured in a mechanical bioreactor for 48 h. Both static and dynamic culture confirmed the biocompatibility of PLCL scaffold and the potential for ligament tissue engineering. *In vivo* characterization was conducted in a rat mode by subcutaneous implantation for 4 weeks, scaffolds with/without MSCs both showed good interaction with surrounding tissue, high vascularization, a dense collagen network formation, no acute degradation and a mild inflammatory response induced by polymer. From a biological point of view and based on these first studies prior to the present work, PLCL was then concluded to constitute a promising candidate material for ligament regeneration.

7.2 PLL/HA LBL modification

In the light of these previous research, this 6-layer braided PLCL scaffold has been initially selected in the present work and PLL/HA PEM has been introduced to modify this scaffold, with the aim to improve cell attachment, distribution and possibly for the future application of delivering growth factors for ligament tissue engineering.

PLL /HA is a classical PEM pair and has been widely used for surface modification to

improve cell interaction (Richert et al. 2004), and both materials were already used for biomedical application (Huang et al. 1983; Zhang et al. 2013; Yamanlar et al. 2011; Hahn and Hoffman 2004). The pair of PLL/HA PEM was expected to be an effective system to improve MSCs behavior on scaffolds. PEM properties varies with respect to parameters such as the solution concentration, pH, electrolyte charge, etc. In our first study, parameters such as the number of PLL/HA bilayer, the order of polycation/polyanion, the ending layer and the solution pH have been evaluated in order to develop an optimized PLL/HA PEM film (X. Liu et al. 2018). In the literature, both pH 6.0-6.5 and pH 7.4 have been used to develop PLL/HA PEM films (Yamanlar et al. 2011; Burke and Barrett 2003). We firstly evaluated the effect of bilayer number and different pH on PLL/HA PEM films development for cell attachment and proliferation.

In the assays, bilayer number was tested up to 5 layers, while for WJ-MSCs results showed that cell metabolic activities did not increase after more than 1 layer. For both BM-MSCs and WJ-MSCs, cell metabolic activities decreased as the layer number increased. As far as the pH was concerned, results demonstrated that both cells showed a better metabolic activity in pH 6.2 than in pH 7.4. In the preliminary study, the outer layer of PLL or HA has also been compared. Results showed that PLL positively promoted cell attachment, while HA was less effective for cell attachment and this corresponded to the results reported in a previous study (Yamanlar et al. 2011). As a conclusion, pH 6.0-6.5 was selected for PEM films development, PLL was used as terminal layer and layer number was kept inferior to one layer.

Cell interaction with scaffold is a complex process related to physicochemical properties of scaffold (surface topography, surface toughness, wettability, stiffness, and crystallinity) and cell properties. The structure of scaffold with PLL/HA modification was detected by FTIR and confirmed the deposition of PLL/HA on PLCL fibers. The morphology of bilayer on scaffold was investigated and reconfirmed with fluorescent microscopy, since the fluorescent intensity increased as the PLL-FITC layer number increased. AFM images permitted to observe the topology of fibers before and after modification, which showed polygonal and particle-like structures of PLL and HA respectively on the fiber surface. After modification, the porous, braided structure from SEM images did not change, and the surface became less smooth after PLL/HA modification. Such results were, to the best of our knowledge, the first of this kind in the literature concerning biomaterial surface modification.

In the biological evaluation, WJ-MSCs and BM-MSCs have been investigated as candidate cell sources because of their self-renew ability, differentiation potential, large availability and easy accessibility. Before MSCs seeding on constructs, their biological properties related to "stemness" have been firstly characterized and confirmed by tests such as CFU, senescence, phenotype and differentiation abilities towards adipocyte, osteocyte and chondrocyte. Then, MSCs behaviors on PLCL scaffolds with or without surface modification have been furtherly evaluated by assessing cell attachment, proliferation, migration, and ECM synthesis. Both types of MSCs attached well on

scaffold and formed cells sheets on the fibers or crossed fibers according to SEM images, while no significant differences about cell attachment were detected for WJ-MSCs and BM-MSCs. It has been previously reported that cell cytoskeleton organization is related to cell fate on scaffold, is beneficial to predict cell commitment, and it also indicates cell senescence (Treiser et al. 2010). Senescent cells are characterized with enlarged, irregular morphology, followed with the decrease of phenotype expression and differentiation abilities (W. Wagner et al. 2008). Cell cytoskeleton and cell nucleus were detected with fluorescent staining in the present study, and MSCs were observed to present an elongated shape along the longitudinal direction of PLCL fibers or crossed fibers, demonstrating the ECM synthesis in accordance with SEM images. The quantification of cell nuclei and the cell morphological changes pointed out that MSCs were more elongated on scaffolds than on TCPS. For BM-MSCs, cell nuclei on scaffolds were smaller than on TCPS. In the literature, it is reported that cells on oriented fibers tend to present an elongated shape, which is called the contact guidance of cells, and then collagen is detected to deposit along the orientation of fiber (Corey et al. 2007; Gnavi et al. 2015; Delaine-Smith et al. 2014; Jingwei Xie et al. 2010). Since it has been reminded previously that native ECM of a tissue is made of oriented fibers, cells were therefore frequently cultured on aligned fibers to mimic native structure (Shang et al. 2010). Therefore, MSCs-PLCL scaffold could be an adaptable, resistant system to response to mechanical stimulation. The results of AB assay indicated that cell proliferated well on scaffolds, and the metabolic activity did not show significant changes after PLL/HA scaffold modification neither

for WJ-MSCs nor for BM-MSCs. The main component of native ligament ECM is known to be collagen (C. B. Frank 2004b), while tenascin-C was also pointed out to be the specific indicator of ligament ECM with collagen I and collagen III (Jarvinen 2003). In this study, collagen I, collagen III, and tenascin-C were secreted by WJ-MSCs and BM-MSCs on the scaffold within 14 days, which could have been encouraged by ascorbic acid in the medium. This pointed out that BM-MSC-scaffold and WJ-MSC-scaffold both exhibit the potentials to form in the future ligamentous tissue. Cell migration is a crucial step in the tissue healing process since cells first migrate to the injury site or target area. Consequently, migration was assessed in this study and our results showed that chemotaxis of WJ-MSCs and BM-MSCs was activated by SB, SP, and S1L. This migration was even more pronounced for scaffold with one-layer surface modification, compared to SB and SP. This may show a possibility to recruit MSC for *in vivo* implantation. These cell-scaffold constructs showed satisfying biocompatibility, and the effect of growth factors incorporation into this PEM layer may be assessed in the forthcoming developments and constitutes therefore an obvious perspective of the present work.

7.3 Limitations of the initial PLCL braided scaffold

A PLCL braided scaffold with PLL/HA modification was designed in our study. The mechanical, morphological and biological results concerning the activity of WJ-MSCs and BM-MSCs showed that such a structure may constitute a promising scaffold for ligament tissue engineering. The incorporation of LBL modification increased cell

chemotaxis, which opens interesting perspectives for *in vivo* application.

In a parallel study, our research group has evaluated the evolution of its initial mechanical properties during hydrolytic degradation (C. P. Laurent et al. 2018). The initial mechanical properties were confirmed to be suitable for ligament regeneration, and the evolution of these mechanical properties of PLCL fibers due to hydrolytic degradation was characterized to quantify the post-implantation mechanical properties changes by using a previously developed numerical model. Surprisingly, PLCL fibers exhibited a non-expected brittle behavior after two months, which may involve a potential risk of premature failure of the scaffold, unless tissue growth compensates this change in mechanical properties (C. P. Laurent et al. 2018). This therefore emphasized a strong limitation of the proposed PLCL scaffold.

7.4 Silk as an alternative to PLCL

Based on the previously mentioned limitation, while the braided structure and the braiding manufacturing process was proved to be adapted to ligament tissue engineering, there was an urgent demand to select an alternative constitutive material. Such a new biomaterial for ligament regeneration should be biocompatible and mechanically strong and exhibit a suitable degradation rate adapted to new tissue growth. Silk is a natural protein-based polymer, which possesses remarkable mechanical properties, excellent biocompatibility, controllable degradability, and low immunogenicity (D. Ma, Wang, and Dai 2018). The *in vivo* biocompatibility of silk has

already been confirmed since it is clinically used on the form of suture wires (Bucknall, Teare, and Ellis 1983). Silk has been also widely examined to be a candidate for ligament/tendon regeneration (Altman et al. 2002; J. L. Chen et al. 2010; Yin et al. 2010; J. L. Chen et al. 2015; X. Chen et al. 2008;). It is slowly biodegradable, since it has been reported that silk degraded in more than two years and been classified as nondegradable biomaterials by FDA (Ethicon 2000). This "non-degradability" may constitute the biggest counteracts for the silk application towards ligament regeneration.

7.5 Proposition of a silk-based braided scaffold

In the light of the studies above, we thus considered to develop silk scaffolds as well as a composite scaffold based on silk and PLCL, in order to offer satisfying biocompatibility, mechanical properties and adaptable degradation rate for ligament tissue engineering. Consequently, we studied the suitability of silk braided scaffold and silk/PLCL composite scaffolds by characterizing their physiochemical and biological properties in order to select the most suited scaffold for ligament regeneration.

The multilayer braided architecture of the scaffold was conserved based on the previous study. Because of the excellent mechanical properties of silk and the elasticity of PLCL, silk was decided to be in the core of scaffold, since it has been previously showed (C. P. Laurent et al. 2012, 2014a) that the inner layers of the scaffold mainly control its overall mechanical properties. The silk layer number was optimized by mechanical tests, and results showed that the stiffness and force at failure does not change as silk layer

exceeded 4 layers. It indicates that only the inner layers play a predominant mechanical role, while outer layers may only modify the morphological properties of the scaffold. From a biological point, metabolic activity of WJ-MSCs did not increase when the layer number exceeded 3 layers. As a result, the maximal layer number was set at 3 layers, and S1, S2, S3 (silk scaffolds with 1,2,3 layers) and SP (Silk/Polymer composite scaffold) have been studied in the present work.

7.6 Characterization of silk and silk/PLCL braided scaffolds

As observed by the different imaging techniques used in the present study, silk and silk/PLCL scaffolds all presented a braided, porous multilayered structure, and scaffolds tended to be more compact as the number of layers increased from one layer to three layers. As a result of this more compacted structure, S3 presented a relatively plan surface for cell attachment which resulted in the formation of cell sheets at the surface of scaffolds as revealed by SEM, and limited cell intergrowth as reflected in histological images. Porosity is linked to gas or nutrient exchange within the scaffold, local pH stability, tissue ingrowth promotion, cell signaling, and is also related to the mechanical properties of the scaffold (Chang and Wang 2011). In our results, the porosity of scaffolds decreased as the number of layers (n=1,2,3) increased. However, the proposition of the SP composite scaffold led to a higher porosity than S3.

Pore size also constitutes a crucial factor to be considered when designing a scaffold (Ge et al. 2006). Increased pore size leads to the reduction of surface area for the whole

scaffold, while an insufficient pore size could limit cell migration. Pore size has also been reported to be associated to cell differentiation (Nehrer et al. 1997; Stenhamre et al. 2011; Kuboki, Jin, and Takita 2001; Roosa et al. 2010; Tsuruga et al. 1997). The computed mean pore size ranged around 20 μm for each scaffold, which is much smaller than the reported optimal pore size for certain cell differentiation. However, the validity of the common watershed algorithm used for μCT image processing is highly debatable in the case of this structure, since pores are largely elongated in the textile structure. Other experimental methods such as mercury porosimetry (C. P. Laurent et al. 2011, 2) may permit to provide with additional information about pore size distribution within the scaffolds, with the same debatable applicability to the elongated pores present in the braided structure. Despite this low reported pore size, cells were detected to migrate among fibrils within yarn, as confirmed by the results of live/dead and histology images that have been reported in section 5.2.2.2.2 & 5.2.2.4. These results have proved that the porosity and pore size of the proposed scaffolds were adapted to cell intergrowth.

From a mechanical point of view, these four scaffolds showed a pronounced J-shape stress-strain response comparable to the typical soft tissue response, with tangent apparent modulus increasing with the prescribed strain. Mechanical strength of the four different scaffolds was comparable to a native ligament (Kendoff, Morgan-Jones, and Haddad 2016), and it is worthy to note that SP may constitute a safer choice since PLCL contributed to scaffold integrity when subject to very large strain due to its large deformability.

MSCs behaviors such as proliferation, migration and ECM synthesis are essential activities towards tissue regeneration (Bružauskaitė et al. 2016). From a biological point, the suitability of scaffolds has been characterized by a series of biocompatibility assays. Results showed that WJ-MSCs appeared more sensible to the decrease of porosity than BM-MSCs. BM-MSCs metabolic activity increased with no significant difference from day1 to day7. Live/dead staining results indicated that WJ-MSCs and BM-MSCs penetrated and proliferated in the smallest units-fibrils among silk yarns. More dead cells were observed on S3, with less cell intergrowth for both types of cells, which may be attributed to the decrease in porosity. Cells migrated and proliferated across silk fibers and PLCL fibers on the SP scaffold, which indicated matrix synthesis. Except for S3, BM-MSCs tended to be more oriented and proliferated along the longitudinal direction of fibers, and probably have a better viability than WJ-MSCs, since less dead BM-MSCs were detected on the same scaffolds. BM-MSCs showed more activated migration behavior than WJ-MSCs under stimulation of silk and silk/PLCL scaffolds, in accordance with our previous study (X. Liu et al. 2018). Moreover, the combination of silk with PLCL appeared to be favorable for cells migration. HES staining revealed the location of MSCs on scaffolds as well as matrix synthesis. Both longitudinal and transverse sections showed that cells migrated into the fibrils within the yarns. Moreover, matrix formed on the outer edges of the scaffolds and also colonized the scaffolds core. Sirius red was used to stain the total collagen as well as to distinguish collagen types in histological sections. For WJ-MSCs, more

collagen was detected on S1 and SP, while very few collagens were detected on S3, which may be attributed to the low porosity of scaffold limiting cell ingrowth and nutrient delivery. For BM-MSCs, more collagens were detected on S1, S2, and SP, resulting in the same conclusion.

7.7 Preliminary study of the effect of mechanical stimulation on MSC-scaffold differentiation

Mechanical stimulations are expected to promote cell-scaffolds differentiation. With the parameters set in the chapter VI, mechanical stimulation did not show a positive effect on cell metabolic activity, however, cell proliferation was observed as more BM-MSCs attachment on the scaffold at D4 and D7 than at D1. MSCs showed elongated shape homogeneously along longitudinal direction of silk fibers, which may constitute a first sign into the development of an organized matrix. Parameters (such as seeding cell density, frequency, period etc.) need to be furtherly optimized in the future to promote cell attachment, proliferation and synthesis ECM.

8 Chapter VIII: Conclusion, limitation and perspectives

8.1 Conclusion of the present work

This thesis mainly focused on the optimization of scaffolds and cell sources towards ligament tissue engineering, and also contained a preliminary study on the effect of mechanical stimulation on cell-scaffold constructs. Firstly, polymers from different sources including PLCL and silk have been investigated to fabricate various kinds of multilayer braided scaffolds. 6-layer braided PLCL scaffold have been showed to support WJ-MSCs and BM-MSCs attachment, proliferation, migration and ECM synthesis. Introduction of PLL/HA PEM on PLCL did not result in a substantial improvement of cell-scaffold interactions except the promotion of cell migration. However, this modification was conserved with the idea to develop a growth factor delivery system in order to promote ligamentous tissue formation, by furtherly integrating growth factors within the LBL modification. Optimized parameters concerning the development of PEM were in pH6.0-6.5 solution with no more than one-layer modification. The combination of silk/PLCL gathered the advantages of both materials together, resulting in a scaffold with a sufficient strength and a degradation rate though to be consistent with the development of neo-tissue. Results showed that silk/PLCL composite presented the best-suited mechanical properties, morphology and biocompatibility for MSCs towards ligament/ tendon regeneration.

For both PLCL and silk, scaffolds were fabricated in a porous braided structure with optimized PLCL fiber diameter and braided angle as previously reported (C. P. Laurent

et al. 2011, 2012). PLCL was fabricated as 6-layer scaffold, while for silk, mechanical properties were not enhanced when layer number exceeded 3 layers. To enhance mechanical strength and increase scaffold porosity, the core layer as well as the outermost layer were built using silk fibers. The middle layer was made of PLCL fibers to enhance porosity, while the main mechanical loading was supported by the inner layer of silk, thus avoiding excessive loading of the PLCL. 6-layer PLCL scaffold and silk-PLCL-silk scaffolds all showed good mechanical properties and biocompatibility.

In this study, WJ-MSCs and BM-MSCs were selected as candidate cell sources. MSCs properties related to CFU, tripotential differentiation and specific phenotype markers were confirmed before seeding them on scaffolds. Results of cell behaviors on PLCL scaffolds with or without modification and silk-based scaffolds demonstrated that there was no significant difference concerning biocompatibility between WJ-MSCs and BM-MSCs, or no preference for ligament tissue engineering. Both cells showed good cell attachment, proliferation, migration and ECM (Col I, Col III and TNC) synthesis.

The attempt of mechanical stimulation did not show any promotion of cell attachment and proliferation as expected, and there is therefore a need to define the suitable mechanical parameters to promote cell-scaffold proliferation and differentiation towards ligament tissue.

8.2 Limitations of the proposed scaffolds and required further characterization

8.2.1   Biodegradation properties

Ideally, the combination of silk and PLCL should result in mechanical properties corresponding to anatomical site, in order to mimic native function and also to support new tissue growth. This process relates to the cooperation of biomaterial degradation and neo-tissue formation rate. The expected cooperation involves a scaffold degradation rate adapted to neo-tissue formation. Previous study has demonstrated that PLCL alone show a brittle behavior after two months of degradation by hydrolytic degradation. This has permitted to conclude that tissue engineered constructs run a risk of construct collapse after post-implantation. However, *in vivo* implantation did not show any scaffold degradation after 4 weeks. To respond to such a doubt, silk was added to the PLCL scaffold since silk has been reported to degrade in more than 2 years *in vivo*. Based on these results, we put forward the hypothesis that the combination of silk and PLCL could permit to obtain a scaffold with sufficient mechanical properties during the post-implantation phase to support neo-tissue growth, and we therefore assumed that such a lower degradation may be adapted to neo-tissue degradation. Therefore, further experiments need to be performed in order to study silk/PLCL composite degradation rate *in vitro* and *in vivo* at different intervals in order to validate these series of assumptions.

8.2.2   *In vivo* implantation

In order to furtherly assess the clinical suitability of the developed scaffolds, *in vivo*

implantation including subcutaneous implantation or *in site* implantation should be performed. Subcutaneous implantations are frequently used to evaluate scaffold biocompatibility or acute inflammation response, and has already been performed for PLCL braided scaffold (C. P. Laurent et al. 2018). The same study could therefore be extended in the future to silk/PLCL composite scaffolds, with or without LBL modification. *In site* implantations usually aim at mimicking native tissue environment and to investigate the clinical consequence of the graft implantation. Such studies are usually performed on large animal models such as pigs (Fan et al. 2009). While such *in vivo* tests need to be considered before clinical application, they are obviously particularly difficult and costly to be carried out.

8.2.3   Quantitative characterization

In the present study, most of biological evaluations including cell morphology and ECM synthesis were performed with qualitative detection. Especially for the analysis of ECM composition, basically including Col I, Col III and TNC, the characterization was conducted with specific protein staining at the protein level. In future work, it may be also interesting to assess specific gene expression with PCR at the gene level, since the collagen ratio may be related ECM remodeling in native tissue. The quantification of ECM components could be evaluated by Western blot. Furthermore, some other specific markers related to ligament/tendon tissue (TNMD, scleraxis) should be also evaluated.

8.3 Perspectives of the present work

It is well-known that microenvironment is one of the three crucial elements for the development of cell-scaffold constructs towards tissue regeneration. As discussed above, both biochemical and mechanical stimulations could positively promote cell differentiation on scaffolds to develop target tissues. The biochemical stimulations are related to the supply of growth factors, cytokines and other bioactive molecules. As discussed in the chapter I, growth factors such as IL-1, TGF-β, VEGF, PDGF, and bFGF have been widely investigated in the literature to enhance cell proliferation, migration, and matrix synthesis, and have been extensively discussed. It is worthy to note that platelet lysate, as a cocktail of growth factors, has recently emerged as an attractive factor for biomedical application, and it has been compared and proposed to replace traditional FBS to support cell proliferation. The development of an effective method to deliver such growth factors is therefore urgently demanded for growth factors application. We reported in chapter II the development of LBL modification on the braided scaffold with the idea to delivery growth factors. Consequently, an obvious perspective of the present study, consists in combining platelet lysate with PLL/HA PEM on silk/PLCL scaffold to promote MSCs behaviors towards ligamentous tissue differentiation. This will firstly be conducted in static culture.

As a second promising perspective of the present study, this delivery system combined with the silk/PLCL composite scaffold should be completed by external mechanical stimulation. The effect of mechanical loading on MSCs activities will therefore be

assessed. Indeed, in our preliminary study described in section 6.2.1 & 6.2.2, while BM-MSCs showed elongated cell morphology on scaffolds and cell number increased from d1 to d7, very few cells were detected on scaffold under a continuous stimulation up to seven days. This point should therefore be furtherly explored, and the parameters of bioreactors including the prescribed strain, frequency, lasting period need to be optimized to positively promote proliferation and differentiation.

References

Abbott, LeRoy C., B. John, M. Saunders, Frederic C. Bost, and Carl E. Anderson. 1944. 'Injuries to the Ligaments of the Knee Joint'. *JBJS* 26 (3): 503–521.

Aibibu, D., M. Hild, and C. Cherif. 2016. '6 - An Overview of Braiding Structure in Medical Textile: Fiber-Based Implants and Tissue Engineering'. In *Advances in Braiding Technology*, edited by Yordan Kyosev, 171–90. Woodhead Publishing Series in Textiles. Woodhead Publishing. https://doi.org/10.1016/B978-0-08-100407-4.00006-5.

Altman, Gregory H., Frank Diaz, Caroline Jakuba, Tara Calabro, Rebecca L. Horan, Jingsong Chen, Helen Lu, John Richmond, and David L. Kaplan. 2003. 'Silk-Based Biomaterials'. *Biomaterials* 24 (3): 401–416.

Altman, Gregory H, Rebecca L Horan, Helen H Lu, Jodie Moreau, Ivan Martin, John C Richmond, and David L Kaplan. 2002. 'Silk Matrix for Tissue Engineered Anterior Cruciate Ligaments'. *Biomaterials* 23 (20): 4131–41. https://doi.org/10.1016/S0142-9612(02)00156-4.

Altman, Gregory H., Helen H. Lu, Rebecca L. Horan, Tara Calabro, Daniel Ryder, David L. Kaplan, Peter Stark, Ivan Martin, John C. Richmond, and Gordana Vunjak-Novakovic. 2002. 'Advanced Bioreactor with Controlled Application of Multi-Dimensional Strain for Tissue Engineering'. *Journal of Biomechanical Engineering* 124 (6): 742–749.

Badylak, Stephen F. 1997. 'Identification of Extractable Growth Factors from Small Intestinal Submucosa'. *Journal of Cellular Biochemistry* 67 (478491).

Bailey, Mark M., Limin Wang, Claudia J. Bode, Kathy E. Mitchell, and Michael S. Detamore. 2007. 'A Comparison of Human Umbilical Cord Matrix Stem Cells and Temporomandibular Joint Condylar Chondrocytes for Tissue Engineering Temporomandibular Joint Condylar Cartilage'. *Tissue Engineering* 13 (8): 2003–2010.

Baksh, Dolores, Raphael Yao, and Rocky S. Tuan. 2007. 'Comparison of Proliferative and Multilineage Differentiation Potential of Human Mesenchymal Stem Cells Derived from Umbilical Cord and Bone Marrow'. *Stem Cells* 25 (6): 1384–1392.

Barfod, Kristoffer Weisskirchner. 2014. 'Achilles Tendon Rupture; Assessment of Nonoperative Treatment'. *Danish Medical Journal* 61 (4): B4837.

Barnes, Catherine P., Scott A. Sell, Eugene D. Boland, David G. Simpson, and Gary L. Bowlin. 2007. 'Nanofiber Technology: Designing the next Generation of Tissue Engineering Scaffolds'. *Advanced Drug Delivery Reviews* 59 (14): 1413–1433.

Barry, F., R. Boynton, M. Murphy, S. Haynesworth, and J. Zaia. 2001. 'The SH-3 and SH-4 Antibodies Recognize Distinct Epitopes on CD73 from Human Mesenchymal Stem Cells'. *Biochemical and Biophysical Research Communications* 289 (2): 519–24. https://doi.org/10.1006/bbrc.2001.6013.

Barry, Frank, Raymond E. Boynton, Beishan Liu, and J. Mary Murphy. 2001. 'Chondrogenic Differentiation of Mesenchymal Stem Cells from Bone Marrow: Differentiation-Dependent Gene Expression of Matrix Components'. *Experimental Cell Research* 268 (2): 189–200.

Baumann, M. Douglas, Catherine E. Kang, Jason C. Stanwick, Yuanfei Wang, Howard

Kim, Yakov Lapitsky, and Molly S. Shoichet. 2009. 'An Injectable Drug Delivery Platform for Sustained Combination Therapy'. *Journal of Controlled Release* 138 (3): 205–213.

Benjamin, M, H Toumi, J R Ralphs, G Bydder, T M Best, and S Milz. 2006. 'Where Tendons and Ligaments Meet Bone: Attachment Sites ("Entheses") in Relation to Exercise and/or Mechanical Load'. *Journal of Anatomy* 208 (4): 471–90. https://doi.org/10.1111/j.1469-7580.2006.00540.x.

Bennett, Neil T., and Gregory S. Schultz. 1993. 'Growth Factors and Wound Healing: Biochemical Properties of Growth Factors and Their Receptors'. *The American Journal of Surgery* 165 (6): 728–37. https://doi.org/10.1016/S0002-9610(05)80797-4.

Benoit, Danielle S. W., and Kristi S. Anseth. 2005. 'Heparin Functionalized PEG Gels That Modulate Protein Adsorption for HMSC Adhesion and Differentiation'. *Acta Biomaterialia* 1 (4): 461–70. https://doi.org/10.1016/j.actbio.2005.03.002.

Bernardi, Martina, Elena Albiero, Alberta Alghisi, Katia Chieregato, Chiara Lievore, Domenico Madeo, Francesco Rodeghiero, and Giuseppe Astori. 2013. 'Production of Human Platelet Lysate by Use of Ultrasound for Ex Vivo Expansion of Human Bone Marrow–Derived Mesenchymal Stromal Cells'. *Cytotherapy* 15 (8): 920–29. https://doi.org/10.1016/j.jcyt.2013.01.219.

Bernardo, Maria Ester, Franco Locatelli, and Willem E. Fibbe. 2009. 'Mesenchymal Stromal Cells'. *Annals of the New York Academy of Sciences* 1176 (1): 101–17. https://doi.org/10.1111/j.1749-6632.2009.04607.x.

Biau, David Jean, Sandrine Katsahian, Jüri Kartus, Arsi Harilainen, Julian A. Feller, Matjaz Sajovic, Lars Ejerhed, Stefano Zaffagnini, Martin Röpke, and Rémy Nizard. 2009. 'Patellar Tendon Versus Hamstring Tendon Autografts for Reconstructing the Anterior Cruciate Ligament: A Meta-Analysis Based on Individual Patient Data'. *The American Journal of Sports Medicine* 37 (12): 2470–78. https://doi.org/10.1177/0363546509333006.

Birch, Helen L. 2007. 'Tendon Matrix Composition and Turnover in Relation to Functional Requirements'. *International Journal of Experimental Pathology* 88 (4): 241–48. https://doi.org/10.1111/j.1365-2613.2007.00552.x.

Birch, Helen L., Chavaunne T. Thorpe, and Adam P. Rumian. 2013. 'Specialisation of Extracellular Matrix for Function in Tendons and Ligaments'. *Muscles, Ligaments and Tendons Journal* 3 (1): 12–22. https://doi.org/10.11138/mltj/2013.3.1.012.

Brandau, Oliver, Alfons Meindl, Reinhard Fässler, and Attila Aszódi. 2001. 'A Novel Gene, Tendin, Is Strongly Expressed in Tendons and Ligaments and Shows High Homology with Chondromodulin-I'. *Developmental Dynamics* 221 (1): 72–80. https://doi.org/10.1002/dvdy.1126.

Brune, T., A. Borel, T. W. Gilbert, J. P. Franceschi, S. F. Badylak, and P. Sommer. 2007. 'In Vitro Comparison of Human Fibroblasts from Intact and Ruptured ACL for Use in Tissue Engineering'. *European Cells & Materials* 14 (December): 78–90; discussion 90-91.

Bružauskaitė, Ieva, Daiva Bironaitė, Edvardas Bagdonas, and Eiva Bernotienė. 2016.

'Scaffolds and Cells for Tissue Regeneration: Different Scaffold Pore Sizes—Different Cell Effects'. *Cytotechnology* 68 (3): 355–69. https://doi.org/10.1007/s10616-015-9895-4.

Bucknall, T. E., L. Teare, and H. Ellis. 1983. 'The Choice of a Suture to Close Abdominal Incisions'. *European Surgical Research* 15 (2): 59–66. https://doi.org/10.1159/000128334.

Budama-Kilinc, Yasemin, Rabia Cakir-Koc, Bahar Aslan, Burcu Özkan, Hande Mutlu, and Eslin Üstün. 2017. 'Hydrogels in Regenerative Medicine'. *Biomaterials in Regenerative Medicine*, December. https://doi.org/10.5772/intechopen.70409.

Burdick, Jason A., and Glenn D. Prestwich. 2011. 'Hyaluronic Acid Hydrogels for Biomedical Applications'. *Advanced Materials (Deerfield Beach, Fla.)* 23 (12): H41-56. https://doi.org/10.1002/adma.201003963.

Burke, Susan E., and Christopher J. Barrett. 2003. 'PH-Responsive Properties of Multilayered Poly(l-Lysine)/Hyaluronic Acid Surfaces'. *Biomacromolecules* 4 (6): 1773–83. https://doi.org/10.1021/bm034184w.

Burks, Chris A., Kirk Bundy, Parwis Fotuhi, and Eckhard Alt. 2006. 'Characterization of 75:25 Poly(l-Lactide-Co-Epsilon-Caprolactone) Thin Films for the Endoluminal Delivery of Adipose-Derived Stem Cells to Abdominal Aortic Aneurysms'. *Tissue Engineering* 12 (9): 2591–2600. https://doi.org/10.1089/ten.2006.12.2591.

Cai, Changbin, Cheng Chen, Guangxing Chen, Fuyou Wang, Lin Guo, Li Yin, Dehong Feng, and Liu Yang. 2013. 'Type I Collagen and Polyvinyl Alcohol Blend Fiber

Scaffold for Anterior Cruciate Ligament Reconstruction'. *Biomedical Materials* 8 (3): 035001.

Caliari, Steven R., Manuel A. Ramirez, and Brendan A.C. Harley. 2011. 'The Development of Collagen-GAG Scaffold-Membrane Composites for Tendon Tissue Engineering'. *Biomaterials* 32 (34): 8990–98. https://doi.org/10.1016/j.biomaterials.2011.08.035.

Cardwell, Robyn D., Linda A. Dahlgren, and Aaron S. Goldstein. 2014. 'Electrospun Fibre Diameter, Not Alignment, Affects Mesenchymal Stem Cell Differentiation into the Tendon/Ligament Lineage'. *Journal of Tissue Engineering and Regenerative Medicine* 8 (12): 937–45. https://doi.org/10.1002/term.1589.

Chan, B. P., S. Fu, L. Qin, K. Lee, C. G. Rolf, and K. Chan. 2000. 'Effects of Basic Fibroblast Growth Factor (BFGF) on Early Stages of Tendon Healing: A Rat Patellar Tendon Model'. *Acta Orthopaedica Scandinavica* 71 (5): 513–18. https://doi.org/10.1080/000164700317381234.

Chang, Hsin-I., and Yiwei Wang. 2011. 'Cell Responses to Surface and Architecture of Tissue Engineering Scaffolds'. *Regenerative Medicine and Tissue Engineering - Cells and Biomaterials*, August. https://doi.org/10.5772/21983.

Chen, Gecai, Aihuan Yue, Zhongbao Ruan, Yigang Yin, Ruzhu Wang, Yin Ren, and Li Zhu. 2015. 'Comparison of Biological Characteristics of Mesenchymal Stem Cells Derived from Maternal-Origin Placenta and Wharton's Jelly'. *Stem Cell Research & Therapy* 6 (1): 228. https://doi.org/10.1186/s13287-015-0219-6.

Chen, Guoping, Takashi Sato, Masataka Sakane, Hajime Ohgushi, Takashi Ushida, Junzo Tanaka, and Tetsuya Tateishi. 2004. 'Application of PLGA-Collagen Hybrid Mesh for Three-Dimensional Culture of Canine Anterior Cruciate Ligament Cells'. *Materials Science and Engineering: C*, 2nd International BMC-NIMS Symposium on Biomaterials and Bionanotechnology at the Tsukuba International Congress Center, Epochal, Japan, 24 (6): 861–66. https://doi.org/10.1016/j.msec.2004.08.041.

Chen, Guoping, Takashi Sato, Takashi Ushida, Rei Hirochika, Yoshio Shirasaki, Naoyuki Ochiai, and Tetsuya Tateishi. 2003. 'The Use of a Novel PLGA Fiber/Collagen Composite Web as a Scaffold for Engineering of Articular Cartilage Tissue with Adjustable Thickness'. *Journal of Biomedical Materials Research Part A* 67A (4): 1170–80. https://doi.org/10.1002/jbm.a.10164.

Chen, Jia Lin, Zi Yin, Wei Liang Shen, Xiao Chen, Boon Chin Heng, Xiao Hui Zou, and Hong Wei Ouyang. 2010. 'Efficacy of HESC-MSCs in Knitted Silk-Collagen Scaffold for Tendon Tissue Engineering and Their Roles'. *Biomaterials* 31 (36): 9438–51. https://doi.org/10.1016/j.biomaterials.2010.08.011.

Chen, Jia Lin, Wei Zhang, Ze Yu Liu, Boon Chin Heng, Hong Wei Ouyang, and Xue Song Dai. 2015. 'Physical Regulation of Stem Cells Differentiation into Teno-Lineage: Current Strategies and Future Direction'. *Cell and Tissue Research* 360 (2): 195–207. https://doi.org/10.1007/s00441-014-2077-4.

Chen, Jiarong, Liu Yang, Lin Guo, and Xiaojun Duan. 2012. 'Sodium Hyaluronate as a

Drug-Release System for VEGF 165 Improves Graft Revascularization in Anterior Cruciate Ligament Reconstruction in a Rabbit Model'. *Experimental and Therapeutic Medicine* 4 (3): 430–34. https://doi.org/10.3892/etm.2012.629.

Chen, Xiao, Yi-Ying Qi, Lin-Lin Wang, Zi Yin, Guo-Li Yin, Xiao-Hui Zou, and Hong-Wei Ouyang. 2008. 'Ligament Regeneration Using a Knitted Silk Scaffold Combined with Collagen Matrix'. *Biomaterials* 29 (27): 3683–3692.

Chevallay, B., and D. Herbage. 2000. 'Collagen-Based Biomaterials as 3D Scaffold for Cell Cultures: Applications for Tissue Engineering and Gene Therapy'. *Medical and Biological Engineering and Computing* 38 (2): 211–18. https://doi.org/10.1007/BF02344779.

Chiara Barsotti, Maria, Paola Losi, Enrica Briganti, Elena Sanguinetti, Angela Magera, Tamer Al Kayal, Roberto Feriani, Rossella Di Stefano, and Giorgio Soldani. 2013. 'Effect of Platelet Lysate on Human Cells Involved in Different Phases of Wound Healing'. *PLoS ONE* 8 (12). https://doi.org/10.1371/journal.pone.0084753.

Chiou, Michael, Yue Xu, and Michael T. Longaker. 2006. 'Mitogenic and Chondrogenic Effects of Fibroblast Growth Factor-2 in Adipose-Derived Mesenchymal Cells'. *Biochemical and Biophysical Research Communications* 343 (2): 644–52. https://doi.org/10.1016/j.bbrc.2006.02.171.

Chiquet, Matthias. 1999. 'Regulation of Extracellular Matrix Gene Expression by Mechanical Stress'. *Matrix Biology* 18 (5): 417–26. https://doi.org/10.1016/S0945-053X(99)00039-6.

Comninou, Maria, and I. V. Yannas. 1976. 'Dependence of Stress-Strain Nonlinearity of Connective Tissues on the Geometry of Collagen Fibres'. *Journal of Biomechanics* 9 (7): 427–33. https://doi.org/10.1016/0021-9290(76)90084-1.

Cooper, James A., LeeAnn O. Bailey, Janell N. Carter, Cynthia E. Castiglioni, Michelle D. Kofron, Frank K. Ko, and Cato T. Laurencin. 2006. 'Evaluation of the Anterior Cruciate Ligament, Medial Collateral Ligament, Achilles Tendon and Patellar Tendon as Cell Sources for Tissue-Engineered Ligament'. *Biomaterials* 27 (13): 2747–2754.

Corey, Joseph M., David Y. Lin, Katherine B. Mycek, Qiaoran Chen, Stanley Samuel, Eva L. Feldman, and David C. Martin. 2007. 'Aligned Electrospun Nanofibers Specify the Direction of Dorsal Root Ganglia Neurite Growth'. *Journal of Biomedical Materials Research Part A: An Official Journal of The Society for Biomaterials, The Japanese Society for Biomaterials, and The Australian Society for Biomaterials and the Korean Society for Biomaterials* 83 (3): 636–645.

Czaplewski, Sarah K., Tsung-Lin Tsai, Sarah E. Duenwald-Kuehl, Ray Vanderby, and Wan-Ju Li. 2014. 'Tenogenic Differentiation of Human Induced Pluripotent Stem Cell-Derived Mesenchymal Stem Cells Dictated by Properties of Braided Submicron Fibrous Scaffolds'. *Biomaterials* 35 (25): 6907–17. https://doi.org/10.1016/j.biomaterials.2014.05.006.

Dahlgren, Linda A, Marjolein C. H van der Meulen, John E. A Bertram, Greg S Starrak, and Alan J Nixon. 2002. 'Insulin-like Growth Factor-I Improves Cellular and

Molecular Aspects of Healing in a Collagenase-Induced Model of Flexor Tendinitis'. *Journal of Orthopaedic Research* 20 (5): 910–19. https://doi.org/10.1016/S0736-0266(02)00009-8.

Dallalana, Richard J., John H. M. Brooks, Simon P. T. Kemp, and Andrew M. Williams. 2007. 'The Epidemiology of Knee Injuries in English Professional Rugby Union'. *The American Journal of Sports Medicine* 35 (5): 818–30. https://doi.org/10.1177/0363546506296738.

De Groot, J. H., F. M. Zijlstra, H. W. Kuipers, A. J. Pennings, J. Klompmaker, R. P. H. Veth, and H. W. B. Jansen. 1997. 'Meniscal Tissue Regeneration in Porous 50/50 Copoly (L-Lactide/ε-Caprolactone) Implants'. *Biomaterials* 18 (8): 613–622.

Deepthi, S., M. Nivedhitha Sundaram, J. Deepti Kadavan, and R. Jayakumar. 2016. 'Layered Chitosan-Collagen Hydrogel/Aligned PLLA Nanofiber Construct for Flexor Tendon Regeneration'. *Carbohydrate Polymers* 153 (November): 492–500. https://doi.org/10.1016/j.carbpol.2016.07.124.

Delaine-Smith, Robin M., Nicola H. Green, Stephen J. Matcher, Sheila MacNeil, and Gwendolen C. Reilly. 2014. 'Monitoring Fibrous Scaffold Guidance of Three-Dimensional Collagen Organisation Using Minimally-Invasive Second Harmonic Generation'. *PloS One* 9 (2): e89761.

Dimasi, Luke. 2011. 'Meeting Increased Demands on Cell-Based Processes by Using Defined Media Supplements'. *BioProcess International* 9 (8): 48–57.

Docheva, Denitsa, Ernst B. Hunziker, Reinhard Fässler, and Oliver Brandau. 2005.

'Tenomodulin Is Necessary for Tenocyte Proliferation and Tendon Maturation'. *Molecular and Cellular Biology* 25 (2): 699–705.

Dodge-Khatami, Ali, Carl L. Backer, Lauren D. Holinger, Constantine Mavroudis, Keith E. Cook, and Susan E. Crawford. 2001. 'Healing of a Free Tracheal Autograft Is Enhanced by Topical Vascular Endothelial Growth Factor in an Experimental Rabbit Model'. *The Journal of Thoracic and Cardiovascular Surgery* 122 (3): 554–61. https://doi.org/10.1067/mtc.2001.116206.

Dong, Chanjuan, and Yonggang Lv. 2016. 'Application of Collagen Scaffold in Tissue Engineering: Recent Advances and New Perspectives'. *Polymers* 8 (2). https://doi.org/10.3390/polym8020042.

Doroski, Derek M., Kelly S. Brink, and Johnna S. Temenoff. 2007. 'Techniques for Biological Characterization of Tissue-Engineered Tendon and Ligament'. *Biomaterials*, Cellular and Molecular Biology Techniques for Biomaterials Evaluation, 28 (2): 187–202. https://doi.org/10.1016/j.biomaterials.2006.08.040.

Doukas, John, Kate Blease, Darren Craig, Chenglie Ma, Lois A. Chandler, Barbara A. Sosnowski, and Glenn F. Pierce. 2002. 'Delivery of FGF Genes to Wound Repair Cells Enhances Arteriogenesis and Myogenesis in Skeletal Muscle'. *Molecular Therapy: The Journal of the American Society of Gene Therapy* 5 (5 Pt 1): 517–27. https://doi.org/10.1006/mthe.2002.0579.

Dunn, Michael G., Lisa D. Bellincampi, Alfred J. Tria, and Joseph P. Zawadsky. 1997. 'Preliminary Development of a Collagen-PLA Composite for ACL

Reconstruction'. *Journal of Applied Polymer Science* 63 (11): 1423–28. https://doi.org/10.1002/(SICI)1097-4628(19970314)63:11<1423::AID-APP4>3.0.CO;2-O.

Eagan, Michael J., Patricia A. Zuk, Ke-Wei Zhao, Benjamin E. Bluth, Elyse J. Brinkmann, Benjamin M. Wu, and David R. McAllister. 2012. 'The Suitability of Human Adipose-Derived Stem Cells for the Engineering of Ligament Tissue'. *Journal of Tissue Engineering and Regenerative Medicine* 6 (9): 702–709.

Erisken, Cevat, Xin Zhang, Kristen L. Moffat, William N. Levine, and Helen H. Lu. 2013. 'Scaffold Fiber Diameter Regulates Human Tendon Fibroblast Growth and Differentiation'. *Tissue Engineering. Part A* 19 (3–4): 519–28. https://doi.org/10.1089/ten.tea.2012.0072.

Ethicon, I. 2000. *Wound Closure Manual. The Suture Specific Suturing Materials. Non-Absorbable Suture*. Ethicon, Inc Somerville, NJ.

Fan, Hongbin, Haifeng Liu, Siew L. Toh, and James C. H. Goh. 2009. 'Anterior Cruciate Ligament Regeneration Using Mesenchymal Stem Cells and Silk Scaffold in Large Animal Model'. *Biomaterials* 30 (28): 4967–77. https://doi.org/10.1016/j.biomaterials.2009.05.048.

Fan, Hongbin, Haifeng Liu, Eugene J. W. Wong, Siew L. Toh, and James C. H. Goh. 2008. 'In Vivo Study of Anterior Cruciate Ligament Regeneration Using Mesenchymal Stem Cells and Silk Scaffold'. *Biomaterials* 29 (23): 3324–37. https://doi.org/10.1016/j.biomaterials.2008.04.012.

Frank, C. B. 2004a. 'Ligament Structure, Physiology and Function'. *Journal of*

Musculoskeletal and Neuronal Interactions 4 (2): 199.

———. 2004b. 'Ligament Structure, Physiology and Function'. *Journal of Musculoskeletal and Neuronal Interactions* 4 (2): 199.

Frank, C., S.L.-Y. Woo, D. Amiel, F. Harwood, M. Gomez, and W. Akeson. 1983. 'Medial Collateral Ligament Healing: A Multidisciplinary Assessment in Rabbits'. *The American Journal of Sports Medicine* 11 (6): 379–89. https://doi.org/10.1177/036354658301100602.

Freeman, Joseph W., Mia D. Woods, Damond A. Cromer, Emmanuel C. Ekwueme, Tea Andric, Emmanuel A. Atiemo, Christian H. Bijoux, and Cato T. Laurencin. 2011. 'Evaluation of a Hydrogel–Fiber Composite for ACL Tissue Engineering'. *Journal of Biomechanics* 44 (4): 694–99. https://doi.org/10.1016/j.jbiomech.2010.10.043.

Friedenstein, A. J., R. K. Chailakhjan, and K. S. Lalykina. 1970. 'The Development of Fibroblast Colonies in Monolayer Cultures of Guinea-Pig Bone Marrow and Spleen Cells'. *Cell Proliferation* 3 (4): 393–403. https://doi.org/10.1111/j.1365-2184.1970.tb00347.x.

Friedenstein, Alexander J. 1976. 'Precursor Cells of Mechanocytes'. In *International Review of Cytology*, edited by G. H. Bourne, J. F. Danielli, and K. W. Jeon, 47:327–59. Academic Press. https://doi.org/10.1016/S0074-7696(08)60092-3.

Frosch, Karl-Heinz, Dirk Stengel, Tobias Brodhun, Immanuel Stietencron, Dirk Holsten, Christian Jung, Dominik Reister, et al. 2010. 'Outcomes and Risks of Operative Treatment of Rupture of the Anterior Cruciate Ligament in Children

and Adolescents'. *Arthroscopy: The Journal of Arthroscopic & Related Surgery: Official Publication of the Arthroscopy Association of North America and the International Arthroscopy Association* 26 (11): 1539–50. https://doi.org/10.1016/j.arthro.2010.04.077.

Fujiwara, Hiroshi, Keiji Tatsumi, Kenzo Kosaka, Yukiyasu Sato, Toshihiro Higuchi, Shinya Yoshioka, Michiyuki Maeda, Masamichi Ueda, and Shingo Fujii. 2003. 'Human Blastocysts and Endometrial Epithelial Cells Express Activated Leukocyte Cell Adhesion Molecule (ALCAM/CD166)'. *The Journal of Clinical Endocrinology and Metabolism* 88 (7): 3437–43. https://doi.org/10.1210/jc.2002-021888.

Galliera, E., L. Girolamo De, P. Randelli, P. Volpi, G. Dogliotti, A. Quaglia, G. Banfi, P. Cabitza, M. M. Corsi, and M. Denti. 2011. 'High Articular Levels of the Angiogenetic Factors VEGF and VEGF-Receptor 2 as Tissue Healing Biomarkers after Single Bundle Anterior Cruciate Ligament Reconstruction.' *Journal of Biological Regulators and Homeostatic Agents* 25 (1): 85–91.

Ge, Zigang, James Cho Hong Goh, and Eng Hin Lee. 2005. 'Selection of Cell Source for Ligament Tissue Engineering'. *Cell Transplantation* 14 (8): 573–583.

Ge, Zigang, Fang Yang, James CH Goh, Seeram Ramakrishna, and Eng Hin Lee. 2006. 'Biomaterials and Scaffolds for Ligament Tissue Engineering'. *Journal of Biomedical Materials Research Part A: An Official Journal of The Society for Biomaterials, The Japanese Society for Biomaterials, and The Australian Society for Biomaterials and the Korean Society for Biomaterials* 77 (3): 639–

652.

Gelse, Kolja, E. Pöschl, and T. Aigner. 2003. 'Collagens—Structure, Function, and Biosynthesis'. *Advanced Drug Delivery Reviews* 55 (12): 1531–1546.

Gerich, T. G., R. Kang, F. H. Fu, P. D. Robbins, and C. H. Evans. 1996. 'Gene Transfer to the Rabbit Patellar Tendon: Potential for Genetic Enhancement of Tendon and Ligament Healing'. *Gene Therapy* 3 (12): 1089–93.

Giai Via, Alessio, Antonio Frizziero, and Francesco Oliva. 2012. 'Biological Properties of Mesenchymal Stem Cells from Different Sources'. *Muscles, Ligaments and Tendons Journal* 2 (3): 154–62.

Gianotti, Simon M., Stephen W. Marshall, Patria A. Hume, and Lorna Bunt. 2009. 'Incidence of Anterior Cruciate Ligament Injury and Other Knee Ligament Injuries: A National Population-Based Study'. *Journal of Science and Medicine in Sport* 12 (6): 622–27. https://doi.org/10.1016/j.jsams.2008.07.005.

Gnavi, Sara, Benedetta Fornasari, Chiara Tonda-Turo, Rossella Laurano, Marco Zanetti, Gianluca Ciardelli, and Stefano Geuna. 2015. 'The Effect of Electrospun Gelatin Fibers Alignment on Schwann Cell and Axon Behavior and Organization in the Perspective of Artificial Nerve Design'. *International Journal of Molecular Sciences* 16 (6): 12925–12942.

Gómez-Pinilla, F., L. Vu, and C. W. Cotman. 1995. 'Regulation of Astrocyte Proliferation by FGF-2 and Heparan Sulfate in Vivo'. *The Journal of Neuroscience: The Official Journal of the Society for Neuroscience* 15 (3 Pt 1): 2021–29.

Gornitzky, Alex L., Ariana Lott, Joseph L. Yellin, Peter D. Fabricant, J. Todd Lawrence, and Theodore J. Ganley. 2016. 'Sport-Specific Yearly Risk and Incidence of Anterior Cruciate Ligament Tears in High School Athletes: A Systematic Review and Meta-Analysis'. *The American Journal of Sports Medicine* 44 (10): 2716–23. https://doi.org/10.1177/0363546515617742.

Graf, Ben K., Richard H. Lange, C. Keith Fujisaki, Gregory L. Landry, and R. K. Saluja. 1992. 'Anterior Cruciate Ligament Tears in Skeletally Immature Patients: Meniscal Pathology at Presentation and after Attempted Conservative Treatment'. *Arthroscopy: The Journal of Arthroscopic & Related Surgery* 8 (2): 229–233.

Gumbiner, Barry M. 1996. 'Cell Adhesion: The Molecular Basis of Tissue Architecture and Morphogenesis'. *Cell* 84 (3): 345–57. https://doi.org/10.1016/S0092-8674(00)81279-9.

Guzzanti, V. 2003. 'The Natural History and Treatment of Rupture of the Anterior Cruciate Ligament in Children and Adolescents'. *The Journal of Bone and Joint Surgery. British Volume* 85 (4): 618–619.

Hahn, Sei Kwang, and Allan S. Hoffman. 2004. 'Characterization of Biocompatible Polyelectrolyte Complex Multilayer of Hyaluronic Acid and Poly-L-Lysine'. *Biotechnology and Bioprocess Engineering* 9 (3): 179–183.

Häkkinen, Lari, Silke Strassburger, Veli-Matti Kähäri, Paul G. Scott, Inge Eichstetter, Renato V. Iozzo, and Hannu Larjava. 2000. 'A Role for Decorin in the Structural Organization of Periodontal Ligament'. *Laboratory Investigation* 80 (12):

1869–80. https://doi.org/10.1038/labinvest.3780197.

Halper, Jaroslava, and Michael Kjaer. 2014. 'Basic Components of Connective Tissues and Extracellular Matrix: Elastin, Fibrillin, Fibulins, Fibrinogen, Fibronectin, Laminin, Tenascins and Thrombospondins'. In *Progress in Heritable Soft Connective Tissue Diseases*, edited by Jaroslava Halper, 31–47. Advances in Experimental Medicine and Biology. Dordrecht: Springer Netherlands. https://doi.org/10.1007/978-94-007-7893-1_3.

Hankemeier, Stefan, Michaela Keus, Johannes Zeichen, Michael Jagodzinski, Tanja Barkhausen, Ulrich Bosch, Christian Krettek, and Martijn Van Griensven. 2005. 'Modulation of Proliferation and Differentiation of Human Bone Marrow Stromal Cells by Fibroblast Growth Factor 2: Potential Implications for Tissue Engineering of Tendons and Ligaments'. *Tissue Engineering* 11 (1–2): 41–49. https://doi.org/10.1089/ten.2005.11.41.

Hardy, A., L. Casabianca, K. Andrieu, L. Baverel, and T. Noailles. 2017. 'Complications Following Harvesting of Patellar Tendon or Hamstring Tendon Grafts for Anterior Cruciate Ligament Reconstruction: Systematic Review of Literature'. *Orthopaedics & Traumatology: Surgery & Research*, Proceedings of the French Arthroscopic Society, 103 (8, Supplement): S245–48. https://doi.org/10.1016/j.otsr.2017.09.002.

Hauser, R. A., E. E. Dolan, H. J. Phillips, A. C. Newlin, R. E. Moore, and B. A. Woldin. 2013. 'Ligament Injury and Healing: A Review of Current Clinical Diagnostics and Therapeutics'. *The Open Rehabilitation Journal* 6 (1).

https://benthamopen.com/ABSTRACT/TOREHJ-6-1.

Haut, R. C. 1983. 'Age-Dependent Influence of Strain Rate on the Tensile Failure of
Rat-Tail Tendon'. *Journal of Biomechanical Engineering* 105 (3): 296–99.
https://doi.org/10.1115/1.3138422.

Hewett, Timothy E., Gregory D. Myer, Kevin R. Ford, Mark V. Paterno, and Carmen
E. Quatman. 2016. 'Mechanisms, Prediction, and Prevention of ACL Injuries:
Cut Risk With Three Sharpened and Validated Tools'. *Journal of Orthopaedic
Research : Official Publication of the Orthopaedic Research Society* 34 (11):
1843–55. https://doi.org/10.1002/jor.23414.

Hildebrand, K. A., C. B. Frank, and D. A. Hart. 2004. 'Gene Intervention in Ligament
and Tendon: Current Status, Challenges, Future Directions'. *Gene Therapy* 11
(4): 368–78. https://doi.org/10.1038/sj.gt.3302198.

Hildebrand, Kevin A., Masataka Deie, Christina R. Allen, David W. Smith, Helga I.
Georgescu, Christopher H. Evans, Paul D. Robbins, and Savio L.-Y. Woo. 1999.
'Early Expression of Marker Genes in the Rabbit Medial Collateral and Anterior
Cruciate Ligaments: The Use of Different Viral Vectors and the Effects of
Injury'. *Journal of Orthopaedic Research* 17 (1): 37–42.
https://doi.org/10.1002/jor.1100170107.

Hildebrand, Kevin A., Savio LY Woo, David W. Smith, Christina R. Allen, Masataka
Deie, Brian J. Taylor, and Christopher C. Schmidt. 1998. 'The Effects of
Platelet-Derived Growth Factor-BB on Healing of the Rabbit Medial Collateral
Ligament'. *The American Journal of Sports Medicine* 26 (4): 549–554.

Hodde, J. P., R. D. Record, H. A. Liang, and S. F. Badylak. 2001. 'Vascular Endothelial Growth Factor in Porcine-Derived Extracellular Matrix'. *Endothelium* 8 (1): 11–24.

Hsieh, C. F., P. Alberton, E. Loffredo-Verde, E. Volkmer, M. Pietschmann, P. E. Müller, M. Schieker, and D. Docheva. 2016. 'Periodontal Ligament Cells as Alternative Source for Cell-Based Therapy of Tendon Injuries: In Vivo Study of Full-Size Achilles Tendon Defect in a Rat Model'. *Eur Cell Mater* 32: 228–240.

Hu, E., P. Tontonoz, and B. M. Spiegelman. 1995. 'Transdifferentiation of Myoblasts by the Adipogenic Transcription Factors PPAR Gamma and C/EBP Alpha'. *Proceedings of the National Academy of Sciences* 92 (21): 9856–60. https://doi.org/10.1073/pnas.92.21.9856.

Huang, Wei-Min, S. J. Gibson, PGUJ Facer, J. Gu, and Julia M. Polak. 1983. 'Improved Section Adhesion for Immunocytochemistry Using High Molecular Weight Polymers of L-Lysine as a Slide Coating'. *Histochemistry* 77 (2): 275–279.

Humbel, Rene E. 1990. 'Insulin-like Growth Factors I and II'. *European Journal of Biochemistry* 190 (3): 445–462.

Ilic, Mirna Z., Phillip Carter, Alicia Tyndall, Jayesh Dudhia, and Christopher J. Handley. 2005. 'Proteoglycans and Catabolic Products of Proteoglycans Present in Ligament'. *Biochemical Journal* 385 (2): 381–88. https://doi.org/10.1042/BJ20040844.

Imanaka-Yoshida, Kyoko, and Hiroki Aoki. 2014. 'Tenascin-C and Mechanotransduction in the Development and Diseases of Cardiovascular

System'. *Frontiers in Physiology* 5. https://doi.org/10.3389/fphys.2014.00283.

Jarvinen, T. A. H. 2003. 'Mechanical Loading Regulates the Expression of Tenascin-C in the Myotendinous Junction and Tendon but Does Not Induce de Novo Synthesis in the Skeletal Muscle'. *Journal of Cell Science* 116 (5): 857–66. https://doi.org/10.1242/jcs.00303.

Järvinen, T. a. H., P. Kannus, T. L. N. Järvinen, L. Jozsa, H. Kalimo, and M. Järvinen. 2000. 'Tenascin-C in the Pathobiology and Healing Process of Musculoskeletal Tissue Injury'. *Scandinavian Journal of Medicine & Science in Sports* 10 (6): 376–82. https://doi.org/10.1034/j.1600-0838.2000.010006376.x.

Jenner, J.M.G.Th., F. van Eijk, D.b.f. Saris, W.j. Willems, W.j.a. Dhert, and Laura B. Creemers. 2007. 'Effect of Transforming Growth Factor-Beta and Growth Differentiation Factor-5 on Proliferation and Matrix Production by Human Bone Marrow Stromal Cells Cultured on Braided Poly Lactic-Co-Glycolic Acid Scaffolds for Ligament Tissue Engineering'. *Tissue Engineering* 13 (7): 1573–82. https://doi.org/10.1089/ten.2006.0208.

Jeong, Ishik, Hye-Sun Yu, Mi-Kyung Kim, Jun-Hyeog Jang, and Hae-Won Kim. 2010. 'FGF2-Adsorbed Macroporous Hydroxyapatite Bone Granules Stimulate in Vitro Osteoblastic Gene Expression and Differentiation'. *Journal of Materials Science. Materials in Medicine* 21 (4): 1335–42. https://doi.org/10.1007/s10856-009-3971-2.

Jeong, Sung In, Byung-Soo Kim, Sun Woong Kang, Jae Hyun Kwon, Young Moo Lee, Soo Hyun Kim, and Young Ha Kim. 2004. 'In Vivo Biocompatibilty and

Degradation Behavior of Elastic Poly(L-Lactide-Co-Epsilon-Caprolactone) Scaffolds'. *Biomaterials* 25 (28): 5939–46. https://doi.org/10.1016/j.biomaterials.2004.01.057.

Jeong, Sung In, Soo Hyun Kim, Young Ha Kim, Youngmee Jung, Jae Hyun Kwon, Byung-Soo Kim, and Young Moo Lee. 2004. 'Manufacture of Elastic Biodegradable PLCL Scaffolds for Mechano-Active Vascular Tissue Engineering'. *Journal of Biomaterials Science. Polymer Edition* 15 (5): 645–60.

Jeong, Sung In, Jae Hyun Kwon, Jin Ik Lim, Seung-Woo Cho, Youngmee Jung, Won Jun Sung, Soo Hyun Kim, et al. 2005. 'Mechano-Active Tissue Engineering of Vascular Smooth Muscle Using Pulsatile Perfusion Bioreactors and Elastic PLCL Scaffolds'. *Biomaterials* 26 (12): 1405–11. https://doi.org/10.1016/j.biomaterials.2004.04.036.

Jun, Indong, Hyung-Seop Han, James Edwards, and Hojeong Jeon. 2018. 'Electrospun Fibrous Scaffolds for Tissue Engineering: Viewpoints on Architecture and Fabrication'. *International Journal of Molecular Sciences* 19 (3): 745.

Juneja, Subhash C., and Christian Veillette. 2013. 'Defects in Tendon, Ligament, and Enthesis in Response to Genetic Alterations in Key Proteoglycans and Glycoproteins: A Review'. Research article. Arthritis. 2013. https://doi.org/10.1155/2013/154812.

Kalpan, G., V. S. Shalini, S. Jonnalagadda, and N. Kumar. 2007. 'Fast Degradable Poly (L-Lactide-Co-e-Caprolactone) Microspheres for Tissue Engineering: Synthesis, Characterization, and Degradation Behavior'. *J Polym Sci A1* 45:

2755–2764.

Kang, Mi-Na, Hee-Hoon Yoon, Young-Kwon Seo, and Jung-Keug Park. 2012. 'Human Umbilical Cord-Derived Mesenchymal Stem Cells Differentiate into Ligament-like Cells with Mechanical Stimulation in Various Media'. *Tissue Engineering and Regenerative Medicine* 9 (4): 185–93. https://doi.org/10.1007/s13770-012-0333-9.

Kaplan, David, W. Wade Adams, Barry Farmer, and Christopher Viney. 1994. 'Silk: Biology, Structure, Properties, and Genetics'. In *ACS Symposium Series (USA)*.

Kawai, K., S. Suzuki, Y. Tabata, Y. Ikada, and Y. Nishimura. 2000. 'Accelerated Tissue Regeneration through Incorporation of Basic Fibroblast Growth Factor-Impregnated Gelatin Microspheres into Artificial Dermis'. *Biomaterials* 21 (5): 489–99.

Kendoff, Daniel, Rhidian Morgan-Jones, and Fares S. Haddad. 2016. *Periprosthetic Joint Infections: Changing Paradigms*. Springer.

Kim, Mihye, Bohee Hong, Jongman Lee, Se Eun Kim, Seong Soo Kang, Young Ha Kim, and Giyoong Tae. 2012. 'Composite System of PLCL Scaffold and Heparin-Based Hydrogel for Regeneration of Partial-Thickness Cartilage Defects'. *Biomacromolecules* 13 (8): 2287–98. https://doi.org/10.1021/bm3005353.

Kimura, Yu, Makoto Ozeki, Takashi Inamoto, and Yasuhiko Tabata. 2003. 'Adipose Tissue Engineering Based on Human Preadipocytes Combined with Gelatin Microspheres Containing Basic Fibroblast Growth Factor'. *Biomaterials* 24

(14): 2513–21.

Kocaefe, Çetin, Deniz Balcı, Burcu Balcı Hayta, and Alp Can. 2010. 'Reprogramming of Human Umbilical Cord Stromal Mesenchymal Stem Cells for Myogenic Differentiation and Muscle Repair'. *Stem Cell Reviews and Reports* 6 (4): 512–522.

Komiyama, Yuske, Shinsuke Ohba, Nobuyuki Shimohata, Keiji Nakajima, Hironori Hojo, Fumiko Yano, Tsuyoshi Takato, et al. 2013. 'Tenomodulin Expression in the Periodontal Ligament Enhances Cellular Adhesion'. *PLOS ONE* 8 (4): e60203. https://doi.org/10.1371/journal.pone.0060203.

Koob, Thomas J., and Daniel J. Hernandez. 2002. 'Material Properties of Polymerized NDGA–Collagen Composite Fibers: Development of Biologically Based Tendon Constructs'. *Biomaterials* 23 (1): 203–212.

Kouroupis, Dimitrios, Athena Kyrkou, Eleni Triantafyllidi, Michalis Katsimpoulas, George Chalepakis, Anna Goussia, Anastasios Georgoulis, Carol Murphy, and Theodore Fotsis. 2016. 'Generation of Stem Cell-Based Bioartificial Anterior Cruciate Ligament (ACL) Grafts for Effective ACL Rupture Repair'. *Stem Cell Research* 17 (2): 448–57. https://doi.org/10.1016/j.scr.2016.04.016.

Kroeze, R. J., M. N. Helder, W. H. Roos, G. J. L. Wuite, R. A. Bank, and T. H. Smit. 2010. 'The Effect of Ethylene Oxide, Glow Discharge and Electron Beam on the Surface Characteristics of Poly (L-Lactide-Co-Caprolactone) and the Corresponding Cellular Response of Adipose Stem Cells'. *Acta Biomaterialia* 6 (6): 2060–2065.

Kuboki, Yoshinori, Qiming Jin, and Hiroko Takita. 2001. 'Geometry of Carriers Controlling Phenotypic Expression in BMP-Induced Osteogenesis and Chondrogenesis'. *JBJS* 83: S1–105.

Kuo, Catherine K., Joseph E. Marturano, and Rocky S. Tuan. 2010. 'Novel Strategies in Tendon and Ligament Tissue Engineering: Advanced Biomaterials and Regeneration Motifs'. *BMC Sports Science, Medicine and Rehabilitation* 2 (1): 20. https://doi.org/10.1186/1758-2555-2-20.

Kurtz, Christopher A., Thomas G. Loebig, Donald D. Anderson, Patrick J. DeMeo, and Phil G. Campbell. 1999. 'Insulin-Like Growth Factor I Accelerates Functional Recovery from Achilles Tendon Injury in a Rat Model'. *The American Journal of Sports Medicine* 27 (3): 363–69. https://doi.org/10.1177/03635465990270031701.

Laurencin, Cato T., and Joseph W. Freeman. 2005. 'Ligament Tissue Engineering: An Evolutionary Materials Science Approach'. *Biomaterials* 26 (36): 7530–36. https://doi.org/10.1016/j.biomaterials.2005.05.073.

Laurent, Cédric, Xing Liu, Natalia De Isla, Xiong Wang, and Rachid Rahouadj. 2018. 'Defining a Scaffold for Ligament Tissue Engineering: What Has Been Done, and What Still Needs to Be Done'. *Journal of Cellular Immunotherapy*, 7th International Symposium Europe China Stem Cells and Regenerative Medicine, 4 (1): 4–9. https://doi.org/10.1016/j.jocit.2018.09.002.

Laurent, Cédric P., Damien Durville, Didier Mainard, Jean-François Ganghoffer, and Rachid Rahouadj. 2012. 'A Multilayer Braided Scaffold for Anterior Cruciate

Ligament: Mechanical Modeling at the Fiber Scale'. *Journal of the Mechanical Behavior of Biomedical Materials* 12 (August): 184–96. https://doi.org/10.1016/j.jmbbm.2012.03.005.

Laurent, Cédric P., Jean-François Ganghoffer, Jérôme Babin, Jean-Luc Six, Xiong Wang, and Rachid Rahouadj. 2011. 'Morphological Characterization of a Novel Scaffold for Anterior Cruciate Ligament Tissue Engineering'. *Journal of Biomechanical Engineering* 133 (6): 065001.

Laurent, Cédric P., Cédryck Vaquette, Xing Liu, Jean-François Schmitt, and Rachid Rahouadj. 2018. 'Suitability of a PLCL Fibrous Scaffold for Soft Tissue Engineering Applications: A Combined Biological and Mechanical Characterisation'. *Journal of Biomaterials Applications* 32 (9): 1276–88. https://doi.org/10.1177/0885328218757064.

Laurent, Cédric P., Cédryck Vaquette, Céline Martin, Emmanuel Guedon, Xiude Wu, Alain Delconte, Dominique Dumas, et al. 2014a. 'Towards a Tissue-Engineered Ligament: Design and Preliminary Evaluation of a Dedicated Multi-Chamber Tension-Torsion Bioreactor'. *Processes* 2 (1): 167–79. https://doi.org/10.3390/pr2010167.

———. 2014b. 'Towards a Tissue-Engineered Ligament: Design and Preliminary Evaluation of a Dedicated Multi-Chamber Tension-Torsion Bioreactor'. *Processes* 2 (1): 167–79. https://doi.org/10.3390/pr2010167.

Lawrence, J. Todd R., Nina Argawal, and Theodore J. Ganley. 2011. 'Degeneration of the Knee Joint in Skeletally Immature Patients with a Diagnosis of an Anterior

Cruciate Ligament Tear: Is There Harm in Delay of Treatment?' *The American Journal of Sports Medicine* 39 (12): 2582–2587.

LEE, THAY Q. 2005. 'Structure and Function of Ligaments and Tendons'. *Basic Orthopaedic Biomechanics & Mechano-Biology*, 301.

Li, Shuzhen, Yueping Chen, Zonghan Lin, Wei Cui, Jingmin Zhao, and Wei Su. 2012. 'A Systematic Review of Randomized Controlled Clinical Trials Comparing Hamstring Autografts versus Bone-Patellar Tendon-Bone Autografts for the Reconstruction of the Anterior Cruciate Ligament'. *Archives of Orthopaedic and Trauma Surgery* 132 (9): 1287–97. https://doi.org/10.1007/s00402-012-1532-5.

Li, Zhenyu, and Ce Wang. 2013. *One-Dimensional Nanostructures: Electrospinning Technique and Unique Nanofibers*. Springer.

Liang, Rui, Savio L.-Y. Woo, Yoshiyuki Takakura, Daniel K. Moon, Fengyan Jia, and Steven D. Abramowitch. 2006. 'Long-Term Effects of Porcine Small Intestine Submucosa on the Healing of Medial Collateral Ligament: A Functional Tissue Engineering Study'. *Journal of Orthopaedic Research* 24 (4): 811–819.

Lifshitz, Veronica, and Dan Frenkel. 2013. 'Chapter 225 - TGF-β'. In *Handbook of Biologically Active Peptides (Second Edition)*, edited by Abba J. Kastin, 1647–53. Boston: Academic Press. https://doi.org/10.1016/B978-0-12-385095-9.00225-6.

'Ligament Injury and Healing: An Overview of Current Clinical Concepts'. 2012. *Journal of Prolotherapy* (blog). 29 March 2012.

http://journalofprolotherapy.com/ligament-injury-and-healing-an-overview-of-current-clinical-concepts/.

Lim, Jit-Kheng, James Hui, Li Li, Ashvin Thambyah, James Goh, and Eng-Hin Lee. 2004. 'Enhancement of Tendon Graft Osteointegration Using Mesenchymal Stem Cells in a Rabbit Model of Anterior Cruciate Ligament Reconstruction'. *Arthroscopy: The Journal of Arthroscopic & Related Surgery* 20 (9): 899–910.

Liu, Haifeng, Hongbin Fan, Yue Wang, Siew Lok Toh, and James C. H. Goh. 2008. 'The Interaction between a Combined Knitted Silk Scaffold and Microporous Silk Sponge with Human Mesenchymal Stem Cells for Ligament Tissue Engineering'. *Biomaterials* 29 (6): 662–74. https://doi.org/10.1016/j.biomaterials.2007.10.035.

Liu, Wei, Bin Chen, Dan Deng, Feng Xu, Lei Cui, and Yilin Cao. 2006. 'Repair of Tendon Defect with Dermal Fibroblast Engineered Tendon in a Porcine Model'. *Tissue Engineering* 12 (4): 775–78. https://doi.org/10.1089/ten.2006.12.775.

Liu, Xing, Cédric Laurent, Qiaoyue Du, Laurie Targa, Ghislaine Cauchois, Yun Chen, Xiong Wang, and Natalia de Isla. 2018. 'Mesenchymal Stem Cell Interacted with PLCL Braided Scaffold Coated with Poly-l-Lysine/Hyaluronic Acid for Ligament Tissue Engineering'. *Journal of Biomedical Materials Research Part A* 106 (12): 3042–3052.

Lou, J., Y. Tu, M. Burns, M. J. Silva, and P. Manske. 2001. 'BMP-12 Gene Transfer Augmentation of Lacerated Tendon Repair'. *Journal of Orthopaedic Research: Official Publication of the Orthopaedic Research Society* 19 (6): 1199–1202.

https://doi.org/10.1016/S0736-0266(01)00042-0.

Lou, J., Y. Tu, F. J. Ludwig, J. Zhang, and P. R. Manske. 1999. 'Effect of Bone Morphogenetic Protein-12 Gene Transfer on Mesenchymal Progenitor Cells'. *Clinical Orthopaedics and Related Research*, no. 369 (December): 333–39.

Lu, Helen H., James A. Cooper Jr, Sharron Manuel, Joseph W. Freeman, Mohammed A. Attawia, Frank K. Ko, and Cato T. Laurencin. 2005. 'Anterior Cruciate Ligament Regeneration Using Braided Biodegradable Scaffolds: In Vitro Optimization Studies'. *Biomaterials* 26 (23): 4805–4816.

Lujan, Trevor J., Clayton J. Underwood, Nathan T. Jacobs, and Jeffrey A. Weiss. 2009. 'Contribution of Glycosaminoglycans to Viscoelastic Tensile Behavior of Human Ligament'. *Journal of Applied Physiology* 106 (2): 423–31. https://doi.org/10.1152/japplphysiol.90748.2008.

Ma, Dakun, Yansong Wang, and Wenjie Dai. 2018. 'Silk Fibroin-Based Biomaterials for Musculoskeletal Tissue Engineering'. *Materials Science and Engineering: C* 89 (August): 456–69. https://doi.org/10.1016/j.msec.2018.04.062.

Ma, Peter X. 2004. 'Scaffolds for Tissue Fabrication'. *Materials Today* 7 (5): 30–40. https://doi.org/10.1016/S1369-7021(04)00233-0.

MacIntosh, Ana C., Victoria R. Kearns, Aileen Crawford, and Paul V. Hatton. 2008. 'Skeletal Tissue Engineering Using Silk Biomaterials'. *Journal of Tissue Engineering and Regenerative Medicine* 2 (2–3): 71–80.

Mackey, Abigail Louise, Katja Maria Heinemeier, Satu Osmi Anneli Koskinen, and Michael Kjaer. 2008. 'Dynamic Adaptation of Tendon and Muscle Connective

Tissue to Mechanical Loading'. *Connective Tissue Research* 49 (3–4): 165–68. https://doi.org/10.1080/03008200802151672.

Mafi, R, S Hindocha, P Mafi, M Griffin, and W.S Khan. 2011. 'Sources of Adult Mesenchymal Stem Cells Applicable for Musculoskeletal Applications - A Systematic Review of the Literature'. *The Open Orthopaedics Journal* 5 (July): 242–48. https://doi.org/10.2174/1874325001105010242.

Majewski, M., Habelt Susanne, and Steinbrück Klaus. 2006. 'Epidemiology of Athletic Knee Injuries: A 10-Year Study'. *The Knee* 13 (3): 184–188.

Maleki, Masoud, Farideh Ghanbarvand, Mohammad Reza Behvarz, Mehri Ejtemaei, and Elham Ghadirkhomi. 2014. 'Comparison of Mesenchymal Stem Cell Markers in Multiple Human Adult Stem Cells'. *International Journal of Stem Cells* 7 (2): 118–26. https://doi.org/10.15283/ijsc.2014.7.2.118.

Malmström, Anders, Barbara Bartolini, Martin A. Thelin, Benny Pacheco, and Marco Maccarana. 2012. 'Iduronic Acid in Chondroitin/Dermatan Sulfate: Biosynthesis and Biological Function'. *Journal of Histochemistry & Cytochemistry* 60 (12): 916–925.

Margheritini, Fabrizio, Jeff Rihn, Volker Musahl, Pier P. Mariani, and Christopher Harner. 2002. 'Posterior Cruciate Ligament Injuries in the Athlete'. *Sports Medicine* 32 (6): 393–408. https://doi.org/10.2165/00007256-200232060-00004.

Marui, T., C. Niyibizi, H. I. Georgescu, M. Cao, K. W. Kavalkovich, R. E. Levine, and S. L. Woo. 1997. 'Effect of Growth Factors on Matrix Synthesis by Ligament

Fibroblasts'. *Journal of Orthopaedic Research: Official Publication of the Orthopaedic Research Society* 15 (1): 18–23. https://doi.org/10.1002/jor.1100150104.

Masoud, Ghorbani, Sadeghi Hossain, Rashidi Bahman, Karimi Zeinab, and Amouzegar Fatemeh. 2014. 'New Look at about Nature, Structure and Function of Trietz Ligament'. *Advanced Biomedical Research* 3 (January). https://doi.org/10.4103/2277-9175.125853.

Menetrey, J., C. Kasemkijwattana, C. S. Day, P. Bosch, F. H. Fu, M. S. Moreland, and J. Huard. 1999. 'Direct-, Fibroblast- and Myoblast-Mediated Gene Transfer to the Anterior Cruciate Ligament'. *Tissue Engineering* 5 (5): 435–42. https://doi.org/10.1089/ten.1999.5.435.

Messenger, Michael P., El M. Raïf, Bahaa B. Seedhom, and Steven J. Brookes. 2010. 'Enamel Matrix Derivative Enhances Tissue Formation around Scaffolds Used for Tissue Engineering of Ligaments'. *Journal of Tissue Engineering and Regenerative Medicine* 4 (2): 96–104. https://doi.org/10.1002/term.210.

Meyers, Michael C., and Bill S. Barnhill. 2004. 'Incidence, Causes, and Severity of High School Football Injuries on FieldTurf versus Natural Grass: A 5-Year Prospective Study'. *The American Journal of Sports Medicine* 32 (7): 1626–38. https://doi.org/10.1177/0363546504266978.

Moffat, Kristen L., Anne S.-P. Kwei, Jeffrey P. Spalazzi, Stephen B. Doty, William N. Levine, and Helen H. Lu. 2009. 'Novel Nanofiber-Based Scaffold for Rotator Cuff Repair and Augmentation'. *Tissue Engineering. Part A* 15 (1): 115–26.

https://doi.org/10.1089/ten.tea.2008.0014.

Molloy, Timothy, Yao Wang, and George Murrell. 2003. 'The Roles of Growth Factors in Tendon and Ligament Healing'. *Sports Medicine (Auckland, N.Z.)* 33 (5): 381–94. https://doi.org/10.2165/00007256-200333050-00004.

Moshaverinia, Alireza, Xingtian Xu, Chider Chen, Sahar Ansari, Homayoun H. Zadeh, Malcolm L. Snead, and Songtao Shi. 2014. 'Application of Stem Cells Derived from the Periodontal Ligament or Gingival Tissue Sources for Tendon Tissue Regeneration'. *Biomaterials* 35 (9): 2642–50. https://doi.org/10.1016/j.biomaterials.2013.12.053.

Muller, Yves A, Hans W Christinger, Bruce A Keyt, and Abraham M de Vos. 1997. 'The Crystal Structure of Vascular Endothelial Growth Factor (VEGF) Refined to 1.93 Å Resolution: Multiple Copy Flexibility and Receptor Binding'. *Structure* 5 (10): 1325–38. https://doi.org/10.1016/S0969-2126(97)00284-0.

Murray, Martha M., Kurt P. Spindler, Eduardo Abreu, John A. Muller, Arthur Nedder, Mark Kelly, John Frino, et al. 2007. 'Collagen-Platelet Rich Plasma Hydrogel Enhances Primary Repair of the Porcine Anterior Cruciate Ligament'. *Journal of Orthopaedic Research* 25 (1): 81–91. https://doi.org/10.1002/jor.20282.

Mustoe, Thomas A., Neal R. Cutler, Richard M. Allman, Patricia S. Goode, Thomas F. Deuel, Jo Ann Prause, Moraye Bear, Cuneyt M. Serdar, and Glenn F. Pierce. 1994. 'A Phase II Study to Evaluate Recombinant Platelet-Derived Growth Factor-BB in the Treatment of Stage 3 and 4 Pressure Ulcers'. *Archives of Surgery* 129 (2): 213–219.

Naghashzargar, Elham, Dariush Semnani, Saeed Karbasi, and Haleh Nekoee. 2014. 'Application of Intelligent Neural Network Method for Prediction of Mechanical Behavior of Wire-Rope Scaffold in Tissue Engineering'. *The Journal of The Textile Institute* 105 (3): 264–74. https://doi.org/10.1080/00405000.2013.835904.

Nakamura, N., K. Shino, T. Natsuume, S. Horibe, N. Matsumoto, Y. Kaneda, and T. Ochi. 1998. 'Early Biological Effect of in Vivo Gene Transfer of Platelet-Derived Growth Factor (PDGF)-B into Healing Patellar Ligament'. *Gene Therapy* 5 (9): 1165–70. https://doi.org/10.1038/sj.gt.3300712.

Nakamura, N., S. A. Timmermann, D. A. Hart, Y. Kaneda, N. G. Shrive, K. Shino, T. Ochi, and C. B. Frank. 1998. 'A Comparison of in Vivo Gene Delivery Methods for Antisense Therapy in Ligament Healing'. *Gene Therapy* 5 (11): 1455–61. https://doi.org/10.1038/sj.gt.3300765.

Nakamura, Norimasa, David A. Hart, Richard S. Boorman, Yasufumi Kaneda, Nigel G. Shrive, Linda L. Marchuk, Konsei Shino, Takahiro Ochi, and Cyril B. Frank. 2000. 'Decorin Antisense Gene Therapy Improves Functional Healing of Early Rabbit Ligament Scar with Enhanced Collagen Fibrillogenesis in Vivo'. *Journal of Orthopaedic Research* 18 (4): 517–23. https://doi.org/10.1002/jor.1100180402.

Nau, Thomas, and Andreas Teuschl. 2015. 'Regeneration of the Anterior Cruciate Ligament: Current Strategies in Tissue Engineering'. *World Journal of Orthopedics* 6 (1): 127–36. https://doi.org/10.5312/wjo.v6.i1.127.

Nehrer, Stefan, Howard A. Breinan, Arun Ramappa, Gretchen Young, Sonya Shortkroff, Libby K. Louie, Clement B. Sledge, Ioannis V. Yannas, and Myron Spector. 1997. 'Matrix Collagen Type and Pore Size Influence Behaviour of Seeded Canine Chondrocytes'. *Biomaterials* 18 (11): 769–76. https://doi.org/10.1016/S0142-9612(97)00001-X.

Niyibizi, C., K. Kavalkovich, T. Yamaji, and S. L. Woo. 2000. 'Type V Collagen Is Increased during Rabbit Medial Collateral Ligament Healing'. *Knee Surgery, Sports Traumatology, Arthroscopy: Official Journal of the ESSKA* 8 (5): 281–85. https://doi.org/10.1007/s001670000134.

Nöth, U., K. Schupp, A. Heymer, S. Kall, F. Jakob, N. Schütze, B. Baumann, T. Barthel, J. Eulert, and C. Hendrich. 2005. 'Anterior Cruciate Ligament Constructs Fabricated from Human Mesenchymal Stem Cells in a Collagen Type I Hydrogel'. *Cytotherapy* 7 (5): 447–55. https://doi.org/10.1080/14653240500319093.

Ohneda, O., K. Ohneda, F. Arai, J. Lee, T. Miyamoto, Y. Fukushima, D. Dowbenko, L. A. Lasky, and T. Suda. 2001. 'ALCAM (CD166): Its Role in Hematopoietic and Endothelial Development'. *Blood* 98 (7): 2134–42.

Pagán, Ana, Salvador D. Aznar-Cervantes, José Pérez-Rigueiro, Luis Meseguer-Olmo, and Jose L. Cenis. 2019. 'Potential Use of Silkworm Gut Fiber Braids as Scaffolds for Tendon and Ligament Tissue Engineering'. *Journal of Biomedical Materials Research Part B: Applied Biomaterials*.

Paletta, G. A., and R. F. Warren. 1994. 'Knee Injuries and Alpine Skiing. Treatment and

Rehabilitation'. *Sports Medicine (Auckland, N.Z.)* 17 (6): 411–23. https://doi.org/10.2165/00007256-199417060-00006.

Pauly, Hannah M., Daniel J. Kelly, Ketul C. Popat, Nathan A. Trujillo, Nicholas J. Dunne, Helen O. McCarthy, and Tammy L. Haut Donahue. 2016. 'Mechanical Properties and Cellular Response of Novel Electrospun Nanofibers for Ligament Tissue Engineering: Effects of Orientation and Geometry'. *Journal of the Mechanical Behavior of Biomedical Materials* 61 (August): 258–70. https://doi.org/10.1016/j.jmbbm.2016.03.022.

Pauly, Hannah M., Binulal N. Sathy, Dinorath Olvera, Helen O. McCarthy, Daniel J. Kelly, Ketul C. Popat, Nicholas J. Dunne, and Tammy Lynn Haut Donahue. 2017. 'Hierarchically Structured Electrospun Scaffolds with Chemically Conjugated Growth Factor for Ligament Tissue Engineering'. *Tissue Engineering Part A* 23 (15–16): 823–836.

Peh, Ruey-Feng, Vallaya Suthikum, Cho-Hong Goh, and Siew-Lok Toh. 2007. 'Novel Electrospun-Knitted Silk Scaffolds for Ligament Tissue Engineering'. In *World Congress on Medical Physics and Biomedical Engineering 2006*, edited by R. Magjarevic and J. H. Nagel, 3287–90. IFMBE Proceedings. Springer Berlin Heidelberg.

Peppas, Nicholas A., J. Zach Hilt, Ali Khademhosseini, and Robert Langer. 2006. 'Hydrogels in Biology and Medicine: From Molecular Principles to Bionanotechnology'. *Advanced Materials* 18 (11): 1345–1360.

Petrigliano, Frank A., David R. McAllister, and Benjamin M. Wu. 2006. 'Tissue

Engineering for Anterior Cruciate Ligament Reconstruction: A Review of Current Strategies'. *Arthroscopy: The Journal of Arthroscopic & Related Surgery* 22 (4): 441–51. https://doi.org/10.1016/j.arthro.2006.01.017.

Phinney, Donald G., and Darwin J. Prockop. 2007. 'Concise Review: Mesenchymal Stem/Multipotent Stromal Cells: The State of Transdifferentiation and Modes of Tissue Repair—Current Views'. *STEM CELLS* 25 (11): 2896–2902. https://doi.org/10.1634/stemcells.2007-0637.

Pierce, Glenn F., Thomas A. Mustoe, Bruce W. Altrock, Thomas F. Deuel, and Arlen Thomason. 1991. 'Role of Platelet☐derived Growth Factor in Wound Healing'. *Journal of Cellular Biochemistry* 45 (4): 319–26. https://doi.org/10.1002/jcb.240450403.

Prockop, Darwin J. 1997. 'Marrow Stromal Cells as Stem Cells for Nonhematopoietic Tissues'. *Science* 276 (5309): 71–74. https://doi.org/10.1126/science.276.5309.71.

Rana, Sohel, and Raul Fangueiro. 2015. *Braided Structures and Composites: Production, Properties, Mechanics, and Technical Applications*. CRC Press.

Rathbone, Sarah, and Sarah Cartmell. 2011. 'Tissue Engineering of Ligaments'. In *Tissue Engineering for Tissue and Organ Regeneration*. IntechOpen.

Rege, Tanya A., and James S. Hagood. 2006. 'Thy-1 as a Regulator of Cell-Cell and Cell-Matrix Interactions in Axon Regeneration, Apoptosis, Adhesion, Migration, Cancer, and Fibrosis'. *FASEB Journal: Official Publication of the Federation of American Societies for Experimental Biology* 20 (8): 1045–54.

https://doi.org/10.1096/fj.05-5460rev.

Reviews, C. T. I. 2016. *Kinn's The Medical Assistant, An Applied Learning Approach: Medicine, Healthcare*. Cram101 Textbook Reviews.

Richert, Ludovic, Fouzia Boulmedais, Philippe Lavalle, Jérôme Mutterer, Emmanuelle Ferreux, Gero Decher, Pierre Schaaf, Jean-Claude Voegel, and Catherine Picart. 2004. 'Improvement of Stability and Cell Adhesion Properties of Polyelectrolyte Multilayer Films by Chemical Cross-Linking'. *Biomacromolecules* 5 (2): 284–294.

Rodrigues, Márcia T., Rui L. Reis, and Manuela E. Gomes. 2013. 'Engineering Tendon and Ligament Tissues: Present Developments towards Successful Clinical Products'. *Journal of Tissue Engineering and Regenerative Medicine* 7 (9): 673–86. https://doi.org/10.1002/term.1459.

Rodríguez, Francisco J., Nuria Gómez, Gabriele Perego, and Xavier Navarro. 1999. 'Highly Permeable Polylactide-Caprolactone Nerve Guides Enhance Peripheral Nerve Regeneration through Long Gaps'. *Biomaterials* 20 (16): 1489–1500. https://doi.org/10.1016/S0142-9612(99)00055-1.

Roosa, Sara M. Mantila, Jessica M. Kemppainen, Erin N. Moffitt, Paul H. Krebsbach, and Scott J. Hollister. 2010. 'The Pore Size of Polycaprolactone Scaffolds Has Limited Influence on Bone Regeneration in an in Vivo Model'. *Journal of Biomedical Materials Research Part A* 92 (1): 359–368.

Rothrauff, Benjamin B., Brian B. Lauro, Guang Yang, Richard E. Debski, Volker Musahl, and Rocky S. Tuan. 2017. 'Braided and Stacked Electrospun

Nanofibrous Scaffolds for Tendon and Ligament Tissue Engineering'. *Tissue Engineering. Part A* 23 (9–10): 378–89. https://doi.org/10.1089/ten.TEA.2016.0319.

S Dhinsa, Baljinder, Anant N Mahapatra, and Wasim S Khan. 2015. 'Sources of Adult Mesenchymal Stem Cells for Ligament and Tendon Tissue Engineering'. *Current Stem Cell Research & Therapy* 10 (1): 26–30.

Saber, Sepideh, Andrew Y. Zhang, Sae H. Ki, Derek P. Lindsey, Robert Lane Smith, Jonathan Riboh, Hung Pham, and James Chang. 2010. 'Flexor Tendon Tissue Engineering: Bioreactor Cyclic Strain Increases Construct Strength'. *Tissue Engineering Part A* 16 (6): 2085–90. https://doi.org/10.1089/ten.tea.2010.0032.

Sahoo, Sambit, Siew Lok Toh, and James CH Goh. 2010. 'A BFGF-Releasing Silk/PLGA-Based Biohybrid Scaffold for Ligament/Tendon Tissue Engineering Using Mesenchymal Progenitor Cells'. *Biomaterials* 31 (11): 2990–2998.

Sakaguchi, Yusuke, Ichiro Sekiya, Kazuyoshi Yagishita, and Takeshi Muneta. 2005. 'Comparison of Human Stem Cells Derived from Various Mesenchymal Tissues: Superiority of Synovium as a Cell Source'. *Arthritis & Rheumatism* 52 (8): 2521–2529.

Sanders, Thomas L., Ayoosh Pareek, Ian J. Barrett, Hilal Maradit Kremers, Andrew J. Bryan, Michael J. Stuart, Bruce A. Levy, and Aaron J. Krych. 2017. 'Incidence and Long-Term Follow-up of Isolated Posterior Cruciate Ligament Tears'. *Knee Surgery, Sports Traumatology, Arthroscopy* 25 (10): 3017–3023.

Sarugaser, Rahul, David Lickorish, Dolores Baksh, M. Morris Hosseini, and John E.

Davies. 2005. 'Human Umbilical Cord Perivascular (HUCPV) Cells: A Source of Mesenchymal Progenitors'. *Stem Cells* 23 (2): 220–229.

Schallmoser, Katharina, Christina Bartmann, Eva Rohde, Andreas Reinisch, Karl Kashofer, Elke Stadelmeyer, Camilla Drexler, Gerhard Lanzer, Werner Linkesch, and Dirk Strunk. 2007. 'Human Platelet Lysate Can Replace Fetal Bovine Serum for Clinical-Scale Expansion of Functional Mesenchymal Stromal Cells'. *Transfusion* 47 (8): 1436–46. https://doi.org/10.1111/j.1537-2995.2007.01220.x.

Sciore, Paul, Raymond Boykiw, and David A. Hart. 1998. 'Semiquantitative Reverse Transcription-Polymerase Chain Reaction Analysis of MRNA for Growth Factors and Growth Factor Receptors from Normal and Healing Rabbit Medial Collateral Ligament Tissue'. *Journal of Orthopaedic Research* 16 (4): 429–37. https://doi.org/10.1002/jor.1100160406.

Sensini, Alberto, and Luca Cristofolini. 2018. 'Biofabrication of Electrospun Scaffolds for the Regeneration of Tendons and Ligaments'. *Materials (Basel, Switzerland)* 11 (10). https://doi.org/10.3390/ma11101963.

Seo, Byoung-Moo, Masako Miura, Stan Gronthos, Peter Mark Bartold, Sara Batouli, Jaime Brahim, Marian Young, Pamela Gehron Robey, Cun Yu Wang, and Songtao Shi. 2004. 'Investigation of Multipotent Postnatal Stem Cells from Human Periodontal Ligament'. *The Lancet* 364 (9429): 149–55. https://doi.org/10.1016/S0140-6736(04)16627-0.

Shang, Shuhuan, Fang Yang, Xiangrong Cheng, X. Frank Walboomers, and John A.

Jansen. 2010. 'The Effect of Electrospun Fibre Alignment on the Behaviour of Rat Periodontal Ligament Cells.'

Shanskii, Ya D., N. S. Sergeeva, I. K. Sviridova, M. S. Kirakozov, V. A. Kirsanova, S. A. Akhmedova, A. I. Antokhin, and V. I. Chissov. 2013. 'Human Platelet Lysate as a Promising Growth-Stimulating Additive for Culturing of Stem Cells and Other Cell Types'. *Bulletin of Experimental Biology and Medicine* 156 (1): 146–51.

Sharifi-Aghdam, Maryam, Reza Faridi-Majidi, Mohammad Ali Derakhshan, Arash Chegeni, and Mahmoud Azami. 2017. 'Preparation of Collagen/Polyurethane/Knitted Silk as a Composite Scaffold for Tendon Tissue Engineering'. *Proceedings of the Institution of Mechanical Engineers, Part H: Journal of Engineering in Medicine* 231 (7): 652–62. https://doi.org/10.1177/0954411917697751.

Shen, Weiliang, Jialin Chen, Zi Yin, Xiao Chen, Huanhuan Liu, Boon Chin Heng, Weishan Chen, and Hong-Wei Ouyang. 2012. 'Allogenous Tendon Stem/Progenitor Cells in Silk Scaffold for Functional Shoulder Repair'. *Cell Transplantation* 21 (5): 943–58. https://doi.org/10.3727/096368911X627453.

Shen, Weiliang, Xiao Chen, Yejun Hu, Zi Yin, Ting Zhu, Jiajie Hu, Jialin Chen, et al. 2014. 'Long-Term Effects of Knitted Silk–Collagen Sponge Scaffold on Anterior Cruciate Ligament Reconstruction and Osteoarthritis Prevention'. *Biomaterials* 35 (28): 8154–63. https://doi.org/10.1016/j.biomaterials.2014.06.019.

Shi, S., P. M. Bartold, M. Miura, B. M. Seo, P. G. Robey, and S. Gronthos. 2005. 'The Efficacy of Mesenchymal Stem Cells to Regenerate and Repair Dental Structures'. *Orthodontics & Craniofacial Research* 8 (3): 191–99. https://doi.org/10.1111/j.1601-6343.2005.00331.x.

Shim, Ann Hye-Ryong, Heli Liu, Pamela J. Focia, Xiaoyan Chen, P. Charles Lin, and Xiaolin He. 2010. 'Structures of a Platelet-Derived Growth Factor/Propeptide Complex and a Platelet-Derived Growth Factor/Receptor Complex'. *Proceedings of the National Academy of Sciences* 107 (25): 11307–12. https://doi.org/10.1073/pnas.1000806107.

Shoulders, Matthew D., and Ronald T. Raines. 2009. 'COLLAGEN STRUCTURE AND STABILITY'. *Annual Review of Biochemistry* 78: 929–58. https://doi.org/10.1146/annurev.biochem.77.032207.120833.

Shukunami, Chisa, Yusuke Oshima, and Yuji Hiraki. 2001. 'Molecular Cloning of Tenomodulin, a Novel Chondromodulin-I Related Gene'. *Biochemical and Biophysical Research Communications* 280 (5): 1323–27. https://doi.org/10.1006/bbrc.2001.4271.

Shukunami, Chisa, Aki Takimoto, Miwa Oro, and Yuji Hiraki. 2006. 'Scleraxis Positively Regulates the Expression of Tenomodulin, a Differentiation Marker of Tenocytes'. *Developmental Biology* 298 (1): 234–247.

Silva Meirelles, Lindolfo da, Aparecida Maria Fontes, Dimas Tadeu Covas, and Arnold I. Caplan. 2009. 'Mechanisms Involved in the Therapeutic Properties of Mesenchymal Stem Cells'. *Cytokine & Growth Factor Reviews*, Bone

Morphogenetic Proteins, Stem Cells and Regenerative Medicine, 20 (5): 419–27. https://doi.org/10.1016/j.cytogfr.2009.10.002.

Singer, Nora G., and Arnold I. Caplan. 2011. 'Mesenchymal Stem Cells: Mechanisms of Inflammation'. *Annual Review of Pathology* 6: 457–78. https://doi.org/10.1146/annurev-pathol-011110-130230.

Sohni, Abhishek, and Catherine M. Verfaillie. 2013. 'Mesenchymal Stem Cells Migration Homing and Tracking'. *Stem Cells International* 2013.

Spiegelman, Bruce M., and Carol A. Ginty. 1983. 'Fibronectin Modulation of Cell Shape and Lipogenic Gene Expression in 3t3-Adipocytes'. *Cell* 35 (3, Part 2): 657–66. https://doi.org/10.1016/0092-8674(83)90098-3.

Stamenkovic, Vera, Stefan Stamenkovic, Tomasz Jaworski, Maciej Gawlak, Milos Jovanovic, Igor Jakovcevski, Grzegorz M. Wilczynski, et al. 2017. 'The Extracellular Matrix Glycoprotein Tenascin-C and Matrix Metalloproteinases Modify Cerebellar Structural Plasticity by Exposure to an Enriched Environment'. *Brain Structure & Function* 222 (1): 393–415. https://doi.org/10.1007/s00429-016-1224-y.

Stanitski, null. 1995. 'Anterior Cruciate Ligament Injury in the Skeletally Immature Patient: Diagnosis and Treatment'. *The Journal of the American Academy of Orthopaedic Surgeons* 3 (3): 146–58.

Steinert, Andre F., Meike Weber, Manuela Kunz, Glyn D. Palmer, Ulrich Nöth, Christopher H. Evans, and Martha M. Murray. 2008. 'In Situ IGF-1 Gene Delivery to Cells Emerging from the Injured Anterior Cruciate Ligament'.

Biomaterials 29 (7): 904–16. https://doi.org/10.1016/j.biomaterials.2007.10.054.

Stenhamre, Hanna, Ulf Nannmark, Anders Lindahl, Paul Gatenholm, and Mats Brittberg. 2011. 'Influence of Pore Size on the Redifferentiation Potential of Human Articular Chondrocytes in Poly (Urethane Urea) Scaffolds'. *Journal of Tissue Engineering and Regenerative Medicine* 5 (7): 578–588.

Sterodimas, Aris, Jose de Faria, Beatriz Nicaretta, and Ivo Pitanguy. 2010. 'Tissue Engineering with Adipose-Derived Stem Cells (ADSCs): Current and Future Applications'. *Journal of Plastic, Reconstructive & Aesthetic Surgery* 63 (11): 1886–92. https://doi.org/10.1016/j.bjps.2009.10.028.

Stoppato, Matteo, Friedrich von Flotow, and Catherine K. Kuo. 2016. 'Application of Hydrogels for Tendon and Ligament Repair and Tissue Engineering'. In *Gels Handbook*, 271–93. WORLD SCIENTIFIC. https://doi.org/10.1142/9789813140394_0009.

Strandberg, Gabriel, Felix Sellberg, Pehr Sommar, Martin Ronaghi, Norbert Lubenow, Folke Knutson, and David Berglund. 2017. 'Standardizing the Freeze-Thaw Preparation of Growth Factors from Platelet Lysate'. *Transfusion* 57 (4): 1058–65. https://doi.org/10.1111/trf.13998.

Swenson, David M., Christy L. Collins, Thomas M. Best, David C. Flanigan, Sarah K. Fields, and R. Dawn Comstock. 2013. 'Epidemiology of Knee Injuries among U.S. High School Athletes, 2005/2006-2010/2011'. *Medicine and Science in Sports and Exercise* 45 (3): 462–69.

https://doi.org/10.1249/MSS.0b013e318277acca.

Tabata, Y., M. Miyao, T. Inamoto, T. Ishii, Y. Hirano, Y. Yamaoki, and Y. Ikada. 2000. 'De Novo Formation of Adipose Tissue by Controlled Release of Basic Fibroblast Growth Factor'. *Tissue Engineering* 6 (3): 279–89. https://doi.org/10.1089/10763270050044452.

Tabata, Y., A. Nagano, M. Muniruzzaman, and Y. Ikada. 1998. 'In Vitro Sorption and Desorption of Basic Fibroblast Growth Factor from Biodegradable Hydrogels'. *Biomaterials* 19 (19): 1781–89.

Tang, Liang, Yadong Yang, Yuezhong Li, Geng Yang, Tao Luo, Yimeng Xu, and Wenyuan Zhang. 2018. 'Knitted Silk Mesh-like Scaffold Incorporated with Sponge-like Regenerated Silk Fibroin/Collagen I and Seeded with Mesenchymal Stem Cells for Repairing Achilles Tendon in Rabbits'. *Acta of Bioengineering and Biomechanics* 20 (4): 77–87.

Texier, A., C. Hulet, Y. Acquitter, E. Tallier, S. Jambou, B. Locker, and C. Vielpeau. 2002. '[Ligamentoplasty of the anterior cruciate ligament after 40 years: a series of 41 patients]'. *Revue De Chirurgie Orthopedique Et Reparatrice De L'appareil Moteur* 88 (2): 149–56.

'The Ligament Injury-Osteoarthritis Connection: The Role of Prolotherapy in Ligament Repair and the Prevention of Osteoarthritis'. 2012. *Journal of Prolotherapy* (blog). 31 March 2012. http://journalofprolotherapy.com/the-ligament-injury-osteoarthritis-connection-the-role-of-prolotherapy-in-ligament-repair-and-the-prevention-of-osteoarthritis/.

Tischer, Thomas, Stephan Vogt, Sebastian Aryee, Erwin Steinhauser, Christopher Adamczyk, Stefan Milz, Vladimir Martinek, and Andreas B. Imhoff. 2007. 'Tissue Engineering of the Anterior Cruciate Ligament: A New Method Using Acellularized Tendon Allografts and Autologous Fibroblasts'. *Archives of Orthopaedic and Trauma Surgery* 127 (9): 735–41. https://doi.org/10.1007/s00402-007-0320-0.

Tohyama, Harukazu, Toshikazu Yoshikawa, Young-Jin Ju, and Kazunori Yasuda. 2009. 'Revascularization in the Tendon Graft Following Anterior Cruciate Ligament Reconstruction of the Knee: Its Mechanisms and Regulation'. *Chang Gung Med J* 32 (2): 133–139.

Treiser, Matthew D., Eric H. Yang, Simon Gordonov, Daniel M. Cohen, Ioannis P. Androulakis, Joachim Kohn, Christopher S. Chen, and Prabhas V. Moghe. 2010. 'Cytoskeleton-Based Forecasting of Stem Cell Lineage Fates'. *Proceedings of the National Academy of Sciences* 107 (2): 610–615.

Tsuruga, Eichi, Hiroko Takita, Hideaki Itoh, Yuichi Wakisaka, and Yoshinori Kuboki. 1997. 'Pore Size of Porous Hydroxyapatite as the Cell-Substratum Controls BMP-Induced Osteogenesis'. *The Journal of Biochemistry* 121 (2): 317–324.

Tuan, Rocky S., Genevieve Boland, and Richard Tuli. 2002. 'Adult Mesenchymal Stem Cells and Cell-Based Tissue Engineering'. *Arthritis Res Ther* 5 (1): 32.

Van Eijk, F., D.b.f. Saris, J. Riesle, W.j. Willems, C.a. van Blitterswijk, A.j. Verbout, and W.j.a. Dhert. 2004. 'Tissue Engineering of Ligaments: A Comparison of Bone Marrow Stromal Cells, Anterior Cruciate Ligament, and Skin Fibroblasts

as Cell Source'. *Tissue Engineering* 10 (5–6): 893–903. https://doi.org/10.1089/1076327041348428.

Vaquette, Cédryck, Cyril Kahn, Céline Frochot, Cécile Nouvel, Jean-Luc Six, Natalia De Isla, Li-Hua Luo, Justin Cooper-White, Rachid Rahouadj, and Xiong Wang. 2010. 'Aligned Poly(L-Lactic-Co-e-Caprolactone) Electrospun Microfibers and Knitted Structure: A Novel Composite Scaffold for Ligament Tissue Engineering'. *Journal of Biomedical Materials Research Part A* 94A (4): 1270–82. https://doi.org/10.1002/jbm.a.32801.

Vieira, N. M., E. Zucconi, C. R. Bueno, M. Secco, M. F. Suzuki, P. Bartolini, M. Vainzof, and M. Zatz. 2010. 'Human Multipotent Mesenchymal Stromal Cells from Distinct Sources Show Different in Vivo Potential to Differentiate into Muscle Cells When Injected in Dystrophic Mice'. *Stem Cell Reviews and Reports* 6 (4): 560–566.

Vuornos, Kaisa, Miina Björninen, Elina Talvitie, Kaarlo Paakinaho, Minna Kellomäki, Heini Huhtala, Susanna Miettinen, Riitta Seppänen-Kaijansinkko, and Suvi Haimi. 2016. 'Human Adipose Stem Cells Differentiated on Braided Polylactide Scaffolds Is a Potential Approach for Tendon Tissue Engineering'. *Tissue Engineering Part A* 22 (5–6): 513–523.

Wagner, Eric R., Dalibel Bravo, Mahrokh Dadsetan, Scott M. Riester, Steven Chase, Jennifer J. Westendorf, Allan B. Dietz, Andre J. van Wijnen, Michael J. Yaszemski, and Sanjeev Kakar. 2015. 'Ligament Tissue Engineering Using a Novel Porous Polycaprolactone Fumarate Scaffold and Adipose Tissue-Derived

Mesenchymal Stem Cells Grown in Platelet Lysate'. *Tissue Engineering. Part A* 21 (21–22): 2703–13. https://doi.org/10.1089/ten.tea.2015.0183.

Wagner, Wolfgang, Patrick Horn, Mirco Castoldi, Anke Diehlmann, Simone Bork, Rainer Saffrich, Vladimir Benes, et al. 2008. 'Replicative Senescence of Mesenchymal Stem Cells: A Continuous and Organized Process'. *PLOS ONE* 3 (5): e2213. https://doi.org/10.1371/journal.pone.0002213.

Wang, Limin, Lindsey Ott, Kiran Seshareddy, Mark L Weiss, and Michael S Detamore. 2011. 'Musculoskeletal Tissue Engineering with Human Umbilical Cord Mesenchymal Stromal Cells'. *Regenerative Medicine* 6 (1): 95–109. https://doi.org/10.2217/rme.10.98.

Wang, Shengyu, Yiyun Wang, Liyang Song, Jiaxin Chen, Yujie Ma, Yunbin Chen, Shunwu Fan, Miaoshang Su, and Xianfeng Lin. 2017. 'Decellularized Tendon as a Prospective Scaffold for Tendon Repair'. *Materials Science and Engineering: C* 77 (August): 1290–1301. https://doi.org/10.1016/j.msec.2017.03.279.

Wang, Tao, Bruce S. Gardiner, Zhen Lin, Jonas Rubenson, Thomas B. Kirk, Allan Wang, Jiake Xu, David W. Smith, David G. Lloyd, and Ming H. Zheng. 2012. 'Bioreactor Design for Tendon/Ligament Engineering'. *Tissue Engineering Part B: Reviews* 19 (2): 133–146.

Weiler, Andreas, Cornelius Förster, Patrick Hunt, Roman Falk, Tobias Jung, Frank N. Unterhauser, Volker Bergmann, Gerhard Schmidmaier, and Norbert P. Haas. 2004. 'The Influence of Locally Applied Platelet-Derived Growth Factor-BB on

Free Tendon Graft Remodeling after Anterior Cruciate Ligament Reconstruction'. *The American Journal of Sports Medicine* 32 (4): 881–891.

Weiss, Jeffrey A., Savio L.-Y. Woo, Karen J. Ohland, Shuji Horibe, and Peter O. Newton. 1991. 'Evaluation of a New Injury Model to Study Medial Collateral Ligament Healing: Primary Repair versus Nonoperative Treatment'. *Journal of Orthopaedic Research* 9 (4): 516–28. https://doi.org/10.1002/jor.1100090407.

Whitlock, Patrick W., Thomas L. Smith, Gary G. Poehling, Jeffrey S. Shilt, and Mark Van Dyke. 2007. 'A Naturally Derived, Cytocompatible, and Architecturally Optimized Scaffold for Tendon and Ligament Regeneration'. *Biomaterials* 28 (29): 4321–29. https://doi.org/10.1016/j.biomaterials.2007.05.029.

Wong, Victor W., Geoffrey C. Gurtner, and Michael T. Longaker. 2013. 'Wound Healing: A Paradigm for Regeneration'. *Mayo Clinic Proceedings* 88 (9): 1022–31. https://doi.org/10.1016/j.mayocp.2013.04.012.

Woo, S. L., M. A. Gomez, T. J. Sites, P. O. Newton, C. A. Orlando, and W. H. Akeson. 1987. 'The Biomechanical and Morphological Changes in the Medial Collateral Ligament of the Rabbit after Immobilization and Remobilization.' *The Journal of Bone and Joint Surgery. American Volume* 69 (8): 1200–1211.

Woo, S. L., M. A. Ritter, D. Amiel, T. M. Sanders, M. A. Gomez, S. C. Kuei, S. R. Garfin, and W. H. Akeson. 1980. 'The Biomechanical and Biochemical Properties of Swine Tendons--Long Term Effects of Exercise on the Digital Extensors'. *Connective Tissue Research* 7 (3): 177–83.

Woo, Savio L.-Y., Steven D. Abramowitch, Robert Kilger, and Rui Liang. 2006.

‘Biomechanics of Knee Ligaments: Injury, Healing, and Repair’. *Journal of Biomechanics* 39 (1): 1–20.

Woo, Savio L-Y., Richard E. Debski, John D. Withrow, and Marsie A. Janaushek. 1999. ‘Biomechanics of Knee Ligaments’. *The American Journal of Sports Medicine* 27 (4): 533–43. https://doi.org/10.1177/03635465990270042301.

Woo, Savio L.-Y., J. Marcus Hollis, Douglas J. Adams, Roger M. Lyon, and Shinro Takai. 1991. ‘Tensile Properties of the Human Femur-Anterior Cruciate Ligament-Tibia Complex: The Effects of Specimen Age and Orientation’. *The American Journal of Sports Medicine* 19 (3): 217–25. https://doi.org/10.1177/036354659101900303.

Wren, Tishya AL, Gary S. Beaupré, and Dennis R. Carter. 2000. ‘Tendon and Ligament Adaptation to Exercise, Immobilization, and Remobilization’. *Journal of Rehabilitation Research and Development* 37 (2): 217–224.

Xie, Jingwei, Matthew R. MacEwan, Wilson Z. Ray, Wenying Liu, Daku Y. Siewe, and Younan Xia. 2010. ‘Radially Aligned, Electrospun Nanofibers as Dural Substitutes for Wound Closure and Tissue Regeneration Applications’. *ACS Nano* 4 (9): 5027–5036.

Xie, Jun, Maki Ihara, Youngmee Jung, Il Keun Kwon, Soo Hyun Kim, Young Ha Kim, and Takehisa Matsuda. 2006. ‘Mechano-Active Scaffold Design Based on Microporous Poly (L-Lactide-Co-ε-Caprolactone) for Articular Cartilage Tissue Engineering: Dependence of Porosity on Compression Force-Applied Mechanical Behaviors’. *Tissue Engineering* 12 (3): 449–458.

Xu, Jia, Jinhui Zhang, Weiquan Gao, Hongwei Liang, Hongyan Wang, and Junfeng Li. 2009. 'Preparation of Chitosan/PLA Blend Micro/Nanofibers by Electrospinning'. *Materials Letters* 63 (8): 658–660.

Xu, Jinping, Wei Wang, Yvonne Kapila, Jeffrey Lotz, and Sunil Kapila. 2008. 'Multiple Differentiation Capacity of STRO-1+/CD146+ PDL Mesenchymal Progenitor Cells'. *Stem Cells and Development* 18 (3): 487–496.

Xu, Yuan, Jinglei Wu, Haoming Wang, Hanqin Li, Ning Di, Lei Song, Sontao Li, et al. 2013. 'Fabrication of Electrospun Poly(L-Lactide-Co-ε-Caprolactone)/Collagen Nanoyarn Network as a Novel, Three-Dimensional, Macroporous, Aligned Scaffold for Tendon Tissue Engineering'. *Tissue Engineering Part C: Methods* 19 (12): 925–36. https://doi.org/10.1089/ten.tec.2012.0328.

Yablonka-Reuveni, Z., R. Seger, and A. J. Rivera. 1999. 'Fibroblast Growth Factor Promotes Recruitment of Skeletal Muscle Satellite Cells in Young and Old Rats'. *The Journal of Histochemistry and Cytochemistry: Official Journal of the Histochemistry Society* 47 (1): 23–42. https://doi.org/10.1177/002215549904700104.

Yamanlar, Seda, Shilpa Sant, Thomas Boudou, Catherine Picart, and Ali Khademhosseini. 2011. 'Surface Functionalization of Hyaluronic Acid Hydrogels by Polyelectrolyte Multilayer Films'. *Biomaterials* 32 (24): 5590–5599.

Yang, Shoufeng, Kah-Fai Leong, Zhaohui Du, and Chee-Kai Chua. 2001. 'The Design

of Scaffolds for Use in Tissue Engineering. Part I. Traditional Factors'. *Tissue Engineering* 7 (6): 679–689.

Yilgor, Caglar, Pinar Yilgor Huri, and Gazi Huri. 2012. 'Tissue Engineering Strategies in Ligament Regeneration'. Research article. Stem Cells International. 2012. https://doi.org/10.1155/2012/374676.

Yin, Zi, Xiao Chen, Jia Lin Chen, Wei Liang Shen, Thi Minh Hieu Nguyen, Ling Gao, and Hong Wei Ouyang. 2010. 'The Regulation of Tendon Stem Cell Differentiation by the Alignment of Nanofibers'. *Biomaterials* 31 (8): 2163–2175.

Yoon, J. Hae, and J. Halper. 2005. 'Tendon Proteoglycans: Biochemistry and Function'. *J Musculoskelet Neuronal Interact* 5 (1): 22–34.

Yoon, Jun Jin, Hyun Jung Chung, Hyuk Jin Lee, and Tae Gwan Park. 2006. 'Heparin-Immobilized Biodegradable Scaffolds for Local and Sustained Release of Angiogenic Growth Factor'. *Journal of Biomedical Materials Research. Part A* 79 (4): 934–42. https://doi.org/10.1002/jbm.a.30843.

Yoshikawa, Toshikazu, Harukazu Tohyama, Taro Katsura, Eiji Kondo, Yoshihisa Kotani, Hideo Matsumoto, Yoshiaki Toyama, and Kazunori Yasuda. 2006. 'Effects of Local Administration of Vascular Endothelial Growth Factor on Mechanical Characteristics of the Semitendinosus Tendon Graft after Anterior Cruciate Ligament Reconstruction in Sheep'. *The American Journal of Sports Medicine* 34 (12): 1918–25. https://doi.org/10.1177/0363546506294469.

Yoshimura, Hideya, Takeshi Muneta, Akimoto Nimura, Akiko Yokoyama, Hideyuki

Koga, and Ichiro Sekiya. 2007. 'Comparison of Rat Mesenchymal Stem Cells Derived from Bone Marrow, Synovium, Periosteum, Adipose Tissue, and Muscle'. *Cell and Tissue Research* 327 (3): 449–62. https://doi.org/10.1007/s00441-006-0308-z.

Zantop, Thore, Thomas W. Gilbert, Mervin C. Yoder, and Stephen F. Badylak. 2006. 'Extracellular Matrix Scaffolds Are Repopulated by Bone Marrow-Derived Cells in a Mouse Model of Achilles Tendon Reconstruction'. *Journal of Orthopaedic Research* 24 (6): 1299–1309. https://doi.org/10.1002/jor.20071.

Zhang, Dongdong, Yanmin Zhang, Lei Zheng, Yingzhuan Zhan, and Langchong He. 2013. 'Graphene Oxide/Poly-l-Lysine Assembled Layer for Adhesion and Electrochemical Impedance Detection of Leukemia K562 Cancercells'. *Biosensors and Bioelectronics* 42: 112–118.

Zhao, Jing. 2008. 'Tendon and Ligament Repair: Regeneration and Maturation'. *All Theses*, May. https://tigerprints.clemson.edu/all_theses/335.
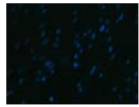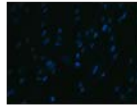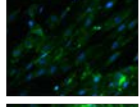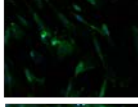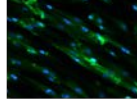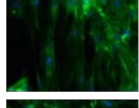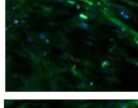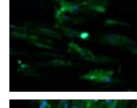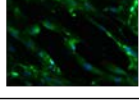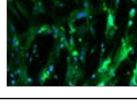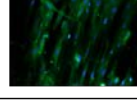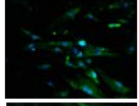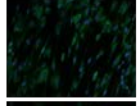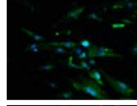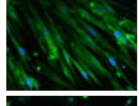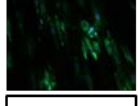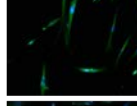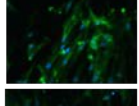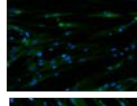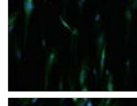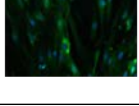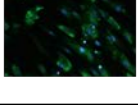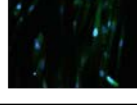
Figure 41 Effect of Growth factor on the synthesis of Col I and Col III by MSCs

(TGF-β: Transforming Growth Factor, FGF-2: Fibroblast growth factor-2)

L'ingénierie tissulaire du ligament constitue une approche prometteuse pour réparer ou remplacer un ligament endommagé. Les trois piliers essentiels de l'ingénierie tissulaire ligamentaire sont la matrice de support (aussi appelée scaffold), la source cellulaire, ainsi que l'apport de stimulations biomécaniques/biochimiques : ces trois piliers ont été partiellement étudiés par le passé dans le but de s'orienter vers une régénération ligamentaire.

Dans la présente étude, le polymère synthétique poly (L-lactide-co-ε-caprolactone) (PLCL) et la soie ont été proposés et comparés comme de potentiels candidats pour la constitution d'une matrice de support. Une série de matrices tressées multicouches à base de PLCL et de soie, ainsi qu'un nouveau composite soie/PLCL ont été développés et comparés. Les caractérisations physico-chimiques et biologiques ont démontré que le PLCL et la soie constituent des candidats pertinents, tant sur les plans mécaniques que biologiques, pour la constitution d'une matrice de support. De plus, nous avons montré que le composite soie/PLCL offrait des propriétés mécaniques et une biocompatibilité accrue par rapport aux autres matrice testées, et constituait probablement le candidat le plus approprié pour l'ingénierie tissulaire du ligament.

Les cellules souches mésenchymateuses (CSM) de la gelée de Wharton (WJ-MSCs) ainsi que les cellules souches mésenchymateuses de la moelle osseuse (BM-MSCs) ont été évaluées et comparées en tant que sources cellulaires potentielles pour la régénération ligamentaire. Les caractéristiques biologiques de ces cellules incluent l'adhésion cellulaire, la prolifération, la migration et la synthèse de matrice extracellulaire. Ces deux types de cellules ont montré une bonne biocompatibilité dans leurs interactions avec les matrices de support en PLCL et en soie. Aucune différence significative n'a été observée entre les WJ-MSCs et les BM-MSCs.

Enfin, l'effet de la stimulation biomécanique sur la différentiation des CSM en tissu ligamentaire a été évalué par le biais d'un bioréacteur de traction-torsion. Bien que peu de cellules aient été détectées la matrice après 7 jours de stimulation, des CSM de forme allongée le long des fibres ont été détectées, ce qui permet de penser qu'il est possible de promouvoir la différenciation des biosubstituts matrice-cellules grâce à la stimulation mécanique en bioréacteur.

En conclusion, cette étude démontre le potentiel prometteur de l'association de cellules souches mésenchymateuses issues de la gelée de Wharton ou de la moelle osseuse avec une matrice de support composite soie/PLCL pour la régénération ligamentaire dans le futur.

Mots-clés : ingénierie tissulaire ligamentaire, poly (L-lactide-co-ε-caprolactone), soie, cellules souches mésenchymateuses de gelée de Wharton, cellules souches mésenchymateuses de la moelle osseuse, bioréacteur

Ligament tissue engineering offers a potential approach to recover or replace injured ligament. The three essential elements that have been investigated towards ligament regeneration consist in a suitable scaffold, an adapted cell source, and the supply of biomechanical/biochemical stimulations. In the current study, synthetic polymer poly (L-lactide-co-ε-caprolactone) (PLCL) and silk have been evaluated as suitable candidates to constitute an adapted scaffold. A series of multilayer braided scaffolds based on PLCL and silk, as well as an original silk/PLCL composite scaffold, have been developed and compared. The conducted physicochemical and biological characterizations have demonstrated that both PLCL and silk constitute adapted candidate material to form ligament scaffolds from the mechanical and biological points of view. Moreover, it has been observed that silk/PLCL composite scaffold resulted in adequate mechanical properties and biocompatibility, and therefore could constitute suitable candidate scaffolds for ligament tissue engineering.

Both Wharton's Jelly mesenchymal stem cells (WJ-MSCs) and Bone marrow mesenchymal stem cells (BM-MSCs) have been evaluated to be cell source for ligament regeneration. MSCs behaviors including cell attachment, proliferation, migration and extracellular matrix synthesis have been investigated. In the present study, both MSCS showed a good biocompatibility to interact with PLCL and silk scaffolds. No significant differences have been detected between WJ-MSCs and BM-MSCs. Finally, the effect of biomechanical stimulation on MSCs differentiation towards ligament tissue has been carried out with a tension-torsion bioreactor. Although few cells were detected on scaffold after 7 days of stimulation, MSCs were observed to exhibit an elongated shape along the longitudinal direction of fibers, which may indicate that an adapted mechanical stimulation could promote MSC-scaffold constructs differentiation towards ligamentous tissue.

As a conclusion, this study demonstrates the potential of WJ-MSCs and BM-MSCs combined with a new silk/PLCL composite scaffold towards ligament regeneration.

Keywords: ligament tissue engineering, poly (L-lactide-co-ε-caprolactone), silk, Wharton's Jelly mesenchymal stem cells, bone marrow mesenchymal stem cells, bioreactor